12-2016

REGULATION OF CANCER METASTASIS BY PROTEIN KINASE D1: A GLOBAL REGULATORY CASCADE

Aditya Ganju

REGULATION OF CANCER METASTASIS BY PROTEIN KINASE D1: A GLOBAL REGULATORY CASCADE

ORCID
http://orcid.org/0000-0003-1258-0105

DOI
10.21007/etd.cghs.2016.0421

REGULATION OF CANCER METASTASIS BY PROTEIN KINASE D1: A GLOBAL REGULATORY CASCADE

A Dissertation
Presented for
The Graduate Studies Council
The University of Tennessee
Health Science Center

In Partial Fulfillment
Of the Requirements for the Degree
Doctor of Philosophy
From The University of Tennessee

By
Aditya Ganju
December 2016

DEDICATION

I want to take this opportunity to dedicate my dissertation which is a byproduct of many years of hard work and sacrifice to my loving parents, Mr. Ashok Ganju and Mrs. Suman Ganju without whose constant support and encouragement I could not have done any of this. I also want to take this opportunity to dedicate this work to my late grandparents (Mr. Somnath Ganju and Mrs. Umashri Ganju) who always taught me the value of hard work and dedication.

ACKNOWLEDGEMENTS

The author wishes to sincerely acknowledge Dr. Meena Jaggi for her mentorship throughout the PhD program. I would also like to thank Dr. Subhash Chauhan for guiding me throughout my PhD program. By providing me the opportunity to work in their lab they gave me an excellent platform to engage in breakthrough research and enhance my understanding of how cancer cells grow and metastasize to different parts of the body. I also would like to thank Drs. Steve Behrman, Yi Lu, Santosh Kumar and Murali Yallapu for not only their mentorship but also giving me excellent feedbacks throughout the course of my program. I also like to thank Dr. Vasudha Sundram, Dr. Bilal Hafeez and Dr. Sheema Khan for providing me valuable inputs on my research work over the years. I would also like to extent my gratitude to Dr. Fathi Halaweish for providing us with the drug ormeloxifene and Dr. Nadeem Zafar for providing assistance with pathology services. Lastly, I would like to thank my family for constant support and encouragement.

ABSTRACT

Protein Kinase D1 (PKD1) is a serine threonine kinase which is downregulated in Prostate, Breast and Colon Cancer. It functions as a tumor suppressor in different cancer cells. Downregulation of PKD1 is known to be associated with aggressiveness of the cancer. PKD1 is known to regulate many key oncogenic signaling pathways such as E-cadherin, β-catenin and Androgen Receptor signaling pathways. Aberrant expression of these oncogenic pathways leads to transformation of cells from normal to malignant phenotype, thereby leading to increased proliferation, growth and metastasis to distant organs of these cancer cells. Literature evidence also points to the fact that E-cadherin β-catenin and PKD1 play a role in regulation of epithelial mesenchymal transition (EMT).

To fully understand how PKD1 regulates β-catenin signaling, we investigated the effect of PKD1 overexpression on β-catenin signaling in colon cancer cells. We observed that PKD1 overexpression is responsible for inhibition of cell proliferation and colony formation ability of different colon cancer cell lines. Moreover, nuclear PKD1 overexpression leads to inhibition of β-catenin transcription activity in colon cancer cells. Further evaluation in *in vivo* mouse model showed that PKD1 is responsible for inhibition of colon cancer tumor growth in xenograft mouse model. This paved way for us to look for the effect of PKD1 on other downstream targets of β-catenin pathway which regulate EMT process in cancer cells such as Metastasis associated Protein 1.

Metastasis associated Protein 1 (MTA1) is a nucleosome remodeling and histone deacetylase protein (NuRD) which is overexpressed in all the cancers. MTA1 is an initiator of epithelial and mesenchymal transition and is responsible for cancer cells metastasizing to different organs of the body. Expression of MTA1 directly correlates with the aggressiveness of the cancer. MTA1 is known to regulate β-catenin and Androgen Receptor signaling pathways leading to cancer cells acquiring metastatic capabilities. Therefore, in our study we evaluated the inverse correlation between MTA1 and PKD1 in different cancer cells.

To investigate the cellular effect of PKD1 in prostate and colon cancer, stable PKD1 overexpressing prostate (C4-2) and colon cancer cells (SW480) were utilized. PKD1 overexpression inhibited MTA1 expression in prostate and colon cancer cells. PKD1 interacts, phosphorylate, translocate and degrades MTA1. Kinase domain and N terminal domain of PKD1 play a significant role in MTA1 interaction and phosphorylation. Phosphorylation of MTA1 leads to nuclear export *via* golgi and trans-golgi network to lysosome. Bryostatin-1 is a macrocyclic lactone which modulates PKD1 activity. Bryostatin-1 was used to activate PKD1 expression in C4-2 cells and MTA1 translocation was then tracked. This translocation of MTA1 to lysosome is a ubiquitin dependent phenomenon leading protein degradation. PKD1 overexpression leads to inhibition of tumor growth and bone metastasis leading to inhibition of osteoblast to osteoclast formation as determined by RANK expression. PTEN Knockout and TRAMP mouse model also show inverse correlation between PKD1 and MTA1 expression in prostate tissues at different weeks. Human tissue microarray of prostate, colon and breast

cancer (MTA1 is overexpressed and PKD1 is downregulated in breast cancer, therefore, we tested our hypothesis in breast cancer as well) showed inverse correlation between PKD1 and MTA1 in different grade tumor tissue signifying clinical relevance of this correlation. For proof of concept of our hypothesis we used ormeloxifene because Bryostatin-1 has mild toxicity issue. Ormeloxifene is a novel modulator of PKD1 activity and it targets rapidly dividing cells Further, we investigated the effect of ormeloxifene on activation of PKD1 leading to inhibition of cancer metastasis. We observed specific activation of PKD1 expression of ormeloxifene which inhibited MTA1 expression leading to inhibition of tumor growth in xenograft mouse.

We further evaluated the efficacy of ormeloxifene to inhibit metastatic prostate cancer cells (PC3 and DU145). Ormeloxifene showed excellent anti-cancer efficacy against prostate cancer as it inhibited cell proliferation, invasion and migration of metastatic prostate cancer cells. Moreoever, ormeloxifene induced cell cycle arrest at G0/G1 phase by regulating key cell cycle regulatory proteins. It also inhibited metastasis of prostate cancer leading to inhibition of key metastatic markers involved to epithelial mesenchymal transition. Ormeloxifene also showed excellent *in vivo* efficacy against metastatic prostate cancer cells. Therefore, ormeloxifene could be a potential therapeutic modality for metastatic cancers as it targets EMT signaling.

To conclude, we for the very first time have elucidated a novel regulatory mechanism of PKD1 mediated regulation of MTA1 that plays an important role in cancer progression and metastasis. For cancer cells to metastasize PKD1 expression is suppressed with subsequent increased expression of MTA1. We elucidated that repression of MTA1 with subsequent activation of MTA1 leads to attenuation of cancer metastasis. Moreover, therapeutic modality that targets this novel regulatory pathway leading to activation of PKD1 and inhibition of MTA1 is an ideal candidate for treatment of advanced stage metastatic cancers.

TABLE OF CONTENTS

LIST OF TABLES

LIST OF FIGURES

LIST OF ABBREVIATIONS

AA	African American
ABC	ATP-Binding Cassette Transporter
ADT	Androgen Deprivation Therapy
AMPK	Adenosine Monophosphate activated Protein Kinase
AR	Androgen Receptor
ATM	Ataxia telangiectasia mutated
ATP	Adenosine Triphosphate
BMI	Body Mass Index
BRCA1	Breast Cancer Susceptibility gene 1
BRCA2	Breast Cancer Susceptibility gene 2
CA	Caucasian American
CBZ	Cabazitaxel
CHEK2	Checkpoint Kinase 2
DTX	Docetaxel
FADH	Flavin adenine Dinucleotide
FAP	Familial Adenomatous Polyposis
FDA	Food and Drug Administration
HNPCC	Hereditary Nonpolyposis Colorectal Cancer
HNSCC	Head and Neck Squamous Cell Carcinoma
MRI	Magnetic Resonance Imaging
MTA1	Metastasis associated Protein 1
NADH	Nicotinamide Adenine Dinucleotide
ORM	Ormeloxifene
PGP	P-glycoproteins
PSA	Prostate Specific Antigen
PTX	Paclitaxel
SEER	Surveillance, Epidemiology and End Results
TBD	Taxol Binding Domain
TME	Tumor Microenvironment
TSC2	Tuberous Sclerosis Complex 2

CHAPTER 1. INTRODUCTION

Colon Cancer

Colon cancer or Colorectal cancer is the development of cancer in the colon or rectum. It occurs due to abnormal growth of cells that can invade to the other parts of body.

Colon Cancer Statistics

Colon cancer is the third most common cancer and third leading cause of all cancer deaths for males and females in the US. There will be 95,270 new cases of colon cancer and 49,120 deaths from colon cancer in the US this year (1) . Of these new cases 23% will be stage I, 31% stage II, 26% stage III, and 20% stage IV (2). Due to innovations in technology and changes in standards of care more colon cancer cases are being caught early (3). With respect to incidence rates and mortality rates there has been a decline of 3% and 2.8% for men and 2.3% and 2.6% for women every year since 1998 (4,5). This is partly due to incidence rates for men and women over 50 years old declining (5). On the other hand, for men and women under age 50, incidence rates have steadily been increasing (6). This increase is thought to be due to obesity and poor diets in children and young adults(6). With the epidemic that obesity, has become in the US over the years it can only be inferred that this increase will continue unabated. Five-year survival for stage I is 74%, IIA is 67%, IIB is 59%, IIC is 37%, IIIA is 73%, IIIB is 46%, IIIC is 28%, and IV is 6% (7) (**Table 1-1**). Stage IV is the most advanced stage of colon cancer and its major differentiation is the presence of metastasis.

Colon Cancer Causes and Risks

Risk factor for colon cancer begin with age. Many factors that contribute to increased risk factors include obesity, lack of physical activity, smoking, eating processed meat, alcohol consumption etc (8). Hereditary and Family history of colorectal cancer also increases the risk due to certain inherited conditions such as hereditary nonpolyposis colorectal cancer (HNPCC) and familial adenomatous polyposis (FAP) (9).

Clinically Relevant Classification

Colon cancer classification is based on either histological grade or staging-the extent of the cancer in the human body. Histological grading is the classification of the cancer cells specifically based on differentiation. The classical grading scheme is broken into well differentiated (grade 1), moderately differentiated (grade 2), poorly differentiated (grade 3), and undifferentiated (grade 4) (10). The World Health Organization (WHO) classifies tumor grade based on the least differentiated portion. The

Table 1-1. 5-year survival by stage from a study of the National Cancer Institute's Surveillance, Epidemiology, and End Results (SEER) database

Stage	5-Year Survival Rate
I	74%
IIa	67%
IIb	59%
IIc	37%
IIIa	73%
IIIb	46%
IIIc	28%
IV	6%

WHO has two categories, low-grade, which is made up of well differentiated and moderately differentiated, and high-grade, which is made up of poorly differentiated and undifferentiated tumors (11).

Histological grading has been previously shown to be a prognostic indicator in colon cancer independent of TNM staging (12). A thorough study looking only at stage IIIa, IIIb, and IIIc found that the following in descending order were the most important in determining patient survival: stage III subgroup, patient age, tumor grade, and first-course treatment (12). However, there has been some criticism for this classification due to two main concerns: The difficulty in objectively distinguishing between grades such as well from moderately differentiated and having a clear standardization for grading for example if one small portion is clearly low grade and the majority of the tumor is high grade (11,13).

New grading models have been suggested due to the objectivity issues. A recent study using Surveillance, Epidemiology, and End Results (SEER) data from 1991-2000 showed statistical significance for differences in 5-year survival between low grade and high grade within specific American Joint Committee on Cancer (AJCC) TNM 5th edition stages except stage I (14). There was no evidence presented overall that suggests tumor grade is a significant indicator of prognosis. Further the differences between the high and low grade within specific stages were typically only 2-10% (14). Therefore, the prognostic value of histological grading as we know is highly debated (15).

The extent of the cancer growth in the patient is the criteria for staging. In the 1940's the TNM staging was first developed by Pierre Denoix (16). The International Union Against cancer (UICC) and the AJCC have both over the years developed and maintained the TNM staging. The AJCC TNM has gone through seven revisions and is currently in its 7th edition. Each edition has improved its clinical relevance to the point in which Dukes and Astler-Coller are outdated and are no longer recommended for use in clinical practice (17,18). **Table 1-2** gives an in-depth guide to TNM staging. Controversy exists over the survival differences between the stages IIIa and IIIb and the stages IIa, IIb, and IIc. The current theory for the higher survival of stage IIIa and IIIb than some subsets of stage II colon cancer is that stage III colon cancers are recommended to always be treated with adjuvant therapy after surgical resection whereas stage II is not (14).

Current Therapy Options

A brief overview of the function of currently used first line chemotherapy drugs: 1) 5-FU inhibits production of dTMP and DNA. 2) Oxaliplatin inhibits DNA replication and transcription. 3) Folic acid used in combination with 5-FU as a rescue treatment. 4) Capecitabine is an oral drug that is converted to 5-FU. 5) Leucovorin is a form of folate used in combination with 5-FU that can function directly without further enzymatic reduction. 6) Irinotecan inhibits topoisomerase I. 7) Levamisole is an immunomodulator that is beneficial in combination treatment with 5-FU (19,20) .

Table 1-2. TNM classification for colon cancer

TNM	Classification
Tx	Tumor cannot be assesed due to incomplete information
Tis	Carcinoma *in-situ*
T1	Cancer cells invade submucosa
T2	Cancer cells invade muscularis propria
T4a	Cancer cells extend through the serosa (outermost layer)
T4b	Tumor invade or is adherent to other organs
Nx	Lymph node cannot be assessed
N0	No cancer cells in nearby lymph nodes
N1a	Cancer cells found in 1 nearby lymph node
N1b	Cancer cells found in 2 or 3 nearby lymph nodes
N1c	Tumor deposit in sub-serosa, or perirectal tissue
N2a	Cancer cells found in 4 to 6 nearby lymph nodes
N2b	Cancer cells found in 7 or more nearby lymph nodes
M0	No distant spread is seen
M1a	Metastasis confined to 1 organ
M1b	Metastases in more than 1 organ/site or the peritoneum

Standardized treatment guidelines for colon cancer are based on the stage of the cancer. Stages 0-III are treated with surgical resection of the tumor with clear margins. Stage II and III patients are also recommended to receive adjuvant therapy after resection whereas for Stage IV patient's chemotherapy before or after surgery is usually recommended (21). Common chemotherapy regimens used for stage III patients are: 1) FOLFOX4 regimen- oxaliplatin, leucovorin, and fluorouracil (5-FU). 2) Levamisole regimen- 5-FU and Levamisole. 3) The Mayo Clinic regimen- 5-FU and low-dose leucovorin. 4) The Roswell Park regimen- 5-FU and high-dose leucovorin (22).

Stage IV and recurrent colon cancer patients have a more complex recommendation based on if the metastatic or recurrent tumor(s) are operable. If the tumor(s) are resectable then the they are treated with neoadjuvant therapy prior to surgical resection (22). If the tumor(s) are not resectable then the following options are recommended: 1) Routine local ablation of tumors through either radiofrequency or cryosurgical ablation. 2) Palliative radiation or chemotherapy treatment. 3) Participation in clinical trials (22). Common chemotherapy regimens used for stage IV and recurrent cancer patients are: 1) FOLFOX4 regimen- oxaliplatin, leucovorin, and fluorouracil (5-FU). 2) FOLFOX6 regimen- a variation of FOLFOX4 with higher doses over a longer duration. 3) German AIO regimen- folic acid, 5-FU, and irinotecan. 4) CAPOX regimen-capecitabine and oxaliplatin. 5) Douillard regimen-folic acid, 5-FU, and irinotecan. 6) FOLFIRI regimen- folic acid, 5-FU, irinotecan. 7) FUFOX regimen-oxaliplatin and 5-FU. 8) FUOX regimen- 5-FU and oxaliplatin. 9) IFL regimen- irinotecan, 5-FU, and leucovorin. 10) XELOX regimen-capecitabine and oxaliplatin. Second line treatments that can be added to first-line regimens are: Aflibercept, a novel anti-VEGF molecule, Cetuximab, a monoclonal antibody for epidermal growth factor receptor (EGFR), and Panitumumab a fully humanized monoclonal antibody for EGFR. Third-line treatments are Regorafenib an inhibitor of multiple tyrosine kinase pathways including VEGF (22).

Adenomatous Polyposis Coli (APC)

The Adenomatous Polyposis Coli (APC) gene product is a 312 kDa protein that has interactions with over 100 different proteins (23). APC binds axin, casein kinase, and glycogen synthase kinase 3β (GSK3β) creating a complex that targets β-catenin for destruction (23).

APC is mutated in sporadic colon cancer as well as in FAP resulting in over 80% of all colon cancer having mutated APC (24). APC mutation is thought to be among the earliest stages in colon tumorigenesis (25). The common site of mutation in APC is the mutation cluster region (MCR), it is in this area that three 20-amino acid repeats exist that contain binding sequences for both β-catenin and axin (26). Mutation at the MCR produces a C-terminal truncated APC which has few binding sites remaining, allowing for binding only of Asef1, Asef2, IQGAPI, and part of the β-catenin site (27). The truncated APC through interaction with Asef1, Asef2, and IQGAPI can cause increased cell migration (27). Truncated APC was previously thought to be unable to bind β-catenin, but recent evidence shows some truncated APC's retain limited ability to bind β-

catenin (28,29). Due to the inability to bind axin or Siah-1, truncated APC cannot facilitate β-catenin interaction with β-catenin destruction complex or the Siah-1 regulatory pathways (28-30).

APC truncation results in APC's inability to bind EB1 and microtubules culminating in the inability of spindle microtubules to attach to chromosomes during metaphase which induces chromosomal instability (CIN) (24,27). CIN is a hallmark of cancer and contributes to tumorigenesis, as previously mentioned, which further supports the importance of APC mutation in early tumorigenesis.

In summary mutations of APC are found in over 80% of colon cancer and are shown to induce numerous regulatory pathways of β-catenin/TCF transcription activity as well as inducing CIN.

β-catenin

β-catenin is a multifunctional protein that is distinguished by an armadillo repeat region which serves as a binding site for numerous partners (31). β-catenin serves a role as the main effector of canonical Wnt signaling and as an important component in cellular adhesion (31). It was the finding of mutated APC involvement in FAP that first connected dysregulated β-catenin and cancer (32). Now it is well known that β-catenin is a dysregulated in 90% or more of all colon cancers (33). Under normal conditions when Wnt is not activated, β-catenin joins classical cadherins to the actin cytoskeleton and is necessary for the correct function of the adherens junctions (34). Any free β-catenin in the cell under normal situations is quickly degraded by the previously mentioned degradation pathways **(Figure 1-1)**.

In the 90% of colon cancer cases that have dysregulated β-catenin, it acts as a co-transcription factor with Transcription Factor (T-cell specific, HMG-Box)/Lymphoid enhancer-binding factor (TCF4/LEF) transcription factors leading to transcription of target genes c-Myc, cyclin-D1, c-Jun, fra-1, urokinase-type plasminogen activator receptor (uPAR), PPARdelta, matrix metalloproteinase-7 (MMP-7), axin-2, Nr-Cam, ITF-2, Gastrin, CD44, EphB/Ephrin-B, bone morphogenetic protein 4 (BMP4), claudin-1, survivin, vascular endothelial growth factor (VEGF), FGF18, c-Myc binding protein, L1, Id2, Jagged, endothelin-1 (EDN1), receptor tyrosine kinase Met, βTrCP, TCF-1, and lef-1 (35-57). These transcription targets and functions are summarized in **Table 1-3**. The three proteins β-TrCP, axin-2, and TCF-1 are thought to be a part of a negative feedback loop to regulate β-catenin/TCF4 transcription (40,43,58). Also noteworthy is EphB/Epnrin-B which compartmentalizes tumors thus suppressing cancer progression, in colon cancer EphB expression is silenced even though it is upregulated by β-catenin (59)

There is some evidence in colon cancer tumors without Smad4 mutation that BMP4 promotes terminal differentiation, apoptosis, and chemosensitization (60). Upon inhibition of β-catenin/TCF4 transcription Hath1 increases, it was found that upon Hath1 increase in colon cancer lines anchorage-independent growth was suppressed,

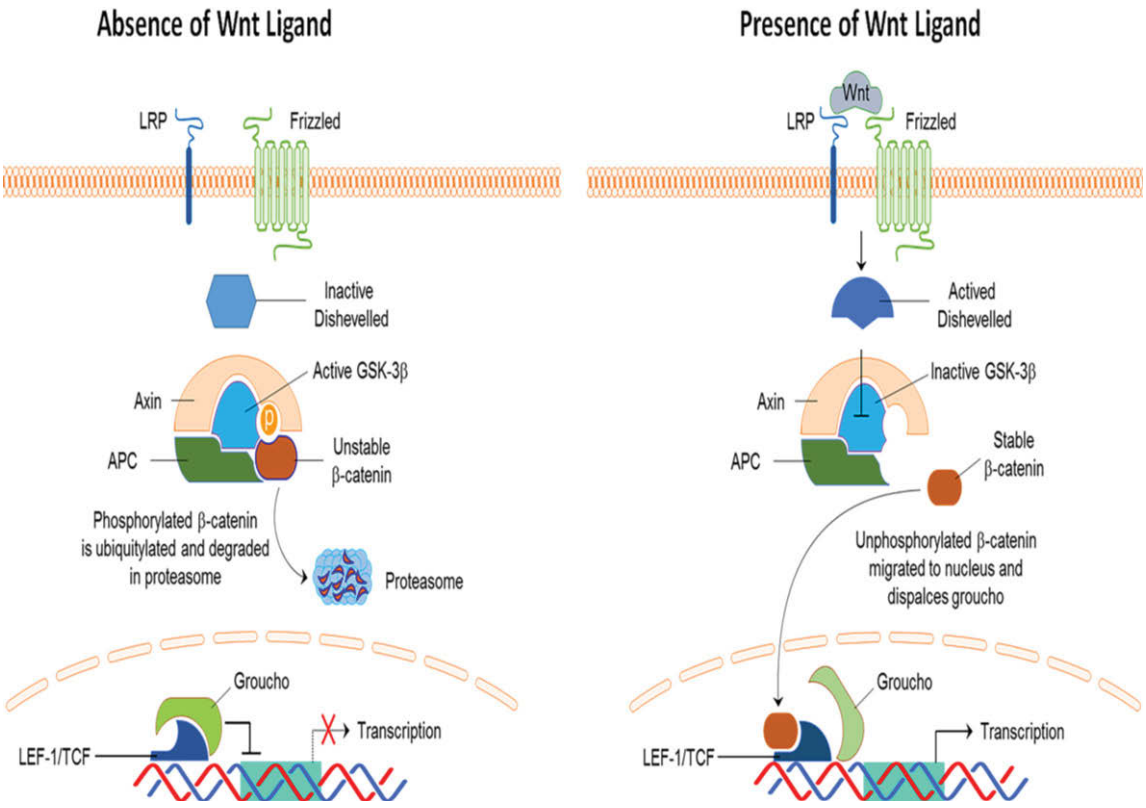

Figure 1-1. Wnt/β-catenin signaling pathway
Original picture made using Motifolio software.

Table 1-3. β-catenin/TCF transcription targets in colon cancer

Target	Function
c-Myc	pro-growth
cyclin-D1	pro-growth
c-Jun	pro-growth
fra-1	pro-growth
uPAR	invasive growth/metastasis formation
PPARdelta	anti-apoptotic
MMP-7	invasive growth/metastasis formation
Axin-2	Canonical Wnt suppressor
TCF-1	Canonical Wnt suppressor
βTrCP	Canonical Wnt suppressor
Nr-Cam	pro-growth/pro cell motility
ITF-2	pro-growth/anti-apoptotic
Gastrin	pro-growth
CD44	pro-cell motility/anti-apoptotic
EphB/Ephrin-B	Suppress progression
BMP-4	May promote terminal differentiation
claudin-1	anti-anoikis
Survivin	anti-apoptotic

proliferation reduced, and reduced xenograft growth in athymic nude mice (61). Upon Wnt activation the GSK3-β destruction complex is inhibited leading to stabilized β-catenin which localizes to the nucleus (62).

β-catenin Shuttling

β-catenin is redistributed via APC and axin shuttling from the nucleus to the cytoplasm. Whereas TCF4 and BCL9 shuttles β-catenin in the opposite direction (63,64). Both truncated and full length APC has been shown in colon cancer cell lines to shuttle β-catenin through the interaction with CRM1/exportin receptor (65). This is an important mechanism for regulation of β-catenin. Whereas, in a normal cell these four proteins simply help retain β-catenin in the original compartment (64).

β-catenin/TCF4 Transcription Repression

APC has been shown to inhibit β-catenin/TCF4 transcription through its direct interaction with βTrCP, CtBP, TLE-1, and HDAC1 (27). In the nucleus of normal colon epithelium APC, ctBP, and βTrCP transiently bind c-Myc enhancer; this is followed by the stable binding of TLE-1 and HDAC1 inhibiting transcription of c-Myc which is a target of β-catenin/TCF transcription (66). Truncated APC has been shown to be unable to bind ctBP and thus unable to participate in this transcriptional regulatory pathway (66).

Prostate Cancer

Prostate cancer is the most prevalent non-epithelial cancer and second leading cause of death among American men in the United States. Metastatic prostate cancer accounts for the majority of cancer-related deaths in males worldwide (1).

Prostate Cancer Statistics

Prostate Cancer Facts and Figures

According to key statistics from the American Cancer Society, 180,890 new prostate cancer cases will be diagnosed within the year 2016, and of those cases approximately 26,120 men will die (1). Majority of survivors of prostate cancer are men above the age of 70 years while less than 1% survivors are under the age of 50 years (67). More than 60% of the cases of prostate cancer worldwide are diagnosed in Developed countries with highest in North and Western Europe and North America with lowest incidence of prostate cancer being in Asia (68). Much of this variation is attributed to the use of Prostate Specific Antigen (PSA) as a marker for diagnosis of prostate cancer.

Prostate Cancer Causes and Risks

PSA testing is no longer used to determine the risk of prostate cancer given the chance of over diagnosis (69). There are many factors contributing to the risk of prostate cancer such as age, race/ethnicity, obesity, family history and genetic mutations.

Incidence of prostate cancer is higher in African American (AA) men than in Caucasian American (CA) men. Prostate Cancer is a critical health problem for men in the United States, including AA population. Recent reports calculated the age-adjusted annual cancer incidence rates from 1975 through 2012 for the Surveillance, Epidemiology and End Results (SEER) areas showed that prostate cancer has become the leading cause of cancer-related deaths among AA men. Clinical reports also suggest that a high proportion of prostate cancer cases in AA are being diagnosed at an advanced stage, when treatment is far less effective and hence have lower cure rates and higher treatment-related morbidities (70). While regular screening can reduce the incidence and mortality rate of prostate cancer, data shows that AA men are experiencing an increasing incidence of prostate cancer. Metastatic prostate cancer in AA men is associated with a 5-yr survival rate of only 28%, compared to 100% in patients with localized or regional disease (70). The underlying cause of high amount of risk in AA descent population is still unknown but genetic mutations may be a factor leading to high susceptibility of prostate cancer in African descent population (71).

Obesity has been associated with risk of prostate cancer mortality (72,73). Obesity has been linked to more aggressive prostate cancer (74). Cohort studies have shown that higher Body Mass Index (BMI) is linked to poor outcome in high risk prostate cancer mortality in obese patients as compared to non-obese healthy adults(75,76). BMI is differently correlated with different age group for the risk of prostate cancer. For early adulthood, higher BMI is not linked to prostate cancer risk but for middle aged and older men, higher BMI is inversely correlated with prostate cancer risk (77). Other components associated with obesity such as high cholesterol is also positively correlated with higher risk of prostate cancer in men with obesity, hypertension and diabetes(78). The underlying correlation between higher BMI and aggressive prostate cancer needs to be further evaluated.

High risk prostate cancer patients have higher DNA repair mutations as compared to low risk prostate cancer patients with higher germline mutations in metastatic, castration resistant prostate cancer patients (79). Homozygous allelic loss or mutation of Breast Cancer Susceptibility gene 2 (BRCA2) is most commonly found in metastatic prostate cancer patients (80). Along with germline mutation, other somatic mutations with higher risk of prostate cancer have been found in other DNA repair genes such as Breast Cancer Susceptibility gene 1 (BRCA1), Ataxia telangiectasia mutated (ATM), and Checkpoint Kinase 2 (CHEK2) genes (79). These mutations indicate that germline and somatic mutations are positively correlates with higher risk of prostate cancer.

Current Therapies for Prostate Cancer

There are currently different treatment options available for prostate cancer treatment. Here we have reviewed some of those treatment options:

Surgery

Surgery remains the main treatment option to cure prostate cancer. Most common type of surgery is radical prostatectomy (81). There are four different types of radical prostatectomy. These are Retropubic, Laparoscopic, Robotic surgery and Perineal. Based on the type of cancer and risk factor involved one or the other type of radical prostatectomy is recommended. A cut is made just below the belly button to the pubic bone in case of Retropubic prostatectomy. In case of Laparoscopic prostatectomy, a several small cuts are made and a laparoscope (video camera) is put inside the cut. When the laparoscopic surgery is performed using robot arms then it is called Robotic surgery. A smaller cut than retropubic surgery is made between the anus and scrotum. In this procedure surgeon removes the seminal vesicles along with the prostate gland and surrounding tissues.

Radiation Therapy

Radiation therapy involves the use of high energy particles to kill the cancer cells. This procedure is generally used if the cancer is localized (82) and low grade or with hormone therapy if the cancer has spread outside of prostate gland (83). Two different types of Radiation therapy used are Brachytherapy and external beam radiation.

Brachytherapy is a form of sealed radiotherapy where radiation source is placed inside or next to the target area through either intracavitary, intraluminal or interstitial route (84). The advantage of brachytherapy over external beam radiation is that unlike external beam radiation it doesn't affect normal tissues and only targets cancer cells because the radiation source is enclosed in a small seed and placed in prostate gland.

External beam radiation is a technique where the beams of radiation are focused on one area from outside of the body. Since the radiation effects large parts of the body it is not specific for cancer cells and equally effects the normal tissues too.

Hormone Therapy

Hormone therapy or androgen deprivation therapy (ADT) as it is commonly known is a standard treatment option for advanced and recurrent prostate cancer where the hormones required for the cancer cells to grow is gradually depleted (85). Cancer cells are hormone responsive and dependent on these hormones for growth and proliferation. Lowering of these male hormones or all together stopping the cells from using these hormones shunts their growth or the cells grow very slowly.

Taxane Based Chemotherapeutic Drugs

Paclitaxel (PTX) is another taxane based chemotherapeutic drug widely used for prostate cancer treatment. PTX is an alkaloid derived from pacific yew tree and it functions predominantly as a microtubule stabilizer by binding to Taxol Binding Domain (TBD) of microtubule and leading to formation of excessive spindle formation and dysfunctional chromosome segregation (86,87).

Docetaxel (DTX) was among the first chemotherapeutic drug approved by Food and Drug Administration (FDA) for metastatic castration-resistant prostate cancer. It became first line of chemotherapeutic drug for treatment of advanced and metastatic prostate cancer drug since FDA approved it in 2004. DTX (chemical formula, $C_{43}H_{53}NO_{14}$ and M.W. 807.9 g mol^{-1}) is a well-established water insoluble anti-mitotic chemotherapeutic agent but it is readily dissolved in 0.1N hydrochloric acid, chloroform, ethanol and methanol. Because of its hydrophobic nature, its transportation inside the cell occurs with the help of plasma proteins such as lipoproteins, albumin and α1 acid glycoprotein (88). Once it is internalized, hydroxylation occurs at the methyl group of the *tert*-butyl group at the C_{13} side chain which is further oxidized and converted into a cyclical form in animals and humans (89,90). This cyclic form of docetaxel is responsible for binding to the microtubule and stabilizing the microtubule structure. Such microtubule polymer hyperstabilization ultimately leads to G_2M phase cell cycle arrest and cell death (91). Metabolism of docetaxel occurs in liver and the cytochrome P450 member, CYP3A4, is a major enzyme responsible for its breakdown (92).

Cabazitaxel (CBZ) is newer class of taxane based chemotherapeutic drug which is nowadays predominantly used as a chemotherapeutic drug for metastatic castration resistant prostate cancer in patients who progressed despite being on hormone and DTX therapy (93). CBZ also binds to the TBD of microtubule promoting its assembly but inhibiting its dissembly leading to hyperstabilization of the microtubule which inhibits mitotic functions (93).

Problems with Taxane Based Therapy

Prostate cancer at the beginning stage is androgen receptor (AR) sensitive and it can be treated with either an androgen-receptor antagonist or chemical castration but as the cancer progresses the majority become androgen-resistant; response to these treatments is poor, leading to high rates of mortality and morbidity (94). Hormone therapy has been frequently used to treat advanced stage prostate cancer (95) and this therapy also works efficiently on androgen sensitive prostate cancer. After a certain period, most of the prostate cancer cells develops resistance to hormone treatment and become androgen independent. Resistance of the cells toward DTX is one of the major challenge in prostate cancer therapy. Newer chemotherapeutic drugs developed to treat docetaxel resistant patients carry significant hematological toxicities that may outweigh their benefits.

Mechanism of DTX Resistance

Docetaxel suppresses AR nuclear translocation through microtubule bundling, leading to cytoplasmic accumulation of the AR. Although tubulin mutations at the taxane binding site may account for clinical taxane resistance including paclitaxel, it does not affect the binding of docetaxel or its inhibition of nuclear AR localization, even though the binding site is shared. This phenomenon is largely due to different binding modes of docetaxel and paclitaxel such that mutation may affect the binding of one but not the other (96-98). Subsequent gene alteration rendering AR trafficking independent of microtubule control leads to docetaxel resistance (98). Furthermore, docetaxel resistance in prostate cancer cells can develop due to increased drug efflux, which lowers the drug concentration inside the cell. Docetaxel resistance in part is due to increased expression of an ATP-binding cassette (ABC) transporter, P-glycoprotein (P-gp), the product of the *MDR1*/*ABCB1* gene (99). P-glycoprotein is a broad spectrum multidrug efflux pump which binds to the hydrophobic substrate through its transmembrane domain and ATP hydrolysis causes conformational change in the transporter leading to release of the drug to the outer leaflet or the extracellular space (100). Drug resistance can also be developed due to increased cellular metabolism of drug detoxifying proteins, such as glutathione-S-transferase, or alterations in β-tubulin isotypes with different kinetics of microtubule formation (101). Solid tumors are heterogeneous in vasculature and increase interstitial fluid pressure (IFP) due to higher vascular permeability and absence of a lymphatic system. In addition, solid tumors with an acidic environment and a lack of oxygen also contribute to the drug resistance.

In addition to activation of the AR and overexpression of ABC or P-gp transporters that account for increased drug efflux, other drug resistance mechanisms include hypoxia, increased IFP, mutation of β-tubulin, overexpression of βIII-tubulin/MAP, and activated RTK, EGFR, IGFR-1, AKT, and Erk1/2 **(Figure 1-2).** Importantly, altered proliferative and anti-apoptotic mechanisms, aberrant angiogenesis and a favorable tumor microenvironment with expression of ECM endothelin receptor A, also contribute to the drug resistance **(Figure 1-2).**

Key Metastatic and Chemo-resistance Signaling Pathways

E-cadherin/N-cadherin and EMT Signaling

Epithelial to mesenchymal transition (EMT) is a phenomenon where de-differentiation of epithelial cells to mesenchymal cells occurs leading to changes in cell plasticity (102). Epithelial-cadherin or E-cadherin is a calcium dependent cell-cell adhesion molecule which plays a pivotal role in maintaining epithelial characteristics of the cell (103). Neural-cadherin or N-cadherin is a calcium dependent cell adhesion molecule which is marker for mesenchymal phenotype (104). These cadherins play an important role in embryogenesis particularly neural crest migration (105,106). These cadherins have also been associated with EMT. Loss of Epithelial markers such as E-cadherin and gain of mesenchymal markers such as N-cadherin, Snail, Slug, Vimentin, ZEB1, ZEB2 and

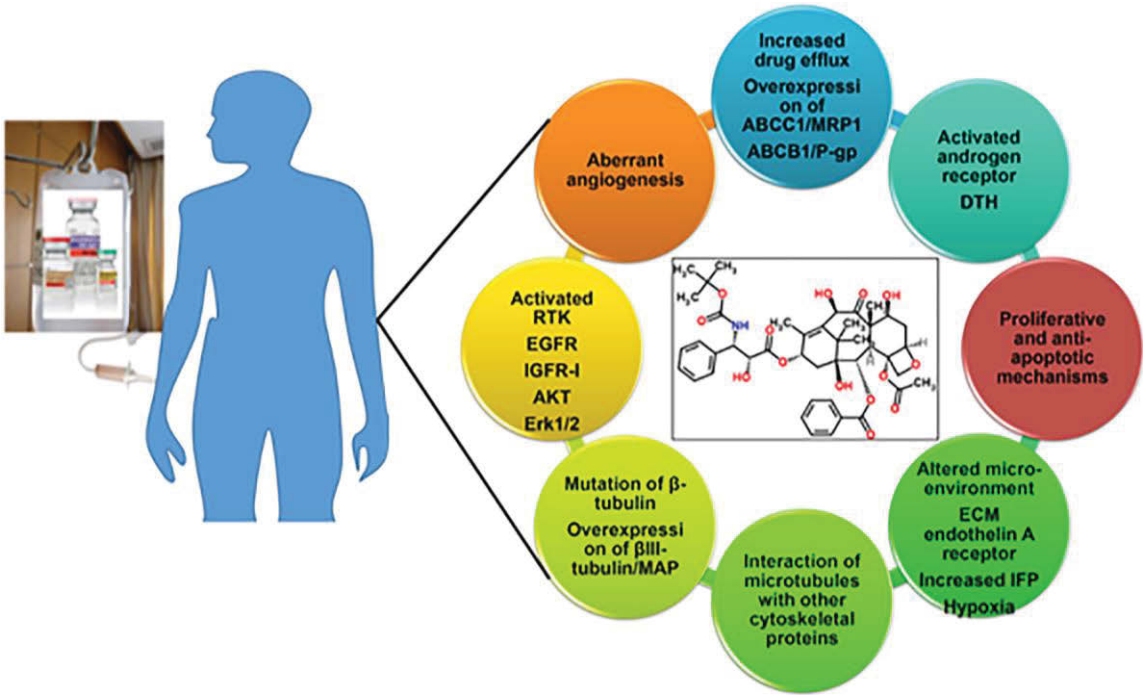

Figure 1-2. ***De novo*** **and acquired resistance mechanisms that mediate docetaxel therapy in many prostate cancer cells and patients**
Original figure was made by Dr. Murali M. Yallapu.

---

*Reprinted with permission. Ganju, A; Yallapu, MM; Khan, S; Behrman, SW; Chauhan, SC; Jaggi M. Nanoways to overcome docetaxel resistance in prostate cancer. *Drug resistance updates*. 2014;17(1-2):13-23.

TWIST characterizes the process of EMT leading to cell proliferation, invasion and metastasis (102). Inappropriate expression of non-epithelial cadherins such as N-cadherin by epithelial cells has been suggested to play a role in promoting invasion and metastasis. This inappropriate expression of cadherin is referred to as "Cadherin Switching" (107). β-catenin is one of the many master regulators of process of EMT (108). β-catenin along with its downstream signaling molecules leads to loss of epithelial markers and gain of mesenchymal markers wherein, cells become more motile and invade surrounding organs (108) **(Figure 1-3)**.

β-catenin/AR Signaling Pathways

Activation of Wnt signaling leads to inhibition of β-catenin degradation, resulting in the accumulation of free cytoplasmic β-catenin. This translocates to the nucleus, in conjunction with TCF4, upregulates the production of various oncogenic signaling components like c-Myc, cyclin-D1, MMP-7, and AR. (109). AR mediated signaling plays a critical role in the development and progression of prostate cancer. Gene amplification and mutations in AR are frequently observed in recurrent prostate cancer, which may account for the hypersensitivity of AR to low castrate levels of androgens and altered ligand specificity. Several mechanisms are proposed for androgen-independent (AI)activation of AR in prostate cancer (1,110-114). One of the mechanisms for androgen-independent activation of AR is through β-catenin (115). We have also reported that β-catenin enhances transactivation of AR in prostate cancer cell (109). Accumulation of nuclear β-catenin and AR, has been reported in advanced stage metastatic prostate cancer (116,117). It has been reported that expression of β-catenin and AR correlates with an increasing prostate tumor grade (117-119) and higher nuclear staining was observed in high Gleason grade metastatic Prostate Cancer, suggesting an involvement of β-catenin and AR signaling pathways in prostate cancer metastasis. We have shown that activation of PKD1 by Bryostatin-1-NPs inhibits prostate cancer cell proliferation through repression of the β- catenin and AR (120). Thus, the strategic suppression of β-catenin/AR signaling pathways would be clinically important for the suppression of prostate cancer metastasis.

Metastasis Associated Protein 1 (MTA1) Signaling

MTA1 is an integral member of the nucleosome remodeling and histone deacetylase (NuRD) complex and multifunctional DNA damage response protein (121). MTA1 is up-regulated in a wide range of cancers and plays an important role in progression and metastasis. MTA1 is highly overexpressed in prostate cancer (122). It has been shown that nuclear expression of MTA1 correlates with progression and metastasis of prostate cancer (123) and up-regulation of MTA1 increases EMT (124). MTA1 is the founding member of the MTA1 family comprised of six different gene products: MTA1, MTA1s, MTA1-ZG29p, MTA2, MTA3 and MTA3L that arise from three different genes (125-129). Six 3 is an important repressor of Wnt signaling (130). Wnt signaling activation causes inhibition of GSK-3β activity and increases nuclear localization of β-catenin, which in turn leads to further up-regulation of MTA1. It has also been reported that up-regulation of MTA1 increases EMT (124).

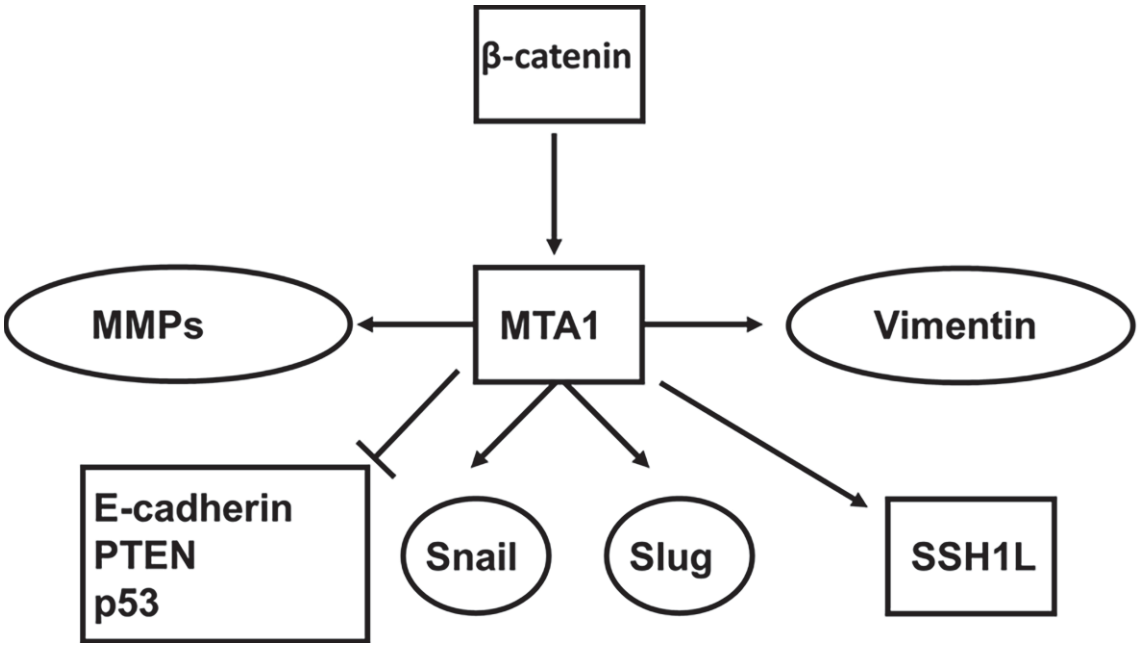

Figure 1-3. Schematic diagram depicting β-catenin mediated regulation EMT signaling

Protein Kinase D1 (PKD1) Signaling

PKD1 is a novel serine threonine protein kinase, a member of PKD family. PKD1 is expressed in various organs of a human body but its expression is found to be the highest in normal prostate cells **(Figure 1-4)**. Because of several distinct structural features of PKD1, including substrate and inhibitor specificity, presence of pleckstrin homology domain, structural identity of the kinase domain among others, it has been assigned to a new protein kinase subfamily called Protein Kinase D (PKD) **(Figure 1-5)** (131). The PKD consists of alanine and proline rich (AP), cysteine-rich (C1a and C1b), pleckstrin homology (PH) and kinase domains (KD), and acidic-rich regions (AC). PKD remains inactive in cytosol via auto-inhibition of catalytic activity by PH domain. DAG binds to C1b domain and induces PKD translocation to plasma membrane, where it is phosphorylated/activated by PKCs. The catalytic domain of PKDs (including PKD1) is distantly related to Calcium Calmodulin-Dependent Kinases (132). Thus, PKD1 combines features of PKC family and CaM Kinase, placing it in a unique position for modulation of many distinct cellular functions. In the recent years, this protein family has been implicated in several characteristics and significant cellular functions including cell survival, cell proliferation, cellular communication, intracellular signaling such as p42, ERK, MAP kinase, and growth factor-induced ERK activation, trans-Golgi organization, vesicle trafficking, oxidative stress signaling, apoptosis and actin remodeling. Its abnormal expression/functions have been associated with cancers (133).

PKD1 has emerged as an important modulator of several kinase signal transduction pathways (133). PKD1 functions as regulator of signal trafficking by growth-factor receptors and also regulates cell shape and tumor cell invasion (133). It has been shown that PKD1 interacts with E-cadherin, whereby PKD1 mediates E-cadherin phosphorylation, and that over-expression of PKD1 is capable of increasing cell aggregation and reducing motility in prostate cancer cells (134).

Both E-cadherin and cytoplasmic β-catenin are down regulated in human prostate cancer, and significantly correlate with increasing Gleason grade. Both these proteins play a significant role in regulation of EMT. PKD1 has been shown to directly interact with β-catenin, and regulate β-catenin subcellular localization (120). In addition, PKD1 mediates phosphorylation and regulation of androgen receptors, establishing a significant role for PKD1 in prostate cancer (109). Despite all of the evidence of PKD1's tumor suppressive role, another research group using a chemical inhibitor approach has claimed that PKD isoforms (PKD1 and PKD3) exhibit an oncogenic function in prostate cancer (135). However, based on the lack of specificity of these chemical inhibitors and their cross-reactivity with other kinases (PKD3 has been recognized as oncogenic) it is not reasonable to claim that PKD1 possesses an oncogenic function.

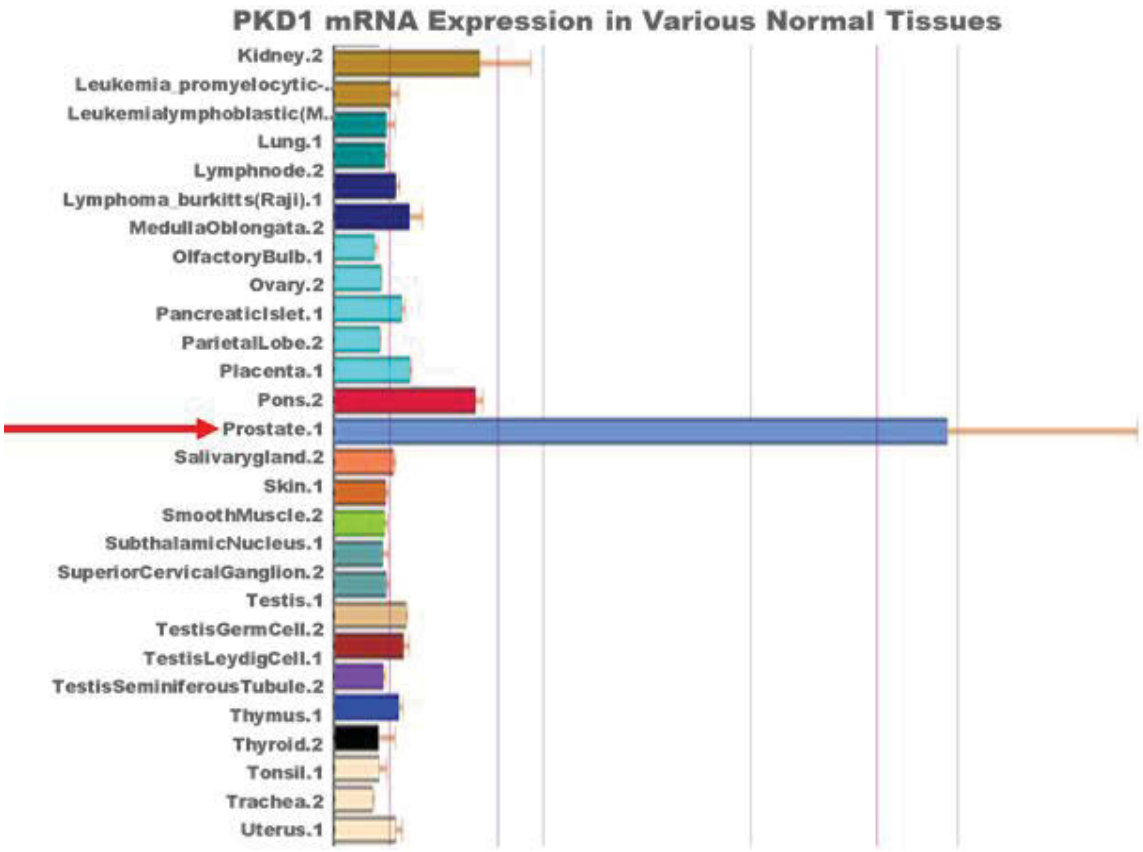

Figure 1-4. PKD1 is highly expressed in prostate compared to any other organs, signifies its crucial role in normal prostate functioning

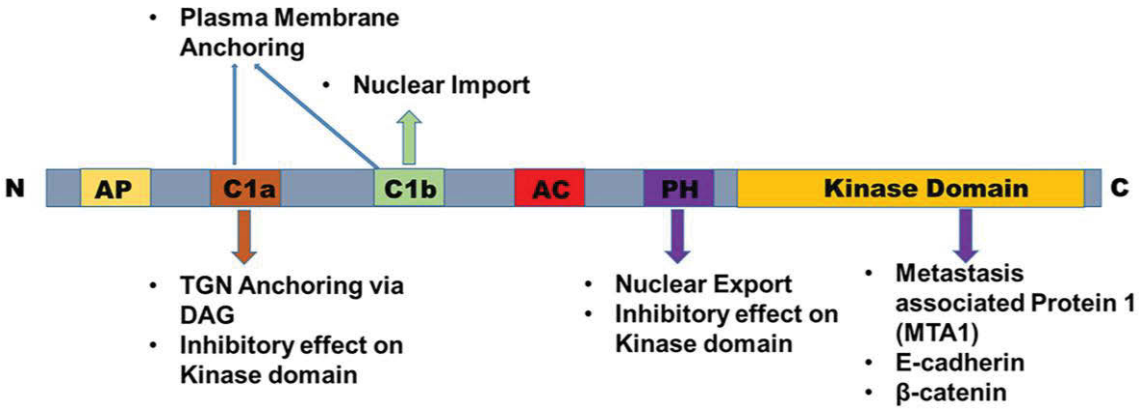

Figure 1-5. PKD1 structure, activation and domain specific functions
AP- alanine proline rich region, C1a and C1b -cysteine rich region, AC- acidic domain, PH- pleckstrin homology domain.

PKD1 Domains and Functions

The domains of PKD1 are vital in the subcellular localization and therefore function of the protein (136).

Alanine Proline (AP)

The alanine proline (AP) rich domain is the least well characterize of all the domains. Little is known about its effects on PKD1 function. It is a hydrophobic region which may be utilized for the correct conformation of the protein structure or important to the stability of PKD1 (137). It also could have a role in binding to lipids thus affecting PKD1's function and localization (138). Another possibility is that it could function as a docking motif with the kinase to help with specificity of the substrates (139).

Cysteine Rich Domain a and b (C1a and C1b)

C1a and C1b are cysteine rich zinc fingers that both bind DAG and phorbol esters. DAG associated with the membrane binds and activates PKC leading to PKD1 recruitment via the C1a and C1b domains (140). C1a quickly and reversibly translocates to the plasma membrane, but C1b does so slowly and persistently allowing for PKD1 to stay activated and attached to the plasma membrane (141). Under oxidative stress the mitochondria rapidly releases DAG (which the mitochondria have a store of) which recruits PKD1 through its C1a and C1b domains to the mitochondria (142). It was found that the deletion of both C1a and C1b, while activating the protein due to removal of inhibition, also removed the ability for PKD1 to respond to Reactive Oxygen Species (ROS) (142). C1a is necessary for PKD1 localization to the golgi and C1b is necessary for nuclear import of PKD1 (143,144). PKD1 is important for membrane fission at the trans golgi network (TGN) and it is recruited there via interaction of C1a to DAG and C1b to Arf1 which is involved in vessiculation of the TGN (145,146).

Acidic Rich Region

The acidic domain (AC) in recent years has been speculated to be a target for activation of the protein via mechanisms that do not involve the activation via phosphorylation (147). It was later shown to be correct, as dextran suflate disrupts the intramolecular interaction between the acidic region and a basic region in the protein, reducing inhibition (147). It has been postulated that other post translational modifications or protein-protein interactions may have a function in activating PKD1 without the activation loop being phosphorylated (148).

Pleckstrin Homology (PH)

Deletion of the entire PH domain (amino acids 429-557) leads to full activation of PKD1 (149). It was also found that even just a partial deletion or single amino acid substitutions within the domain such as R447C and W538A was adequate to activate PKD1 to some degree (149). Other mechanisms for PKD1 activation are through the

interaction of nonreceptor tyrosine kinases C-Abl and Src. C-Abl phosphorylates PKD1 at tyr 463 in the PH domain, then Src phosphorylates at tyr 95. This creates a docking site for the C2 domain of PKCδ which then phosphorylates PKD1 activation loop Ser 738 and Ser 742 (150). Other activation pathways involve the Gβγ site of the PH domain which will be further elaborated in the next section. The PH domain does not seem to interact with any specific lipids (141). Export of PKD1 from the nucleus requires the PH domain (143).

PKD1 Activation Mechanisms

There are five phosphorylation sites on PKD1, two (Ser203 and Ser255) are in the regulatory domain, two (Ser748 and Ser744) are in the catalytic domain, one at c terminus (Ser916)(151). Ser744 and Ser748 are phosphorylated by PKC and are a part of the activation loop of PKD1. Ser 916 is auto-phosphorylated and does not correlate to PKD1 activity, however Ser 916 phosphorylation is necessary for the auto-phosphorylation of Ser 748 which does correlate with PKD1 activity(152). Ser203 can be auto-phosphorylated which may regulate its interaction with 14-3-3 proteins(151,153). Ser 255 is a phosphorylation site targeted by PKC and phorbol esters. Phosphorylated PKD1 kinase activity can be attenuated by 14-3-3 binding at the C1a domain which alters localization of PKD1(136).

PKD1 activation consists of three main pathways: Phospholipase C (PLC), Gβγ, and proteolytic cleavage(154). PLC mediates hydrolysis of phosphatidylinositol 4,5-bisphosphate, producing Inositol (1,4,5) P_3 and DAG. Inositol (1,4,5)P_3 binds a ligand-gated calcium ion channel, releasing calcium and DAG activates PKC(155). DAG recruits PKD1 via C1b domain, PKC phosphorylates PKD1 at Ser-744 and Ser-748 (activation loop), phosphorylation of activation loop removes PH inhibition of PKD1, culminating in PKD1 being stabilized and active(136,154). Gβγ activates PKD1 through release of PH inhibition with the help of Gβγ –induced phospholipase Cβ/PKC(156). PKD1 is activated after its cleavage by caspase-3 between C1 and PH(150). This cleavage activates PKD1 due the release of the majority of the regulatory region of the protein(157). Another study looked at cleaved PKD1 and showed that without the C1 domain interaction with phosphatidylserine/PMA it cannot reach its maximal activity and thus that its activity overall is inconsequential(158).

PKD1 Function

PKD1 inhibits actin incorporation in actin remodeling, inhibiting actin-mediated motility through phosphorylation of SSH1L(159). PKD1 further inhibits cell migration through phosphorylation of RIN1 affecting its association with Abl kinase(160). PKD1 inhibits EMT through phosphorylation of Snail leading to its export from the nucleus via 14-3-3σ binding(161). PKD1 phosphorylates S400 of Par-1b which leads to 14-3-3 proteins binding Par-1b, sequestering the protein at the cytoplasm thus regulating cell polarity(162). PKD1 and kinase dead PKD1 were found in prostate cancer to inhibit

androgen receptor (AR) mediated growth through repressing AR transcription. Most notable, was this was kinase independent(163). In breast cancer, PKD1 was shown to inhibit invasion through decreasing MMP-2, MMP-7, MMP-9, MMP-10, MMP-11, MMP-13, MMP-14, and MMP-15 expression; which is thought to be through interaction with HDAC's(164).

PKD1 phosphorylates E-Cadherin in prostate cancer leading to decreased cellular motility and increased aggregation(165). In prostate cancer, PKD1 was also found to phosphorylate Thr112 and Thr120 of β-catenin. Phosphorylation of Thr120 was found to be important in mediating β-catenin binding to α-catenin and consequently the cytoskeleton. Further, Thr120 phosphorylation leads to β-catenin accumulation in the TGN(166). This appears to play a role in the shuttling of free β-catenin to the E-cadherin-cell adhesion complex(167).

PKD1 can inhibit HDAC's through phosphorylation of HDAC5/7 which leads to 14-3-3 protein binding and nuclear export of HDAC5/7 leading to angiogenic gene expression(140). In response to oxidative stress PKD1 activates NF-κB through its kinase function(168). PKD1 can also promote DNA synthesis and proliferation through its interaction with Erk and JNK(169).

PKD1 and EMT

Inhibition of PKD1 expression is thought to promote invasion and metastasis thereby upregulating EMT machinery within the cells. Wnt signaling activation causes inhibition of GSK-3β activity and increases nuclear localization of β-catenin, which in turn leads to further up-regulation of MTA1. It has also been reported that up-regulation of MTA1 increases EMT (124). MTA1 is an integral member of the nucleosome remodeling and histone deacetylase (NuRD) complex and multifunctional DNA damage response protein (121). MTA1 is up-regulated in a wide range of cancers and plays an important role in tumorigenesis, tumor invasion and metastasis. MTA1 is highly expressed in prostate cancer (122). It has been shown that nuclear expression of MTA1 correlates with disease progression and shows highest expression levels in metastatic prostate cancer (123). Since, PKD1 regulates β-catenin expression, therefore it may also inhibit MTA1 which is regulated by β-catenin signaling. Thus, strategic activation/overexpression of PKD1 may inhibit metastasis by inhibiting MTA1 and EMT signaling.

PKD1 Modulators

PKD1 modulators are class of drug molecules which regulate PKD activity. PKD activity can be regulated many different molecules such as TPA, bombesin etc (170,171). Drug molecules which can lead to upregulation of PKD1 activity could potentially be a promising therapeutic modality for treatment of metastatic cancers. Herein, we have discussed two such molecules:

Bryostatin-1

Bryostatin-1 is a natural marine derived macrocyclic lactone (**Figure 1-6**) which has shown anti-neoplastic activity and has been used in clinical trial with limited success (120). Bryostatin-1 has many modes of action such as apoptosis modulation, T cell activation, neutrophil and monocyte activation, etc. It is also a very potent activator of PKD1 (120). Bryostatin-1 is known to modulate β-catenin subcellular localization by activation PKD1 (120)**.** Bryostatin-1 has been used synergistically with other anti-cancer drugs. It has been used in prostate cancer, acute lymphoblastic leukemia, ovarian cancer and non-small cell lung cancer (172-175). Bryostatin-1 is known to inhibit the effects of TPA and is involved in apoptosis modulation, interaction with MDR-1, T Cell activation, neutrophil/monocyte activation (120).

Ormeloxifene

Ormeloxifene, also known as Centchroman (**Figure 1-7**), is a non-hormonal, non-steroidal synthetic molecule (176,177). Recently, its anti-cancer activity has been reported against advanced breast cancer (178) and head and neck squamous cell carcinoma (HNSCC) (179). Additionally, our recent studies show a potent anti-cancer activity of ormeloxifene (ORM) in various cancer cell lines such as pancreatic and ovarian cancer cell lines (180-182). In our study, we observed that ORM modulates PKD1 expression and inhibits mesenchymal markers such as N-cadherin, Snail, Slug, Vimentin and MMPs such as MMP-2 and 9 to inhibit prostate cancer metastasis. Moreover, ORM is reported to have an excellent therapeutic index and is safe for chronic administration (183). Therefore, ORM has a great repurposing potential for prostate cancer chemoprevention/treatment. Successful examples of drugs repurposing are anti-diabetic drug metformin and the birth control hormone medroxyprogesterone acetate.

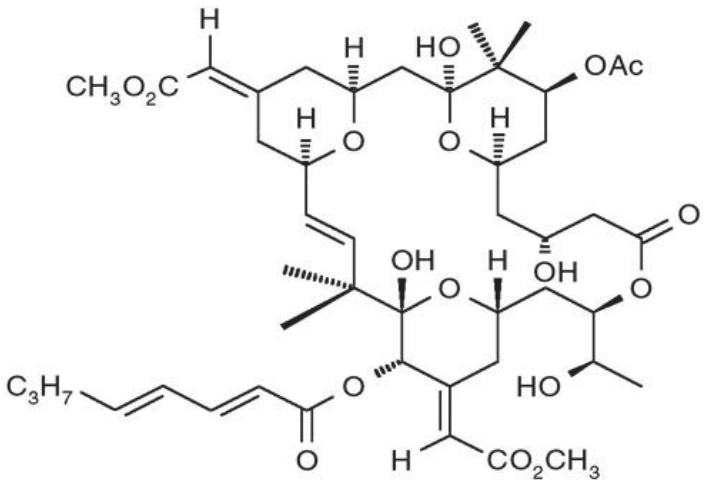

Figure 1-6. **Chemical structure of Bryostatin-1**

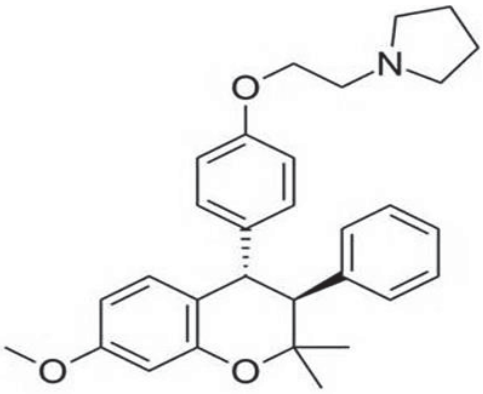

Figure 1-7. Chemical structure of ormeloxifene (MW 490.50)

CHAPTER 2. PROTEIN KINASE D1 ATTENUATES TUMORIGENESIS IN COLON CANCER BY MODULATING BETA-CATENIN/T CELL FACTOR ACTIVITY*

Introduction

Colorectal cancer is the third most commonly diagnosed cancer and the second leading cause of cancer death in the US with approximately 51,000 deaths per year (184). It often begins as a benign polyp in the colon, which over time may become cancerous. The deregulation of the β-catenin signaling pathway due to mutations in the *APC-Axin* or *β-catenin* genes is correlated with over 80% of colon cancer (185). Therefore, understanding the expression, localization and regulation of β-catenin protein and modulation of β-catenin signaling pathway function is critical for developing novel strategies for treatment and/or preventing of colon cancer.

Studies have identified that inhibitors of the PTEN/Akt/GSK3β signaling cascade and regulation of /β-catenin act as potential agents to effectively target cancer stem cells and tumorigenic cancer cells (186,187). β-catenin is a highly conserved, bi-functional protein that functions as a transcription factor in the Wnt signaling pathway to regulate cell proliferation and differentiation (188,189). In addition, at the cell membrane, it plays a key role in regulating E-cadherin mediated cell-cell adhesion by binding to and anchoring E-cadherin to the actin cytoskeleton through the adaptor protein, α-catenin. In the absence of Wnt-signaling, β-catenin is primarily bound to cadherin and N-terminus of free cytosolic β-catenin is targeted for phosphorylation, ubiquitination and degradation by APC-Axin-GSK3β-CK1 complex. β-catenin is also phosphorylated on some sites by the diverse kinases PKA, AKT, and JNK2 that promotes β-catenin activity and its nuclear translocation (190). Mutations in APC, Axin, or these N-terminal phosphorylation sites of β-catenin are found in multiple types of human cancers, where these mutations elevate β-catenin posttranscriptional stability, signaling (191) and formation of nuclear β-catenin/TCF complexes (192). In these scenarios, β-catenin localizes to the nucleus and enhances the transcription of proto-oncogenes such as c-Myc, c-Jun and Cyclin D1, resulting in initiation and progression of cancer (188,189).

Protein Kinase D1 (PKD1) is a ubiquitously expressed serine/threonine kinase that plays a key role in several signal-transduction pathways (133,193,194) through regulatory domains that are homologous to the PKC family and the presence of functional kinase domain with substrate specificity homologous to those of the CaMK family (193). Therefore, PKD1 has been found to modulate a number of cellular processes including cell proliferation, cellular motility, invasion, aggregation and

---

*Modified with permission. Sundram, V; Ganju, A; Hughes, JE; Khan, S; Chauhan, SC; Jaggi, M. Protein kinase D1 attenuates tumorigenesis in colon cancer by modulating beta-catenin/T cell factor activity. *Oncotarget* 2014;5(16):6867-84.

epithelial-mesenchymal transition (120,134,195-201). Downregulation of PKD1 has been documented in breast and prostate cancers (193,195,201,202). In breast cancer, epigenetic silencing of *PRKD1* gene promoter has been reported to directly correlate with the loss of PKD1 expression and the invasive potential of breast tumors or cells (202). Suppression of PKD1 expression was found to be associated with enhanced cellular invasion *via* modulation of multiple matrix metalloproteinases (MMPs) in breast cancer cells (195). Previous work from our group has implicated an important role for PKD1 in prostate cancer (120,134,201) including modulation of E-cadherin, β-catenin functions, and androgen receptor signaling pathways (109,134,197,203-205). Herein, we have investigated the role of PKD1 in colon cancer. We examined the staining pattern of PKD1 expression in tissue of normal colon and colon cancer and demonstrated that PKD1 co-localized with β-catenin in normal colon tissues. In addition, PKD1 expression was downregulated in colon cancer tissues and this coincides with a corresponding change in the subcellular localization of β-catenin. For *in-vitro* analyses, we used SW480 and SW48 colon cancer cell lines to investigate and evaluate the effect of PKD1 overexpression on cellular characteristics. *In-vitro* and *in-vivo* studies using xenograft mouse model revealed that PKD1 overexpression suppresses cell proliferation, clonogenic potential, enhances cell-cell aggregation and alters the tumor histo-architecture *via* modulation of β-catenin functions in cells.

Methods

Cell Lines and Other Materials

Colon cancer cells SW480 and SW48 were purchased from ATCC (ATCC, Manassas, Virginia). The cell lines LoVo, HT29 and T-84 were kindly provided by Prof. Keith Johnson (University of Nebraska Medical Center, Omaha, Nebraska). These cell lines were propagated in high glucose DMEM media supplemented with glutamine, 100 mM sodium pyruvate, 10% fetal bovine serum (FBS) and 1X antibiotic and antimycotic solution. The media components were purchased from Hyclone (Hyclone Laboratories, South Logan, UT), unless mentioned otherwise. OPTI-MEM reduced serum growth media was purchased from Invitrogen (Life Technologies, Carlsbad, CA). All other chemicals were purchased from Sigma (Sigma-Aldrich, St. Louis, MO) unless mentioned otherwise.

Antibodies

Rabbit polyclonal PKD1 antibody (C-20) and Histone H1 were procured from Santa Cruz Biotechnologies (Santa Cruz, CA). Rabbit monoclonal PKD1, cofilin, phospho-cofilin, Arp3, LIMK, phospho-LIMK and Cyclin D1 were purchased from Cell Signaling Technologies (Danvers, MA). Ki67, CD31, Glut1 and β-actin antibodies were purchased from Sigma-Aldrich. The mouse monoclonal β-catenin antibody is a generous gift of Dr. Keith Johnson (University of Nebraska Medical Center, Omaha, Nebraska),

the use and specificity of which has been previously described (206). The HRP conjugated secondary antibodies were purchased from Promega, (Madison, WI) and fluorescence tagged anti-mouse secondary antibodies were purchased from Jackson ImmunoResearch Laboratories (Westgrove, PA).

Immunohistochemical (IHC) Staining of Tissue Samples

The tissue microarray slides (AccuMax, ISU Abxis Co., Ltd, Seoul, Korea) and the slides from colon cancer xenograft mouse tumor were stained using heat-induced antigen retrieval immunohistochemistry techniques with the Vector ABC kit (Vector Laboratories, Burlingame, CA) or Biocare kit (Biocare Medical, Concord, CA) and analyzed as previously described (207). Briefly, the slides containing the tumor tissues were deparaffinized, rehydrated, treated with 0.3% hydrogen peroxide or peroxidazed solution (Biocare Medical) and processed for antigen retrieval using heat-induced technique. After blocking nonspecific binding with background sniper (Biocare Medical), the tissues were incubated with primary antibodies (PKD1 (1:100), β-catenin (1:100), Ki67 (1:25), CD31 (1:25) or Glut1 (1:100)). The final detection for the expression of the specific protein was carried out by using either fluorescently labeled secondary antibodies (1:150) or chromogenic dyes. For the detection of protein using fluorescent antibodies, the slides were incubated in the dark with fluorescently labelled secondary antibodies (1:150), washed and mounted using Vectamount (Vector Laboratories). For the final detection of protein using chromogenic dyes 3,3′-diaminobenzidine (DAB) or Vulcan red, the samples were processed using MACH 4 Universal HRP Polymer detection kit (Biocare Medical) according to manufacturer's instructions and developed using DAB (DAB substrate kit, Vector Laboratories). These slides were counter-stained using hematoxylin and mounted using Vectamount (Vector Laboratories). The slides stained with fluorescent secondary antibodies were processed for laser scanning confocal microscopy with an Olympus Fluoview FV1000 confocal microscope (Olympus Corporation, Tokyo, Japan), while the chromogenically stained slides were visualized using an Olympus BX 41 Microscope (Olympus Corporation).

Analysis of IHC Samples

Quantitative examination of the TMA samples were independently analyzed by two pathologists at the Sanford School of Medicine and the mean composite score (MCS) was calculated as previously mentioned (208,209). The samples were evaluated for staining intensity on a scale of 0 to 4 (0 for no immunostaining, and 4 for very high staining). In addition, the samples were also analyzed for the extent of staining and expressed as percentage of cancer cells that had stained for the protein of interest. This percentage of stained cells was also scored on the scale of 0 to 4 (0 for less than 5% staining, 1 for 5-25%, 2 for 26-50%, 3 for 51-75% and 4 for >75% positively stained cells). The MCS for each sample was calculated by multiplying the percentage of cancer cells positively stained with the intensity of staining (range of 0-16).

Western Blotting

Actively growing colon cancer cells were used for immunoblot analysis as described earlier (207). Briefly, cells (70-80% confluent) were washed with ice-cold phosphate buffer saline (PBS) and lysed in 2X SDS lysis buffer. Equivalent amounts of protein samples were electrophoretically resolved on 4-20% SDS-PAGE gels, blotted onto PVDF membrane (Bio-Rad Laboratories, Hercules, CA), blocked with 10% bovine serum albumin (BSA; 5 ml for one hour) and probed for various proteins using specific primary antibodies. The western blots were incubated with HRP-labeled secondary antibody and the protein bands were developed using Lumi-Light Plus chemi-luminescent reagent (Roche, Indianapolis, IN).

Immunofluorescence

SW480 or SW48 cells expressing various GFP tagged constructs ($1.5x10^5$) were seeded in a 4-well chamber slides (Thermo Scientific Nunc, Waltham, MA) for 48 h and processed for immunofluorescence as previously described (207). In brief, the cells were fixed in 2% paraformaldehyde (PFA) for 15 min, mounted in Vectashield (Vector Laboratories) and processed for laser scanning confocal microscopy with an Olympus Fluoview FV1000 confocal microscope (Olympus Corporation). In order to detect the localization of β-catenin in these cells, following PFA fixation the cells were permeabilized for 5 min with chilled methanol, incubated with anti-β-catenin primary antibody (1:10) for 1 h, and detected by incubating with Cy3 labeled secondary antibodies for 1 h. The slide was mounted in Vectashield mounting media (Vector Laboratories) and processed for laser confocal microscopy.

Transfection and Generation of Stable Cell Line

The pEGFP vector containing PKD1, GFP-NLS-PKD1, Mem-PKD1-GFP and PKD1-KD (kinase-dead) were kind gift from Drs K.C. Balaji (Wake Forest School of Medicine, Salem, NC) and Cheng Du (University of Massachusetts Medical School, Worcester, MA). Colon cancer cell lines (SW480 or SW48) were transfected with pEGFP vector or pEGFP vector containing PKD1 gene or GFP-NLS-PKD1 gene (PKD1 gene tagged to a nuclear localization signal), or Mem-PKD1-GFP gene (PKD1 gene tagged to a membrane localization signal) or PKD1-KD (PKD1 gene with a point mutation at the 618 residue that renders it kinase dead (PKD1 K618W)) using Lipofectamine2000 (Invitrogen) in a serum free media, as previously described (209). After 6 hours of transfection, the media was replaced with 10% serum containing media. The transfected cells were propagated in the presence of a selection agent (500 µg/mL of G418; Invitrogen) and used for experiments within 2-3 passages following transfection. The SW480 cells were also transfected with pcDNA3.1 or PKD1 gene cloned in pcDNA3.1 vector as mentioned above. In order to isolate SW480 stable cell lines overexpressing PKD1-GFP or control GFP, actively growing SW480 cells (80% confluent) were transfected with PKD1 gene cloned in pEGFP.C1 vector or empty vector using

Lipofectamine2000 (Invitrogen) and propagated in the presence of 500 µg/mL of G418 (Invitrogen) selection agent for the selection of stably transfected cells as previously described (209). A pool of stably transfected SW480 cells overexpressing PKD1-GFP (referred to as SW480-PKD1-GFP) or control SW480 cells stably overexpressing GFP (referred to as SW480-GFP) were enriched for stably transfected cells by subjecting these cells to fluorescence assisted cell sorting (FACS). The enriched pool of cells, maintained under constant G418 selection, were expanded and frozen into multiple aliquots of stock. To maintain authenticity of the stable cell lines, the cells were always maintained in the presence of G418 selection agent and used for 30-35 passages, after which a fresh cell line stock was thawed and used. As wild-type and vector control cells did not show any significant differences, and in order to avoid redundancy, the results are primarily shown for vector control.

Cell Proliferation

Cell proliferation was determined by either using CellTiter-Glo Luminescent cell viability assay (Promega) or by manual counting method. The measurement using the CellTiter-Glo Luminescent cell viability assay was carried out according to manufacturer's instructions. Briefly, $5x10^3$ cells of SW480-GFP or SW480-PKD1-GFP were plated in 96-well plates and incubated for 48h in a humidified incubator at 37°C/5% CO_2. Cell proliferation was assessed by measuring the amount of ATP in the cells using CellTiter-Glo Reagent. The determination of cell proliferation by manual counting method was carried out as previously described (209). Briefly, cells ($2x10^4$) were seeded in 6-well plates in triplicate and after varying periods of time (24, 48, 72, and 96 h) the cells were harvested and manually counted using a hemocytometer.

Anchorage Dependent and Anchorage Independent Colony Formation Assay

Both colony formation assays were performed as described earlier (207,210). To determine the anchorage dependent colony formation, cells ($2x10^3$) were plated in 100mm cell culture dishes for 12 days. The colonies formed were fixed with methanol, stained with hematoxylin and number of visible colonies were manually counted and plotted as previously described (207). The anchorage independent colony formation assay was carried out in 6-well plates as previously described (207). A bottom 0.6% agarose layer was first cast in the plates. Following solidification, the top 0.35% agarose layer containing cells ($4x10^4$) was cast. Following 14 days of incubation in 4 ml media per well, the colonies were either directly imaged or stained with 0.05% crystal violet and imaged using a phase contrast microscope. Average numbers of colonies were counted from five independent areas and plotted.

Aggregation Assay

The aggregation assay was performed as described earlier (207). In brief, actively growing cells were trypsinized (0.01% trypsin-EDTA) and washed with PBS containing 5mM $CaCl_2$. $3x10^6$ cells ($1x10^6$ cells/ml) were resuspended in 15ml polystyrene tubes in DMEM containing 5mM $CaCl_2$, incubated for 7h at 37°C under mild mixing/shaking conditions and imaged for number of aggregates formed using a phase contrast microscope. A second type of aggregation assay was also performed as preciously described (120). Actively growing cells were trypsinized, resuspended at $2x10^4$ cell/ml and 25 µl drops were spotted onto the inner side of a 25 mm petri plate lid. The lid was carefully inverted over the petri plate containing 2ml PBS and incubated for 24h in a humidified incubator at 37°C in the presence of 5% CO_2. The cells were gently resuspended and imaged under microscope for aggregate formation.

Cell Motility Assay

The scratch assay for determining cell motility was performed as previously described (134,211). Briefly, cells ($1x10^6$cells/plate) were cultured in 35mm plates until confluent and using the sharp side of a 20µl sterile tip, the confluent cell culture was scratched to generate a wound/gap and incubated at 37°C in the presence of 5% CO_2. The scratch was periodically imaged using an EVOS microscope (Advanced Microscope Group, Bothell, WA) at varying time intervals. A second assay to determine cellular motility using the agarose beads (agarose bead motility assay) was carried out as described earlier (209). Equal volumes of cells ($1x10^7$ cells/ml) and 0.7% low melting agarose were mixed and 25 µl drops were spotted onto 6-well plates pretreated with Fibrinonectin (15µg/ml) and BSA (10µg/ml). Following gelling, the beads were incubated in 2ml media at 37°C and photographed at regular time intervals using a phase contrast microscope. The average number of motile cells that had escaped out of each bead was counted and plotted.

β-catenin/TCF Luciferase Reporter Assay

The reporter constructs were a generous gift from Dr. R. Moon (University of Washington, Seattle, WA). The luciferase reporter assay to determine β-catenin/TCF transcription activity was carried out as previously described (120,207). Briefly, actively growing stable cell lines of SW480 overexpressing either PKD1 or GFP cells ($1.5x10^5$ cells/well) were plated in triplicate in 12-well plates for 24-36h and transiently co-transfected with TCF-firefly luciferase reporter construct (pTOP-FLASH) and *Renilla* luciferase internal control plasmid (pRL-TK) (Promega). Non-specific/background transcription activity was determined by transiently transfecting the control wells with mutant TCF promoter construct (pFOP-FLASH) and *Renilla* luciferase construct (pRL-TK). After 24h, the cell lysates were prepared and assayed for firefly luciferase and *Renilla* luciferase activity using Dual Glo reagents (Promega) according to the manufacturer's instructions and the luciferase signal was measured in a GloMax 96

Microplate Luminometer (Promega). The β-catenin/TCF transcription activity was determined by normalizing the firefly luciferase activity to that of *Renilla* luciferase activity and calculating the ratio of TOP-FLASH signal to FOP-FLASH signal.

Transient transfection of the colon cancer cell lines was also used to examine the effect of the various construct of PKD1 on β-catenin transcription activity. Briefly, actively growing cells ($1.5x10^5$ cells/well) were plated as mentioned above and transiently co-transfected with TCF-firefly luciferase reporter construct (pTOP-FLASH) and *Renilla* luciferase construct along with one of the various PKD1 constructs or control plasmid. Non-specific/background transcription activity was determined by transiently transfecting the control wells with mutant TCF promoter sites (pFOP-FLASH) and *Renilla* luciferase construct (pRL-TK) and the corresponding PKD1 constructs or control plasmid. The cell lysates were prepared and assayed as mentioned above.

Tumor Xenograft Model

Six-week-old male athymic nude (nu/nu) mice (Charles River Laboratories, Wilmington, MA) were used to generate colon cancer xenografts as described earlier (207). The mice were maintained in a pathogen-free environment and all procedures were carried out as approved by the Sanford Research/University of South Dakota Institutional Animal Care and Use Committee. Briefly, SW480 cells overexpressing PKD1 or GFP (5×10^6 cells/100µl/per mouse) were mixed with 100 µl Matrigel (BD Biosciences, Sparks, MD) and injected subcutaneously (sc) into the flank of the left hind limb. The animals were periodically monitored for tumor development and the tumor volume was measured from day 12 after injection using a digital Vernier caliper. The tumor volume was calculated using the ellipsoid volume formula: tumor volume (mm^3) = $\boldsymbol{\pi} / 6 \times \boldsymbol{L} \times \boldsymbol{W} \times \boldsymbol{H}$, wherein $\boldsymbol{L}$ is length, $\boldsymbol{W}$ is width, and $\boldsymbol{H}$ is height. The tumor growth was regularly monitored till either the end of the study or until the tumor burden reached a volume of $700mm^3$. The mice were sacrificed, the tumors fixed in formalin, embedded in paraffin, and sliced into 5µm sections for further processing and analysis.

Statistical Analyses

Student's t test was used for analysis of statistical significance and the significance was determined using a paired t-test. A p value of < 0.05 was considered significant.

Results

PKD1 Is Downregulated in Colon Cancer

The deregulation of PKD1 expression is associated with various cancers including prostate and breast cancer (120,193,195,201). However, the expression profile of PKD1 in colon cancer is not known. Therefore, we investigated the expression pattern of PKD1 by immunofluorescence staining of colon tissue using anti-PKD1 antibody and fluorescently labeled secondary antibodies (red) (**Figure 2-1A**). Additionally, tissues were also simultaneously co-stained for β-catenin expression using anti-β-catenin antibody. Representative images from normal colon tissue stained for PKD1 and β-catenin are shown in **Figure 2-1A**. PKD1 expression was predominantly detected in the cytoplasm with some expression on the membrane and in the nucleus of the cells, while β-catenin expression (green staining) was primarily localized to the membrane of the cells. The immunohistochemical (IHC) staining also revealed co-localization of PKD1 and β-catenin in colon tissues (**Figure 2-1A,** lower panel). This suggests a role for PKD1-β-catenin interaction in colon tissues. In order to investigate the expression profile of PKD1 in colon cancer tissues and quantitatively analyze changes in PKD1 or β-catenin expression, IHC analysis was performed on tissue microarray (TMA) slides containing normal (n=8) and colon cancer tissues (n=45) using chromogenic dyes (**Figure 2-1B**). The tissue samples were grouped based on the Dukes' staging of colon cancer into non-neoplastic, Duke's stage B (wherein the cancer has invaded the bowel walls, but has not spread to the lymph nodes) and Duke's stage C colon cancer (wherein the cancer has spread to the nearby lymph node) and analyzed for the levels of expression and the localization pattern of the proteins. PKD1 expression was significantly ($p<0.05$) downregulated in the cancerous tissues compared to normal tissues (**Figure 2-2A**). We also detected a trend in the progressive downregulation of PKD1 expression from non-neoplastic stage to Duke's stage B and Duke's stage C colon cancer (**Figure 2-1B**). The suppression of PKD1 expression coincided with the distinct change in the β-catenin localization in cancer tissues. While β-catenin was primarily localized on the membrane of normal colon glandular cells, a higher β-catenin staining was detected in the cytoplasm and the nucleus as the cancer progressed from Duke's stage B to Duke's stage C colon cancer, when the cancer had spread to the nearby lymph node. The association between downregulation of PKD1 expression with the change in β-catenin localization in colon cancer seems to suggest a role for PKD1 in regulating β-catenin functions in colon cancer. Based on these results, we proposed that PKD1 functions as a tumor suppressor *via* modulating β-catenin signaling pathway and inhibiting nuclear β-catenin function to suppress colon cancer growth. Thus, an increase in PKD1 levels in colon cancer cells can inhibit the progression of colon cancer.

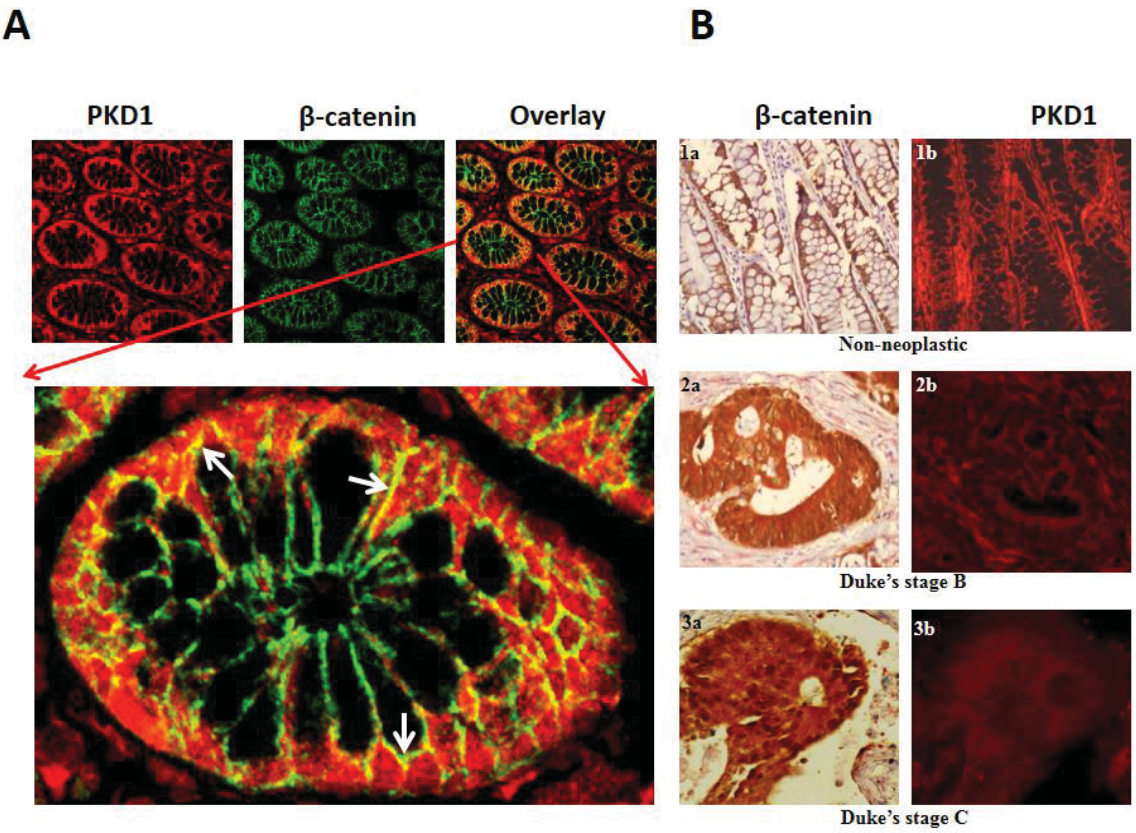

Figure 2-1. Expression of PKD1 is downregulated in colon cancer
(A) Immunohistochemical analysis of PKD1 and β-catenin in colon tissues: Normal colon tissues were immunostained for PKD1 (red) and β-catenin (green). PKD1 expression was detected in the cytoplasm and membrane of colon cells, while β-catenin was primarily localized to the membrane. Co-localization of PKD1 with β-catenin was also detected (yellow). A magnified image of a single colon gland is shown to demonstrate co-localization of PKD1 and β-catenin (white arrows). Original magnification 200X. **(B)** Tissue microarray (TMA): Colon cancer TMA slides were stained for β-catenin (brown) and PKD1 (red). β-catenin staining revealed distinct change in subcellular localization in colon cancer. It was primarily localized on the membrane of non-neoplastic samples (1a), while distinct cytoplasmic and prominent nuclear staining was detected in Duke's stage B (2a) and Duke's stage C colon cancer, respectively (3a). PKD1 expression was strongly detected in non-neoplastic samples (1b, red). However, PKD1 was progressively downregulated in Duke's stage B (2b) and Duke's stage C (3b) colon cancer. Original magnification 400X.

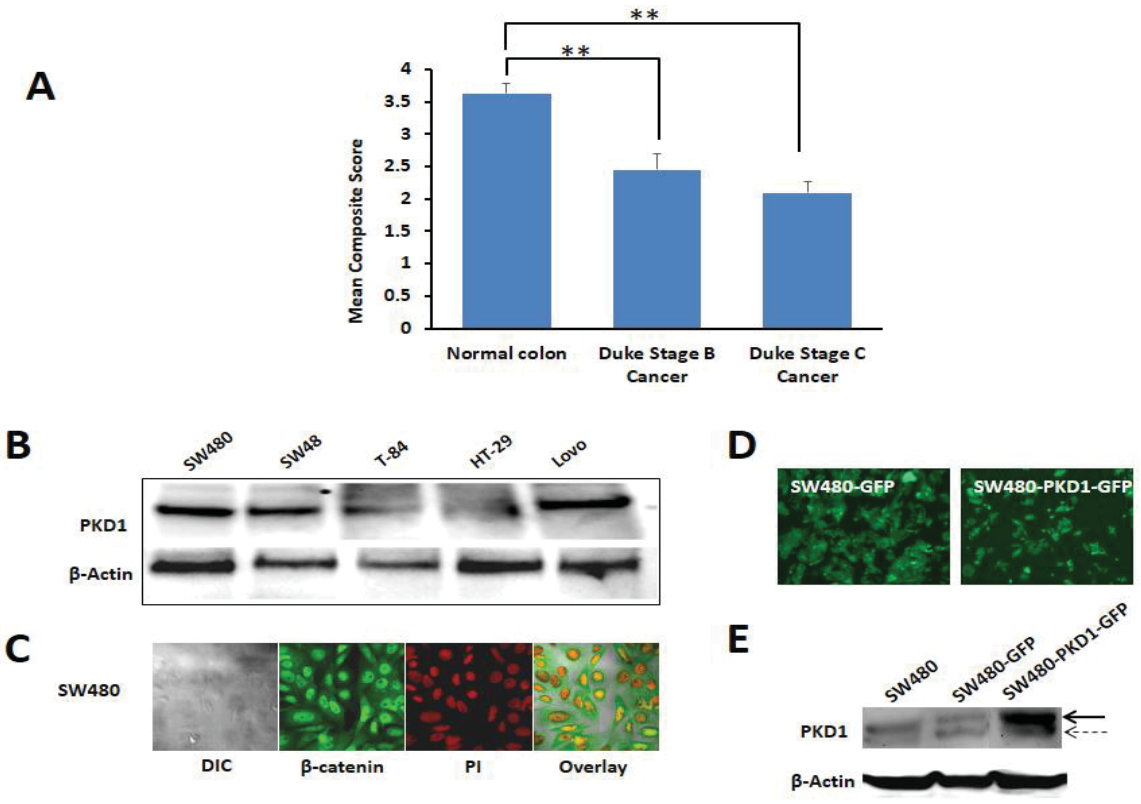

Figure 2-2. PKD1 and β-catenin expression in tissue microarray slides and SW480 colon cancer cells

(**A**) *Quantitative analysis of PKD1 staining in Tissue microarray*: The colon cancer TMA samples stained for PKD1 (red) were evaluated by two pathologists for the intensity and extent of staining. The mean composite score (MCS) for each TMA sample was calculated as detailed in the Methods Section and the MCS was graphed with respect to the Duke's stages of colon cancer. A substantial and significant decrease in the expression of PKD1 was detected in Duke's B and C stages of colon cancer compared to control tissues. (**B**) *PKD1 expression in colon cancer cell lines*. Representative western blot of whole cell lysates isolated from various colon cancer cell lines and probed for PKD1 expression. β-actin was used as loading control. (**C**) *β-catenin in SW480 cells*. SW480 cells were seeded in chamber slides for 24h. The cells were fixed and processed for immunostaining using anti-β-catenin antibody (green), and the nuclei (red) was counter-stained using propidium iodide (PI). The overlay image shows distinct localization of β-catenin in the nucleus (yellow). Original magnification 400X. (**D**) *PKD1 expression in stable cell lines*. Fluorescent and phase contrast microscopic images of stably transfected SW480 cells overexpressing either GFP tagged PKD1 or GFP. Original magnification 100X. (**E**) *Western blot analysis of stable cell lines*. Cell lysates from SW480, SW480-GFP and SW480-PKD1-GFP were resolved on SDS-PAGE, blotted on PVDF membrane and probed for PKD1 expression using anti-PKD1 antibody. β-actin was used as loading control. The intrinsic PKD1 (dotted arrow) and exogenous overexpressed GFP tagged PKD1 (solid arrow) are indicated in the blot.

Exogenous Expression of PKD1

In order to investigate the functional role of PKD1 and the importance of PKD1-β-catenin interaction in colon cancer, we sought to overexpress PKD1 in a cell line that would expresses low or no PKD1 and express high amounts of nuclear β-catenin, to mimic advanced stage colon cancer. Therefore, we screened a panel of five colon cancer cell lines for PKD1 expression using immunoblotting techniques. Moderate level of PKD1 expression was detected in almost all the cancer cell lines (SW480, SW48, T-84 and LoVo), except the HT-29 cell line, which showed very little PKD1 expression (**Figure 2-2B**). These cell lines were also analyzed by confocal microscopy to determine the expression pattern of β-catenin in cells. The SW480 cells primarily expressed β-catenin in the nucleus (**Figure 2-2C**). This is clearly evident by the appearance of the yellow color in the overlay image between β-catenin staining (green) and nuclear staining (red). The other remaining cells lines revealed a predominant cytoplasmic staining of β-catenin (data not shown). Therefore, we used the SW480 colon cancer cells to stably overexpress PKD1 and analyze its role in the regulation of nuclear β-catenin activity and colon carcinogenesis. Actively growing SW480 cells were chemically transfected with either GFP tagged PKD1 (pEGFP.PKD1) or control GFP vector (pEGFP) and subjected to fluorescence assisted cell sorting to enrich a pool of SW480 cells overexpressing either GFP tagged PKD1 or GFP. Over 60% of the stably transfected SW480 cells overexpressed our protein of interest **(Figure 2-2D)**. Analysis of protein lysates from these cells by immunoblotting using anti-PKD1 antibody **(Figure 2-2E)** also revealed the overexpression of GFP tagged PKD1 in addition to endogenous PKD1 in the PKD1 overexpressing cells. For ease of description, from here onwards, the SW480 cells overexpressing GFP tagged PKD1 will be referred to as SW480-PKD1-GFP and the control cells overexpressing GFP vector will be referred as SW480-GFP.

Exogenous Expression of PKD1 Inhibits Cell Proliferation

The stable SW480-PKD1-GFP and control SW480-GFP cells were examined for the effect of PKD1 overexpression on tumorigenic characteristics like cell proliferation and colony formation. PKD1 overexpression significantly ($p<0.05$) decreased cell proliferation compared to control SW480-GFP cells (**Figure 2-3A**). We next examined the clonogenic potential of these cells, an important parameter that reflects the ability of single cancer cells to survive, grow and colonize. PKD1 overexpression (SW480-PKD1-GFP) significantly reduced the ability of colon cancer cells to form anchorage dependent colonies, compared to control cells (**Figure 2-3B**). The anchorage independent clonogenic assay attempts to mimic the *in-vivo* situation and evaluates the ability of cells to form independent colonies when suspended in a gel or viscous medium in the absence of any anchor. Similar to results observed in anchorage dependent assay, SW480-PKD1-GFP cells formed fewer number of colonies compared to control SW480-GFP cells in anchorage independent assay. These results indicate a tumor suppressor function for PKD1 in colon cancer.

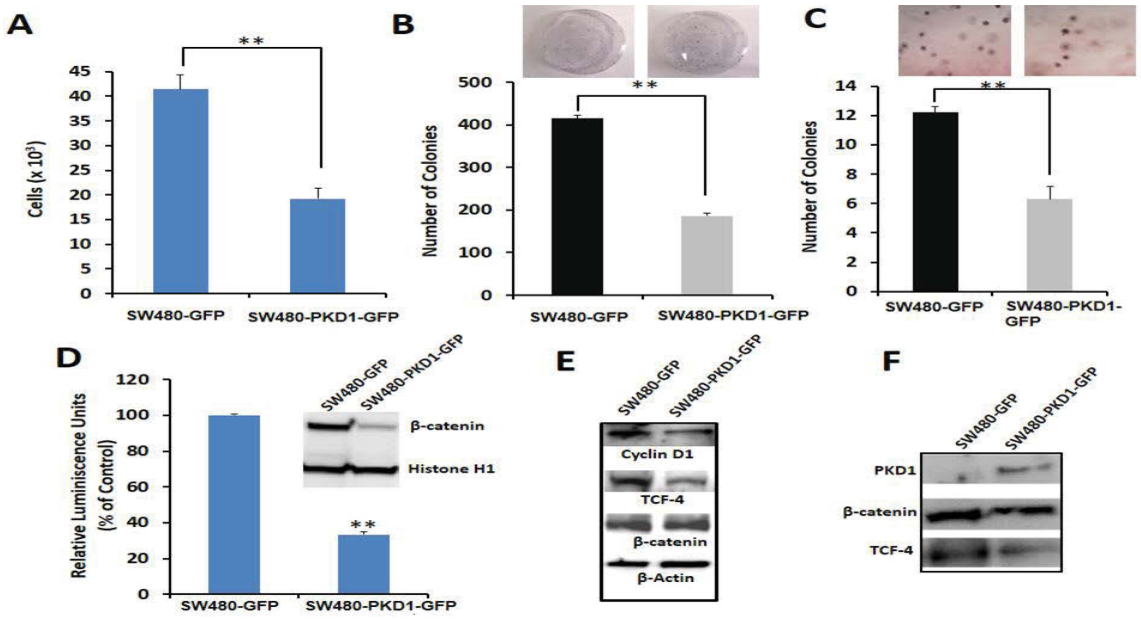

Figure 2-3. PKD1 overexpression decreases tumorigenic phenotypes by inhibiting the nuclear transcriptional activity of β-catenin in SW480 colon cancer cells
(A) *Cell proliferation.* PKD1 overexpression decreased cell proliferation by over 50%. Mean ± SE; n=3; **p<0.05. **(B)** *Anchorage dependent colony formation.* SW480 cells overexpressing either PKD1 or GFP vector ($2x10^3$) were plated in 100mm dishes for 12 days and the average number of colonies formed was counted and graphed. PKD1 overexpression inhibited anchorage dependent colony formation in SW480 cells. **(C)** *Anchorage independent colony formation.* SW480-GFP and SW480-PKD1-GFP cells ($4x10^4$) were seeded in 0.3% agarose and grown for 14 days. The number of colonies formed was enumerated and plotted. PKD1 overexpression decreased anchorage independent colony formation in SW480 cells. Mean ± SE; n=3; **p<0.05. **(D)** *Effect of PKD1 overexpression on β-catenin transcription activity*. Reporter luciferase assay was used to measure β-catenin transcription activity. The β-catenin transcription activity was measured, normalized to the control *Renilla* luciferase activity and expressed as a ratio of TCF-promoter-luciferase activity to mutant TCF-promoter luciferase activity. PKD1 overexpression decreased nuclear β-catenin expression in SW480 cells by over 70%. The inset depicts representative blots of nuclear lysates isolated from SW480-GFP or SW480-PKD1-GFP cells and probed for β-catenin expression. Histone H1 was used as internal control **(E)** *Effect on downstream targets*. Total protein isolated from SW480-PKD1-GFP or control SW480-GFP cells was resolved on gel and immunoblotted using specific antibodies. β-actin was used as loading control. PKD1 overexpression decreased Cyclin D1 and TCF4 levels, both of which are downstream products of β-catenin/TCF transcription activity. **(F)** *Immunoprecipitation (IP)*. Equal amounts of nuclear extract isolated from the PKD1 overexpressing cells or control cells were subjected to IP using anti-TCF4 antibody. The immune-complexes were resolved on gel and sequentially probed for β-catenin, TCF4 and PKD1. PKD1 overexpression decreased the amount of β-catenin-TCF4 complex in the nucleus.

To ensure these results were not specific to one cancer cell line, a different colon cancer cell line, SW48, was also used to overexpress PKD1 or GFP and examine the effect on cell proliferation. This cell line was chosen since SW48 cells express a relatively low amount of PKD1 protein and is amenable to assess nuclear β-catenin transcription activity. In addition, unlike the SW480 cells, SW48 cells do not harbor any mutation in the *APC* gene which plays vital role in the regulation of β-catenin levels within the cells. Therefore, the SW48 cells were transiently transfected to overexpress PKD1 or GFP and analyzed for cell proliferation and clonogenic potential (**Figure 2-4**). Fluorescent and phase contrast image of the cells showed over 70% expression of the exogenous proteins (**Figure 2-4A**). Analysis of cell proliferation revealed that PKD1 overexpression significantly ($p<0.05$) decreased cell proliferation of SW48 cells, compared to control SW48-GFP cells (**Figure 2-4B**). PKD1 overexpression also significantly decreased both anchorage dependent and anchorage independent clonogenic potential of SW48 cells (**Figure 2-4C** and **2-4D**) indicating that the anti-carcinogenic functions of PKD1 in colon cancer were a cell line independent phenomenon.

PKD1 Overexpression Modulates β-catenin Functions and Subcellular Localization

Dysregulation of β-catenin expression or functions leads to enhanced carcinogenesis by up-regulating the expression of various proto-oncogenes, thereby increasing cell proliferation, survival, motility, invasion and epithelial-mesenchymal transition (EMT) (185,188,193). To investigate the underlying mechanism responsible for the anti-proliferative potential of PKD1 and given that PKD1 co-localized with β-catenin in colon tissues, we used a reporter assay to analyze the effect of PKD1 overexpression on the co-transcription activity of β-catenin. PKD1 overexpression significantly ($p<0.05$) downregulated β-catenin co-transcription activity by over 60% compared to control cells (**Figure 2-3D**). Decrease in the β-catenin co-transcription activity was a result of lower nuclear β-catenin that was suggested by finding the decreased β-catenin expression in the nucleus on PKD1 overexpression (inset of **Figure 2-3D**). Additionally, we observed that PKD1 overexpression substantially decreased Cyclin D1 (downstream target of β-catenin), TCF4 expression (that is regulated by TCF4/β-catenin) in SW480-PKD1-GFP cells compared to control cells. However, no change in the overall expression of β-catenin was observed in PKD1 overexpressing cells compared to control.

In order to detect complex formation between nuclear β-catenin, TCF4 and PKD1, equal amounts of protein extracted from the nuclear lysates of SW480-PKD1-GFP or SW480-GFP cells were subjected to immuno-precipitation using anti-TCF4 antibody (**Figure 2-3F**). The immuno-precipitated complex was resolved on a gel, blotted on a membrane and probed using specific antibodies against β-catenin, PKD1 and TCF4. A lower level of TCF4 and β-catenin and therefore lower β-catenin/TCF4 transcription complex was detected in the PKD1 overexpressing cells compared to the control cells (**Figure 2-3F**). This result indicates that the lower β-catenin co-transcription activity detected in the PKD1 overexpressing cells was a consequence of a decrease in nuclear TCF4-β-catenin complex in the PKD1 overexpressing cells compared to GFP control cells. The effect of PKD1 overexpression in attenuating β-catenin transcription activity

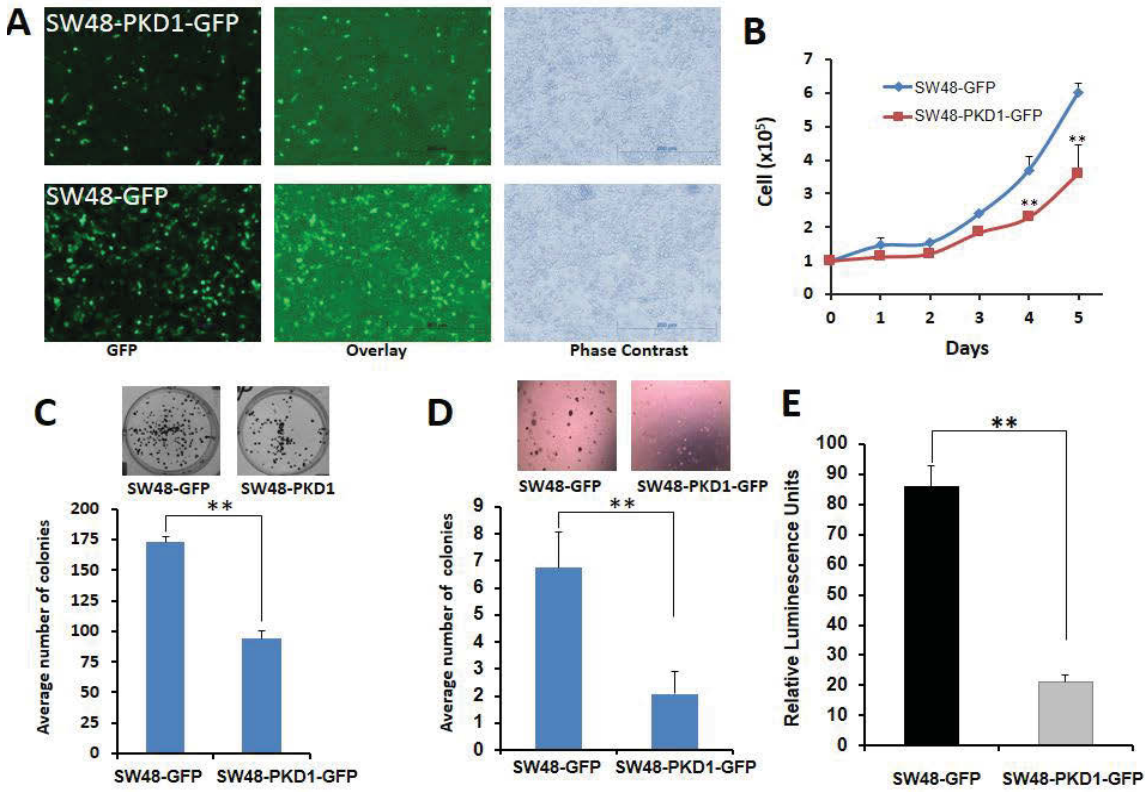

Figure 2-4. Effect of PKD1 overexpression in SW48 colon cancer cells
(A) Overexpression of PKD1 in SW48 cells. Fluorescent and phase contrast microscopic images of SW48 cells overexpressing either PKD1 or GFP are shown. Original magnification 100X. **(B)** Cell proliferation of SW48 cells. Equal numbers of SW48-GFP and SW48-PKD1-GFP cells were plated in multiple cell culture plates. The cells were harvested for five consecutive days, enumerated and graphed. PKD1 overexpression significantly decreased cell proliferation compared to control cells. Mean ± SE; n=3; **p<0.05. **(C)** Anchorage dependent colony formation. SW48 cells overexpressing either PKD1 or GFP vector (2x103) were plated in 100mm dishes for 12 days and the number of colonies formed was counted and graphed. Representative images of colonies are shown below the graph. PKD1 overexpression suppressed anchorage dependent colony formation in SW48 cells. Mean ± SE; n=3; **p<0.05. **(D)** Anchorage independent colony formation. SW48-GFP and SW48-PKD1-GFP cells (4x104) were seeded in soft agar and grown for 14 days and the number of colonies formed was enumerated and plotted. Representative images of colonies are shown above the graph. PKD1 overexpression decreased anchorage independent colony formation in SW48 cells. Mean ± SE; n=3; **p<0.05. **(E)** β-catenin transcription activity. SW48 cells were transiently transfected with vector (pEGFP) or PKD1 (pEGFP-PKD1) along with reporter luciferase construct and an internal control plasmid. The cells were harvested after 48h and assayed to measure β-catenin co-transcription activity as mentioned earlier. PKD1 overexpression significantly decreased β-catenin transcription activity by over 75%.

was also detected in SW48 colon cancer cells. In these cells PKD1 overexpression decreased β-catenin transcription activity by over four-fold (**Figure 2-4E**). These data suggest a critical role of PKD1 in the regulation of nuclear β-catenin transcription activity.

Enzymatically Functional Kinase Activity of PKD1 Is Required for the Suppression of Nuclear β-catenin Transcription

The inhibition of β-catenin transcription activity was also confirmed using another independent construct. The PKD1 gene (pcDNA-PKD1) or control plasmid (pcDNA) was transiently overexpressed along with the luciferase reporter construct and evaluated for its effect on β-catenin transcription activity. As expected, PKD1 overexpression significantly inhibited β-catenin transcription activity (**Figure 2-5A**). In order to investigate if the kinase activity of PKD1 is necessary for the suppression of nuclear β-catenin transcription activity, we overexpressed a kinase dead mutant of PKD1 using a kinase-dead construct (pcDNA-PKD1-K618W) and analyzed the effect on β-catenin transcription activity. Interestingly, the kinase dead mutant of PKD1 failed to inhibit nuclear β-catenin transcriptional activity compared to vector control. In fact, an enhancement of β-catenin activity was observed in kinase dead mutant PKD1 overexpressing cells. This probably occurred due to a dominant-negative role in inhibiting the intrinsic functions of wild type PKD1 for this kinase dead mutant.

Nuclear-targeted PKD1 More Efficiently Attenuates Nuclear β-catenin Transcription Activity

PKD1 is primarily present in the cytoplasm, with a small amount being present in the Golgi complex, the mitochondria, the nucleus and on the inner side of the cell membrane. To examine if nuclear PKD1 is required for the repression of nuclear β-catenin transcriptional activity, nucleus targeted PKD1-GFP construct (GFP-NLS-PKD1) and membrane targeted PKD1-GFP construct (Mem-GFP-PKD1) were overexpressed in SW480 cells. The site-specific overexpression of PKD1 was confirmed by confocal microscopy (**Figure 2-5B**). Cells overexpressing PKD1 with a nuclear localization signal (GFP-NLS-PKD1) revealed exogenous PKD1 expression primarily in the nucleus (as seen by the green and cyan color in the overlay image of GFP-NLS-PKD1 (green) and nuclear signal DAPI (blue) (**Figure 2-5B**, top row). Cells overexpressing PKD1 with a membrane localization signal, however, revealed PKD1 expression primarily on the cell membrane (**Figure 2-5B**, bottom row). We then examined the effect of site-specific expression of PKD1 on β-catenin transcription activity. While PKD1 overexpression inhibited β-catenin transcription activity, the overexpression of nuclear-targeted PKD1 (GFP-NLS-PKD1) further enhanced the suppression of β-catenin transcription activity (**Figure 2-5C**). In contrast, the overexpression of membrane targeted PKD1 (Mem-PKD1-GFP) failed to suppress β-catenin transcription activity in the SW480 cells. To further confirm these findings, we prepared nuclear lysate from SW480 cells overexpressing compartment targeted PKD1 and immunoblotted for nuclear β-catenin

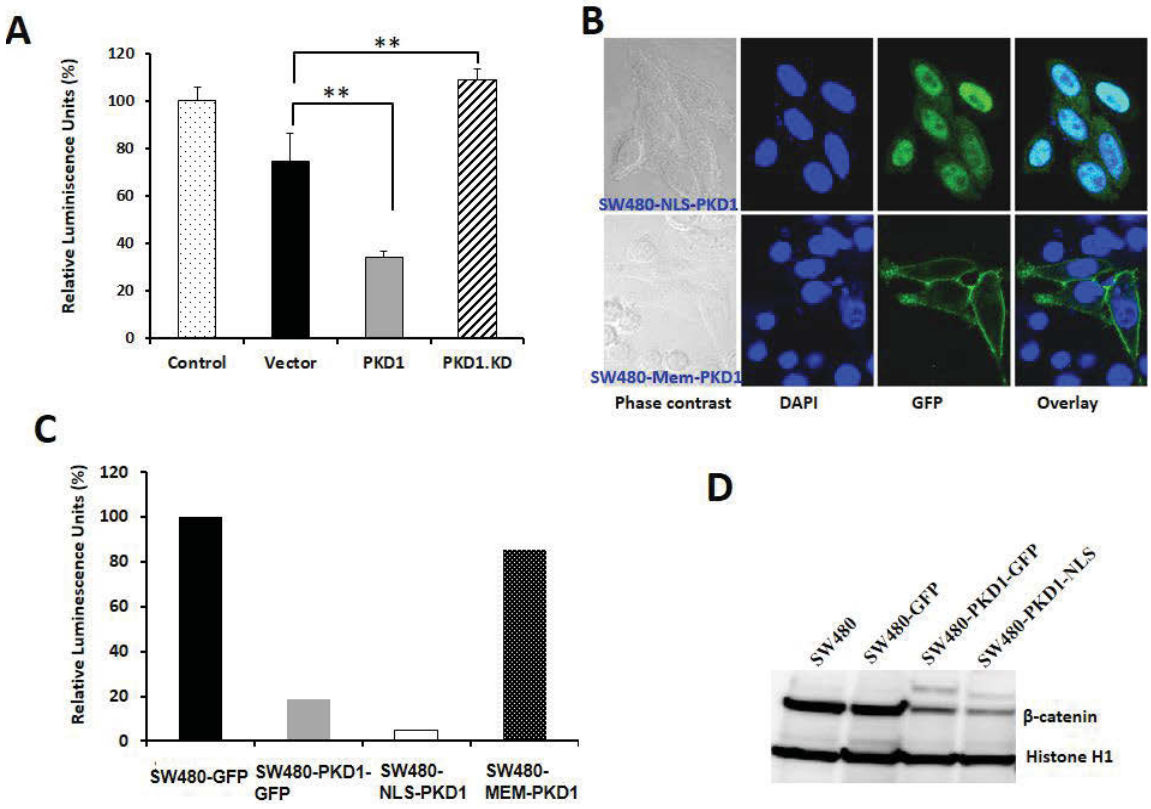

Figure 2-5. **Enzymatically active PKD1 is required for decreasing β-catenin co-transcription activity**

(**A**) *Effect of kinase-dead PKD1 on β-catenin transcription activity*. SW480 cells were transiently transfected with vector (pcDNA), PKD1 (pcDNA-PKD1) or PKD1-KD (kinase dead pcDNA-PKD1-K618W) along with reporter luciferase construct (a TCF-promoter-luciferase construct or a mutant TCF-promoter luciferase construct) and control plasmid expressing *Renilla* luciferase gene. PKD1 overexpression significantly decreased the β-catenin transcription activity, while overexpression of the kinase dead PKD1 released this inhibition, indicating the requirement of active PKD1 molecules for modulating β-catenin transcription activity. (**B**) *Site-specific expression of PKD1 in SW480 cells*. PKD1 overexpression was targeted to the nucleus or the membrane by transient transfection of SW480 cells with nuclear targeted PKD1 (NLS-PKD1) or membrane targeted PKD1 (Mem-PKD1). Nuclear targeted PKD1 (top row) was predominantly localized to the nucleus, while membrane targeted PKD1 (bottom row) was primarily localized on the cell membrane. Original magnification 1000X. (**C**). *Effect of site-specific expression of PKD1 on β-catenin transcription activity.* Nuclear targeted PKD1 most effectively inhibited β-catenin transcription activity, while membrane localization of PKD1 released this inhibition, suggesting the need for nuclear PKD1 to inhibit β-catenin transcription activity. (**D**) *Expression of nuclear β-catenin*. Nuclear extract from cells overexpressing control vector, PKD1-GFP, and NLS-PKD1 were resolved on gel and immune-blotted for β-catenin and Histone H1 (internal control). Overexpression of nuclear PKD1 decreased nuclear β-catenin levels the most compared to control lysates.

and internal control Histone H1 (**Figure 2-5D**). While GFP overexpression did not cause any change in the expression of nuclear β-catenin, the overexpression of PKD1 or nuclear targeted PKD1 (GFP-NLS-PKD1) considerably decreased nuclear β-catenin levels (**Figure 2-5D**). The overexpression of nuclear targeted PKD1 (GFP-NLS-PKD1) caused the highest reduction in nuclear β-catenin levels in the SW480 cells compared to overexpression of either PKD1 or GFP. These results suggest a critical role for enzymatically active and nuclear localized PKD1 for the suppression of nuclear β-catenin transcription activity by lowering the levels of nuclear β-catenin within the cells.

PKD1 Overexpression Enhances Membrane Localization of β-catenin

In addition to its role in signaling as a transcription factor, β-catenin plays a vital role in cell adhesion. It interacts with E-cadherin to form the cell-surface adhesion complex and enhances cell-cell adhesion (134). Since the overexpression of PKD1 regulated the sub-cellular localization of β-catenin and decreased nuclear β-catenin expression, we then examined if PKD1 overexpression affects the expression of β-catenin on the cell membrane. Actively growing SW480-PKD1-GFP or SW480-GFP cells were fixed, stained using anti-β-catenin antibody and subjected to confocal microscopic analysis (**Figure 2-6A**). The expression of β-catenin was primarily nuclear (arrowheads) in the control cells, as is the case in the parent cell line. However, overexpression of PKD1 substantially enhanced the membrane localization of β-catenin compared to control cells (white arrows). A functional output of enhanced membrane localization of β-catenin might result in increased cell-cell adhesion. Therefore, to examine the functional consequence of enhanced membrane localization of β-catenin, the PKD1 overexpressing cells and control cells were subjected to two types of aggregation assays (**Figure 2-6B and C**). In the hanging-drop aggregation assay, the cells were trypsinized, spotted on the inner lid of a petri dish and incubated in an inverted position to form aggregates. The numbers of aggregates formed were examined after 24h (**Figure 2-6B**). Cells overexpressing PKD1 formed significantly higher numbers of aggregates (at least 3 fold) compared to control cells. Similar results were also observed in a second independent aggregation assay, wherein cells trypsinized under mild conditions were subjected to aggregate formation by incubating under gentle rocking conditions for 7h. PKD1 overexpressing cells formed markedly larger and a higher number of aggregates compared to control cells (**Figure 2-6C**).

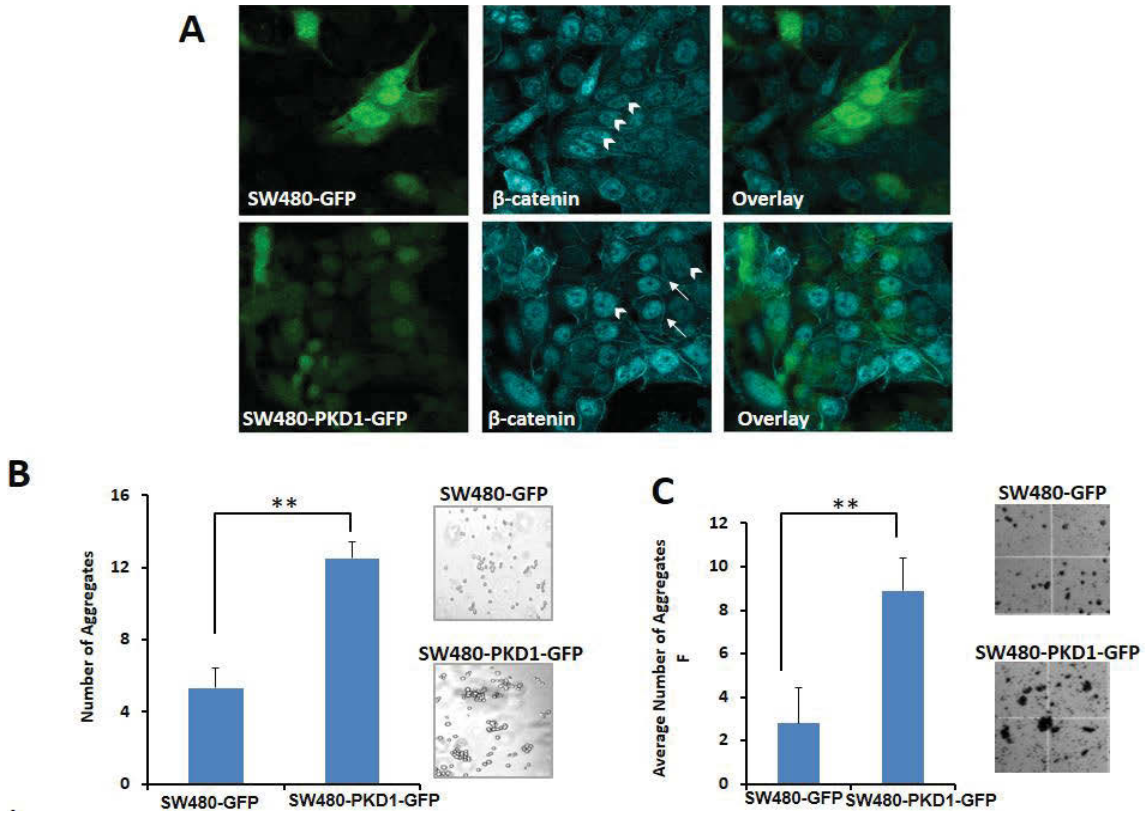

Figure 2-6. PKD1 overexpression enhances membrane localization of β-catenin and decreases nuclear β-catenin transcription activity

(**A**) *β-catenin staining*. SW480 cells overexpressing PKD1 or GFP were seeded in chamber slides for 24h. The cells were fixed and processed for immunostaining using anti-β-catenin antibody. Representative confocal images of cells are shown for SW480-PKD1-GFP or SW480-GFP (green) and β-catenin (cyan) staining. The control cells (SW480-GFP) predominantly exhibited nuclear localization of β-catenin (arrow head) with very low membrane staining. However, PKD1 overexpressing cells showed relatively enhanced membrane localization of β-catenin (white arrows) along with nuclear localization. Original magnification 600X. (**B**) *Hanging drop cell-aggregation assay*. Equal volume of freshly trypsinized cells was spotted on the lid of a petri-dish and incubated under moist conditions for 24h. The aggregates formed were counted and photographed. PKD1 overexpression enhanced cell-cell aggregation, compared to control cells. Representative images of the cell-cell aggregates are also shown. Mean ± SE; n=3; **p<0.05. (**C**) *Cell-aggregation assay.* Freshly trypsinized SW480-PKD1-GFP or SW480-GFP cells were incubated in the presence of 2.5mM $CaCl_2$ under mild shaking conditions to facilitate aggregate formation. The numbers of aggregates formed after 7h of incubation were enumerated, imaged and graphed. Representative images of the cell aggregation assay are also shown. PKD1 overexpression enhanced cell-cell aggregation, compared to control cells. Mean ± SD; n=2; **p<0.05.

PKD1 Overexpression Suppresses Cell Motility

PKD1 plays a significant role in regulating cellular motility (200,212,213). PKD1 has been shown to inhibit cellular motility by interacting with proteins at the leading edge of the motile cells. It negatively regulates cellular motility in part by indirectly maintaining the depolymerizing factor cofilin in its inactive phosphorylated form. PKD1 achieves this by enhancing cofilin phosphorylation (through PAK4-LIMK pathway) or by inhibiting its de-phosphorylation (through the direct phosphorylation and inhibition of SS1L phosphatase function) to shift the equilibrium towards maintaining the phosphorylated and inactive form of cofilin (196,200). Therefore, we evaluated the effect of PKD1 overexpression on motility of SW480 colon cancer cells using the agarose bead assay. In this test, the SW480-PKD1-GFP or SW480-GFP cells were embedded within agarose beads and spotted on cell culture plates pre-coated with fibrinonectin to examine the ability of cells to escape the beads and migrate on the surface of the plate (**Figure 2-7A**). PKD1 overexpression inhibited the motility of colon cancer cells compared to control SW480-GFP cells (**Figure 2-7B**). The ability of PKD1 to inhibit motility of SW480 colon cancer cells was also confirmed using a wound-healing assay (**Figure 2-7C**). A wound (or scratch) was created using the pointed edge of a sterile pipette tip on the surface of confluent plates of SW480-PKD1-GFP or SW480-GFP cells and the plates were examined at regular intervals to document and evaluate wound healing (or gap closure) by motile cells. SW480-GFP cells more effectively closed the gap/wound compared to PKD1 overexpressing cells (SW480-PKD1-GFP). In order to examine the molecular mechanisms regulating the cellular motility of the PKD1 overexpressing colon cancer cells, total protein lysates from SW480-PKD1-GFP or SW480-GFP cells were immunoblotted and examined for the expression of various motility related proteins (**Figure 2-7D**). We observed enhanced expression and phosphorylation of cofilin in PKD1 overexpressing cells compared to control cells. Little to no change was observed either in the expression or phosphorylation of other proteins involved in actin remodeling, including LIMK, Arp2 and Arp3. Thus, PKD1 overexpression appeared to inhibit cellular motility partly by inhibiting the activity of cofilin, a protein critical for depolymerization of filamentous actin filaments to generate new monomeric actin for formation/extension of actin fibers at the leading edge.

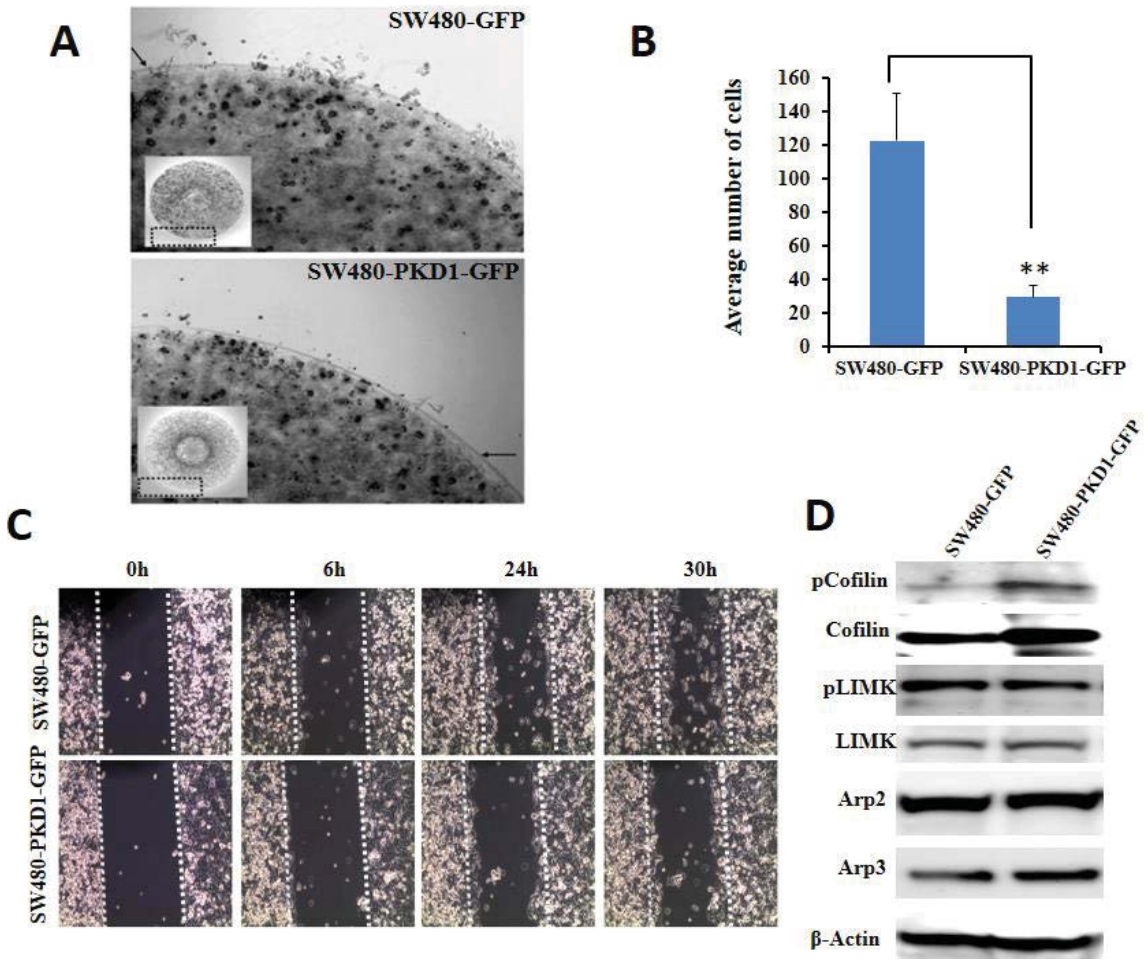

Figure 2-7. Overexpression of PKD1 inhibits cellular motility
(**A**). *Cell migration assay.* SW480 cells overexpressing PKD1 or GFP were mixed with agarose and equal volume was placed on fibrinonectin/BSA coated plates. Representative images of an agarose bead edge with motile cells are shown. The inset shows the corresponding whole agarose bead. PKD1 overexpression decreased the motility of SW480 cells. (**B**) *Quantitative analysis of cell migration assay*. The number of cells that migrated from the agarose bead was counted and plotted. PKD1 overexpression significantly inhibited migration of SW480 cells. Mean ± SE; n=3; **p<0.05. (**C**) *Scratch assay.* Confluent growth of SW480-PKD1-GFP or SW480-GFP cells was 'wounded' by a scratch using a micropipette tip. The 'wound' was periodically monitored for 'wound healing' and photographed. PKD1 overexpression decreased the motility of SW480 cells compared to vector control. (**D**) *Immunoblot analysis*. Representative blots of whole cell lysates from SW480-PKD1-GFP and control SW480-GFP cells were probed for proteins regulating cellular motility. PKD1 overexpression enhanced the expression levels of inactive phospho-cofilin and cofilin.

PKD1 Influences *in-vivo* Colon Tumorigenesis

To investigate the tumor suppressor potential of PKD1 in colon carcinogenesis *in-vivo*, we examined the tumor growth pattern of PKD1 overexpressing cells in a xenograft mouse model. Equal number of SW480 cells overexpressing PKD1 or control vector (GFP) were subcutaneously (sc) injected into the hind flank of nude mice for tumor formation (n=8 per group). The mice were periodically examined for tumor appearance and tumor growth was monitored by calculating the volume of the tumor. By the 12^{th} day of injection, visible tumors could be seen and measured in most control animals. However, PKD1 overexpression in SW480 cells delayed the tumor appearance in nude mice compared to control SW480 cells overexpressing empty vector (**Figure 2-8A**). Analysis of the time taken for visible tumor formation (volume of $50mm^3$ or more) in each animal clearly showed a delay in tumor appearance in the PKD1 overexpressing cells compared to control group (**Figure 2-8A**). In addition, PKD1 overexpression also significantly decreased the average tumor size (volume) in nude mice compared to the tumor formed by control GFP overexpressing cells (**Figure 2-8B**). The shape and overall appearance of tumors formed by the control SW480-GFP cells and the PKD1 overexpressing SW480-PKD1-GFP cells were considerably different. The tumors formed by control SW480-GFP cells appeared flat, nodulated, light pink/white in appearance and displayed well-formed blood vessels on the tumor surface. On the other hand, the tumors formed by PKD1 overexpressing cells appeared round, smooth and very dark in appearance (**Figure 2-8C**). The dark appearance of the tissue prompted us to examine the tissue for necrosis and vascularization. Therefore, the tumors were fixed, paraffin embedded and sliced into 5μm sections. These sections were stained with H&E to detect necrosis and also immunostained with PKD1 and β-catenin antibodies to confirm the presence of PKD1 overexpression and to analyze for change in the subcellular localization of the β-catenin. Additionally, we performed immunostaining for CD31 to detect vasculature in tumors. Interestingly, tumors formed by PKD1 overexpressing cells exhibited a higher degree of necrosis compared to control tumors and also demonstrated higher expression of PKD1 **(Figure 2-8D)**. Importantly, akin to *in-vitro* observations, PKD1 overexpressing cells revealed considerably higher levels of membrane β-catenin on the surface of the cells than the control tumors, strongly implicating to the role of overexpressed PKD1 in modulating the functions and subcellular localization of β-catenin *in-vivo*. Additionally, PKD1 overexpressing tumors displayed higher number of blood vessels and more branching than control tumors (**Figure 2-8D**). A consequence of higher vasculature is oxygenation of the tumors and accordingly a lower expression of Glut1, a marker for hypoxia. Therefore, these tumors were stained for Glut1 to verify the degree of hypoxia. Indeed, tumor tissues formed by PKD1 overexpressing cells showed much lower expression of Glut1 compared to control tumors. These results indicate that PKD1 overexpressing cells not only initially delayed the appearance of tumor, but they eventually formed relatively smaller and necrotic tumors compared to control cells, strongly supporting a tumor suppressor function for PKD1 in colon cancer. These data also suggest a role of PKD1 in tumor necrosis.

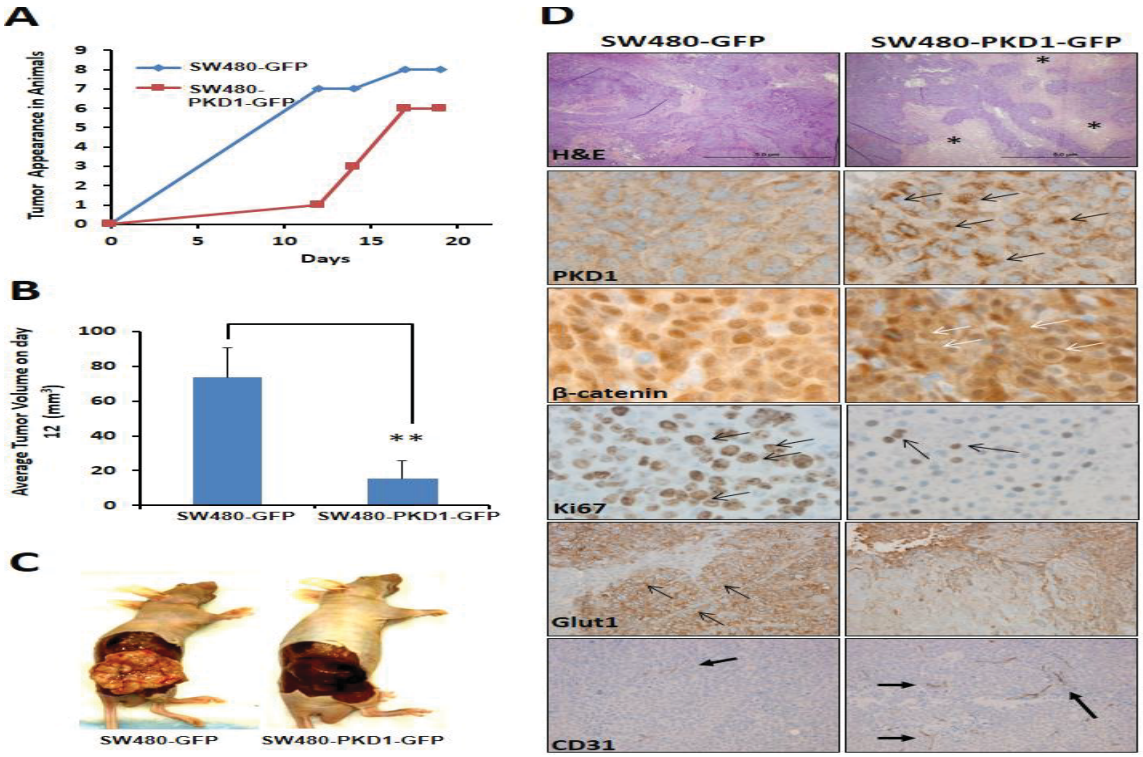

Figure 2-8. PKD1 overexpression delays tumor growth in xenograft mouse model **(A)** Tumor appearance. SW480-PKD1-GFP and SW480-GFP cells (5x106) were injected into the hind flank of nude mice and tumor appearance was periodically monitored. The time required for visible tumor growth was graphed against the number of mice exhibiting the appearance of visible and measurable tumor (> 50mm3). PKD1 overexpression delayed tumor formation compared to GFP control cells. (n=8 mice/group). **(B)** Tumor volume. The average volume of the tumors formed by SW480-PKD1-GFP and SW480-GFP cells was measured on day 12 and plotted. The PKD1 overexpressing cells formed significantly smaller tumors by day 12 than control GFP cells. **(C)** Tumor in nude mice. Representative photographs of nude mice showing tumors developed from SW480-PKD1-GFP or control SW480-GFP colon cancer cells. The tumors formed by SW480-GFP cells were nodulated, flat, and lighter in appearance. In contrast, the tumors formed by SW480-PKD1-GFP cells were smooth, round, and dark in appearance. **(D)** Immuno-histochemistry of tumor tissues. Paraffin embedded tumor xenografts were sectioned and immunohistochemically stained for necrosis (H and E), PKD1 overexpression, β-catenin localization, Ki67 (a marker for cell proliferation), Glut1 (a marker for hypoxia) and CD31 (marker for cellular vasculature). Compared to control tumors, the tumors formed by PKD1 overexpressing cells showed enhanced necrosis (necrotic regions are indicated by *), higher PKD1 staining (black arrows), elevated membrane localization of β-catenin (white arrows) and decreased Ki67 staining (arrows) that indicates lower cell proliferation. PKD1 overexpressing tumors also exhibited lower Glut1 staining and higher CD31 staining. This indicates that PKD1 overexpression decreased hypoxic conditions and increased vasculature in the tumor compared to GFP control tumors.

Discussion

The highly conserved β-catenin protein regulates cell proliferation, polarity and cellular fate determination and thereby plays a prominent role in tightly controlling multiple processes including embryogenesis and cellular homeostasis (188,189,214). herefore, the dysregulation of β–catenin functions leads to major problems in cellular proliferation and differentiation, eventually resulting in the development of a number of cancers (214). The role of β-catenin is especially well documented in colon cancer (185). In fact, mutation in the Wnt/β-catenin signaling pathway is responsible for over 80% of all types of colon cancer (185). Therefore, an in-depth understanding of the regulation and modulation of the Wnt/β-catenin signaling pathway will aid in developing effective treatment strategies for colon cancer. This study aims to delineate a molecular association between PKD1 and β-catenin to develop an effective therapeutic strategy for colon cancer.

The serine-threonine kinase PKD1 has previously been shown to bind, phosphorylate and regulate the functions of β-catenin. The phosphorylation of β-catenin by PKD1 results in translocating β-catenin out of the nucleus and suppressing the transcription functions of the nuclear β-catenin (133,193), (120,215). This decreased transcriptional activity of β-catenin results in reduced expression of oncogenes like c-Myc and cyclin D1 and ultimately the inhibition of cell proliferation and cancerous properties of the cells (120). Additionally, the activation of PKD1 using natural compounds like curcumin or Bryostatin-1, in concurrence with the observed tumor suppressor function for PKD1, also leads to decreased nuclear β-catenin functions and lower cell proliferation in prostate cancer cells (120,207). PKD1 has also been attributed to possess a tumor suppressor function in breast cancer. The overexpression of PKD1 in breast cancer cells inhibited multiple metalloproteinases, suppressed cellular motility, prevented epithelial to mesenchymal transition and modulated the tumor microenvironment leading to the suppression of tumor growth/progression (195,216-218). Although PKD1 has been shown to be downregulated in many cancers, including prostate and breast cancers, its expression patterns and role in colon cancer has never been investigated.

Herein, for the first time, we sought to investigate the role of PKD1 in colon cancer. We examined its function in the regulation of β-catenin signaling pathway since this is one of the main pathways which usually operates aberrantly in colon cancer. Our expression analysis revealed a conspicuous decrease in PKD1 levels in higher grade colon cancer samples compared to normal colon and early grade samples (**Figure 2-1**). In our *in-vitro* studies, the overexpression of PKD1 significantly decreased the nuclear β-catenin levels and β-catenin transcriptional activity and thus reduced expression of the pro-carcinogenic downstream targets like cyclin D1. It was an intriguing observation to find that the nuclear β-catenin transcriptional activity was predominantly influenced by nucleus targeted PKD1. Further investigations revealed that this subcellular modulation of β-catenin results in enhanced membrane localization of β-catenin and thereby, increases cell-cell adhesion which is severely compromised in cancer cells. A similar function of PKD1 was demonstrated in prostate cancer cells (120,134). This eventually

resulted in decreasing cell proliferation and clonogenic potential in colon cancer cells. These anti-proliferative results are consistent with the findings in prostate and breast cancer, wherein the overexpression or activation of PKD1 suppressed cancerous phenotype of the cells (120,195,201,207,217). Herein, we have also shown that the attenuation of nuclear β-catenin functions is accomplished by enzymatically active PKD1 that is primarily present in the nucleus. Our results also revealed that PKD1 overexpression reduced the cellular motility of colon cancer cells by inhibiting the functions of the cofilin protein that are critical for the actin remodeling and cellular motility. Thus, overexpression of PKD1 in colon cancer cells not only enhanced cell-cell interaction, but also inhibited cell motility. Our studies suggest the role of PKD1 in suppression of cellular motility of cancer cells which has been validated by other studies as well (196,200,212,213,219). Additionally, the disruption of β-catenin/TCF complex formation was found on PKD1 expression that is important to regulate the proliferation and progression of colon cancer cells. This also controls the resulting activation of the genetic program in colorectal transformation process (192).

Our *in-vitro* results of PKD1 were recapitulated in xenograft *in-vivo* animal experiments. The *in-vivo* investigation using a xenograft mouse model revealed that PKD1 overexpression delayed the time of tumor appearance and tumor development compared to control GFP overexpressing cells. The detection of lower nuclear β-catenin levels, higher membrane localization of β-catenin and reduced staining of Ki67 (a marker for cell proliferation) was observed in the tumors formed by PKD1 overexpressing cells compared to control GFP overexpressing tumors. This data strongly suggests that PKD1 overexpression attenuates nuclear β-catenin functions and thus suppresses tumor growth. The tumors formed by PKD1 overexpressing cells revealed higher necrotic cell death compared to control tumors. Previous work has suggested a role for PKD1 in inducing programmed necrotic cell death and autophagy (220,221). Upon activation by oxidative stress, activated PKD1 in turn may activate the JNK pathway resulting in the programmed necrosis (220,222). Our results provide the first *in-vivo* evidence implicating a role of PKD1 in necrosis. However, the higher degree of tumor necrosis observed was not due to hypoxia within the tumor. The hypoxic core in tumors is a common occurrence due to dense and rapid cellular growth of the cancer cells without the simultaneous development of blood capillaries, leading to necrotic cell death. Our results suggest that the tumors formed by control GFP overexpressing cells were highly hypoxic compared to the tumors formed by PKD1 overexpressing cells. This observation is significant, since hypoxia within tumors leads to the activation of the transcription factor, hypoxia inducing factor (HIF), that eventually induces the synthesis of proteins resulting in highly aggressive tumor metastasis (223,224). A possible reason for the lower hypoxia might be due to sufficient blood vessel growth. Our results suggest that PKD1 overexpression enhances the formation of blood vessels. The ability of PKD1 to decrease tumor hypoxia and enhance tumor vasculature suggest that PKD1 can improve delivery of cancer drug(s) in tumors. Previous reports implicate a role for PKD1 in VEGF induced angiogenesis through the modulation of class II histone deacetylases (225-227). PKD1 plays a critical downstream role in VEGF-mediated activation of downstream targets enhancing blood vessel formation (227). Due to these molecular alterations, PKD1 overexpression causes conspicuous change in tumor morphology, structure and histo-architecture. The change in

tumor shape might be a result of modulation of not only the protein involved in adherent junctions but also other cell-cell binding and cell-stroma binding factors. Important roles of PKD1 in regulating E-cadherin and β-catenin mediated adherent junctions have previously been shown in prostate cancer cells (120,134,228). Together, these results suggest that the overexpression or activation of PKD1 in tumors enhanced tumor cell death and lowered hypoxia within the tumors. Further analysis of patient sample and PKD1 activators in animal mouse models will yield important information on the role of PKD1 in tumor metastasis and the development of effective treatment strategies.

In conclusion, our studies revealed a novel tumor suppressor function for PKD1 in colon cancer. We have found a correlation of PKD1 downregulation with the aberrant expression and nuclear localization of β-catenin in human colon cancer tissues. *In vitro* investigation revealed that PKD1 directly interacts with β-catenin and attenuates β-catenin transcriptional activity by decreasing nuclear β-catenin levels. Moreover, functional assays including PKD1 overexpression in colon cancer cells inhibited cellular motility and enhanced cell-cell adhesion. The *in-vivo* experiments suggest that PKD1 overexpression delayed tumor appearance and formed smaller tumors by modulating β-catenin functions in colon cancer. Based on these results, we propose that PKD1 may act as a tumor suppressor in colon cancer by modulating the nuclear β-catenin/Wnt signaling. Therefore, strategies for the up-regulation of PKD1 expression levels and/or activation in colon cancer cells are desired to modulate the nuclear β-catenin/Wnt signaling in colon cancer. Thus, the identification of drug molecules that induce PKD1 overexpression/activation may be important for the development of novel therapeutic modalities to inhibit tumorigenesis and colon cancer progression. Herein, we conclusively showed how PKD1 mediates β-catenin regulation. Thus, we now wanted to see if PKD1 can also regulate downstream targets of β-catenin such as Metastasis-associated Protein 1 (MTA1).

CHAPTER 3. PROTEIN KINASE D1 ATTENUATES METASTASIS VIA MODULATING METASTASIS ASSOCIATED PROTEIN 1 ACTIVITY

Introduction

Cancer is the second leading cause of death in US after heart diseases (1). Prostate cancer is the most common cancer and second leading cause of death among American men (1). According to American Cancer Society, it is estimated that about 29,000 American men will die due to prostate cancer in the year 2016 (1). Colon cancer is the third most common and third leading cause of death among both American men and women (1). It is estimated about 95, 000 people will be diagnosed and about 49,000 will die due to colon cancer in year 2016 (1). Most of these deaths will occur due to cancer metastasizing to the other parts of the body leading to a stage where cancer becomes incurable (229,230). However, another impediment in treatment of metastatic cancer cells is the development of chemo-resistance in cancer cells thus rendering the chemotherapeutic drugs ineffective for successful treatment of cancer (231,232). There is a general lack of understanding of mechanisms that leads cells to metastasize to the different parts of the body. Understanding of critical metastasis regulatory pathway is critical for developing novel strategies for treatment and prevention of metastatic cancer.

Metastasis-asscciated Protein 1 (MTA1) is a nucleosome remodeling and histone deacetylation (NuRD) complex protein (233). MTA1 is abundantly expressed in most of the cancers cells (128). It largely acts as a transcriptional co-repressor as well as transcriptional co-activator of large number of genes (234) and its role in tumor metastasis and invasion is very well characterized (235). Nuclear expression of MTA1 has positively correlated with severity of disease progression and shows highest expression levels in metastatic cancers such as prostate cancer (123,124). MTA1 initiates epithelial to mesenchymal transition in cancer cells thus leading cancer cells to break through basal membrane and enter blood stream through intravasation (124). It acts as a transcriptional corepressor for number of tumor suppressor genes such as p53 and PTEN (236). At the same time, it also co-activates pro-oncogenic signals such as Breast Cancer Amplified Sequence 3 (BCAS3) in human breast cancer (237). MTA1 is known to be localized to nucleus and is regulated by Wnt/β-catenin pathway leading to cancer progression and invasion (237). Further, MTA1 has been found to induce chemo-resistance against docetaxel in prostate cancer cells (238).Therefore, any therapeutic modality that targets this key metastasis regulatory signaling pathways can therefore lead to inhibition of not only metastatic capabilities of cancer cells but also chemo-sensitize cancer cells to chemotherapeutic drug.

Protein Kinase D1 (PKD1) is a serine-threonine kinase which is downregulated in prostate and colon cancer (207,239). PKD1 belongs to Protein Kinase D family of protein kinases which are homologous to Protein Kinase C (PKC) family of protein kinases in regulatory domain but are homologous to Calcium-calmodulin Kinases (CAMK) in their kinase domain (193). PKD1 mediates variety of cellular functions such as signal transduction, membrane trafficking, and cell survival, migration and proliferation (194).

PKD1 is known to interact and directly regulate β-catenin/TCF4 pathway in both prostate and colon cancer cells (207,239). Further, PKD1 is known to interact and transcriptionally attenuate Androgen Receptor (AR) expression in prostate cancer cells thus demonstrating a role in Androgen dependent to androgen independent progression of prostate cancer cells (109). PKD1 is known to localize to cytosol, nucleus, membrane, Golgi and mitochondria (193). Herein, we have demonstrated the role of PKD1 in regulation of metastasis in cancer cells. We examined the expression of PKD1 and MTA1 in different prostate and colon cancer cell line and demonstrate that PKD1 expression is negatively correlated with MTA1 expression at both Protein and RNA levels and aggressiveness of cancer cells. Subsequently, when PKD1 expression was inhibited in cancer cell line it resulted in increased expression of MTA1. We used C4-2-GFP, SW480-GFP and C4-2-PKD1-GFP, SW480-PKD1-GFP overexpressing cells to study and evaluate the effect of PKD1 overexpression on MTA1 expression. Bryostatin-1, a macrocyclic lactone is known to activate PKD1 expression (120). We demonstrated that Bryostatin-1 activated PKD1 interacts, phosphorylate, and mediates nuclear export via Golgi and Trans-Golgi network to lysosome. Further, it mediates degradation of MTA1 by ubiquitin pathway by polyubiquitination at lysine 48. We also confirmed the negative correlation of PKD1 and MTA1 in PTEN Knockout (KO) and TRAMP mouse model. Human tissue microarray further showed that PKD1 is downregulated and MTA1 is upregulated as the cancer progresses from low Gleason grade tumor to high Gleason grade tumor. Therefore, any therapeutic modality that activates PKD1 leading to inhibition of MTA1 expression could potentially be a potent anti-cancer drug for metastatic cancers. We therefore investigated the potential of Ormeloxifene, a non-steroidal selective estrogen receptor modulator (SERM) as a potential activator of PKD1 in prostate cancer cells. We for the first time observed specific activation of PKD1 expression by ORM.

Materials and Methods

Materials

RPMI-1640 media containing glutamine were supplemented with 10% Heat-inactivated FBS (Atlanta Biologics, Atlanta, GA), 1X 100mM Sodium Pyruvate, and 100X Antibiotic and Antimycotic Solution purchased from Gibco (Gibco, Thermo Fisher Scientific, Waltham, MA). G418 sulphate solution was purchased from MP Biomedicals (Fisher Scientific, Waltham, MA). Cycloheximide was purchased from Sigma (Sigma-Aldrich, St. Louis, MO). For PKD1 and MTA1 inhibition studies, selective PKD1 siRNA and MTA1 siRNA were purchased from Life technologies (Thermo Fischer Scientific, Carlsbad, CA). Bryostatin-1 and MG132 was purchased from Sigma (Sigma-Aldrich, St. Louis, MO).

Cell Lines and Other Materials

LNCaP (ATCC, Manassas, VA) and C4-2 (Urocor, Oklahoma City, OK) were grown in RPMI-1640 (Lonza, Walkersville, MD) media supplemented with 10% FBS (Atlanta Biologicals, Atlanta, GA), Antibiotic and Antimycotic solution. C4-2 transfected with PKD1-GFP vector or GFP vector was grown in G418 selection media for neomycin resistance. SW480, SW48, MB231, MCF7 (ATCC, Manassas, VA) were grown in DMEM (Lonza, Walkersville, MD) supplemented with 10% FBS and Antibiotic and Antimycotic solution. Other chemicals were purchased from Sigma (Sigma-Aldrich, St. Louis, MO) unless otherwise mentioned.

Antibodies

Rabbit Polyclonal PKD1 (C-20) and Mouse monoclonal MTA1 (A-11) were purchased from Santa Cruz Biotechnology (Santa Cruz, CA). Rabbit polyclonal MTA1 was purchased from Bethyl Laboratories (Bethyl Laboratories Inc., Montgomery, TX). Phospho-PKD1 (S916), PKD1 substrate antibody, K48-linkage specific polyubiquitin, α-tubulin, GAPDH were purchased from Cell Signaling (Cell Signaling Inc., Danvers, MA). Golgi and trans-Golgi antibodies (Golgi Sampler Kit; BD Transduction Laboratories). Ubiquitin and RANK antibody was purchased from abcam (Cambridge, MA). β-actin antibody was purchased from Sigma (Sigma-Aldrich, St. Louis, MO). HRP-conjugated secondary antibody was purchased from Promega (Promega Inc., Madison, WI).

Western Blotting

Cancer cells (70-80% confluent) were washed with ice-cold phosphate buffer saline (PBS) and lysed in 2X SDS lysis buffer. Equivalent amounts of protein samples were electrophoretically resolved on 4-20% SDS-PAGE gels and transferred on a PVDF membrane (Biorad Laboratories, Hercules, CA). Membrane was blocked with 5% BSA or Milk in TBST and incubated with primary antibody for overnight at 4°C. After three subsequent TBST washes the membrane was incubated in secondary antibody for 1 hour at room temperature, washed again and developed with the help of Immobilon Western Chemiluminescent HRP substrate (EMD Millipore, Billerica, MA, USA).

Real Time PCR Array Analysis

Briefly, the RNA samples from C4-2-PKD1-GFP, C4-2-GFP, SW480-PKD1-GFP and SW480-GFP cells were prepared and cDNA was synthesized as described earlier using superscript II RNAase H (High capacity RNA to cDNA kit). The cDNA was amplified by Taqman real time PCR using gene specific primers. The PCR amplification was performed in the Roche Lightcycler 480 (Roche, Indianapolis, IN).

Transfection

Prostate cancer cells (C4-2) and Colon Cancer (sw480) cells were serum starved overnight in opti-MEM media (Thermo Fischer Scientific, Carlsbad, CA) and then transfected with pEGFP vector or pEGFP vector containing PKD1 gene using Lipofectamine 2000 (Thermo Fischer Scientific, Carlsbad, CA). After 6 hours of transfection, the media was replaced with 10% serum containing media. The transfected cells were propagated in the presence of a selection agent (G418) and used after 48 hours of stable transfection.

Immunoflourescence

Cancer cells were seeded in a 4 wells chamber (Thermo Scientific, Nunc, Waltham, MA) slides with $1x10^5$ cells in each well. The cells were fixed in 2% paraformaldehyde (PFA) for 15 min, permeabilized for 5 min with Triton-X (0.2%) in PBS solution. After subsequent PBS washes the slides were incubated in PKD1 (1:500), MTA1 (1:1000), GM130 (1:250), p230 (1:250), Ubiquitin (1:500) antibodies for 1 hour at room temperature. After PBS washes, the slides were incubated in anti-mouse cy3 and anti-rabbit Alexa Fluor 488 (1:200) (Thermo Fisher Scientific, Carlsbad, CA) labelled secondary antibody for 1 hour. The slides were then mounted with Vectashield Mounting Medium containing DAPI and processed for confocal microscopy laser with Zeiss 710 confocal microscope (Zeiss, Germany). Similarly, C4-2 cells were fixed, permeabilized and stained lysotracker Red DND-99 (Thermo Fisher Scientific, Carlsbad, CA).

Immunohistochemistry

Prostate cancer PTEN KO and WT and TRAMP mouse tissues were obtained from University of Wisconsin, Madison and are a generous gift from Dr. Bilal Hafeez which were stained using heat-induced antigen retrieval immunohistochemistry techniques with Biocare kit (Biocare Medical, Concord, CA) and analyzed as previously described (208). Prostate cancer Human Tissue Microarray was purchased from AccuMax (ISU Abxis Co., Ltd) whereas Breast and Colon Cancer Human Tissue Microarray were purchased from US Biomax (Rockville, MD). Paraffin-embedded tissue slides were heated at 65^{o}C for 30 minutes and deparaffinized in 2 changes of SlideBrite (Biocare Medical, Concord, CA) and rehydraded in graded alcohol. Tissue slides were incubated in Peroxidazed solution for 5 minutes and antigen retrieval was performed in Biocare Decloacking Chamber at 125^{o}C for 30 seconds while the slides were immersed 1X Diva solution. Slides were then outlined with PAP pen and incubated in Background sniper for 30 minutes. Tissues were washed with TBST (0.1% Tween-20) and incubated in Rabbit PKD1 (C-20) (1:3500) antibody overnight at 4^{o}C or Mouse MTA1 (1:50) antibody in Da Vinci Green diluent for 1 hour at room temperature (in case of double stain IHC). The slides were again washed in TBST and incubated with mouse probe for 30 minutes and HRP-polymer probe for another 30 minutes. Slides were again washed in incubated in 3,3'- diaminobenzidine reagent (DAB) solution for 3 minutes. Hematoxylin

was used as counterstain before dehydrating the slides and mounting with Ecomount mounting media. Slides which were treated with no primary antibody control were used as negative controls.

Animal Studies

Athymic nude male mice were used for these experiments. The mice were maintained in a pathogen-free environment and all procedures were carried out as approved by the UTHSC Institutional Animal Care and Use Committee (UTHSC-IACUC). All the procedures and methods were carried out in "accordance" with the approved guidelines of UTHSC-IACUC.

Subcutaneous Tumors

Athymic nude mice (Cancer Research Animal Core, UTHSC, Memphis, TN) (7 per group) were injected Subcutaneously with C4-2-PKD1-GFP and C4-2-GFP cells. Briefly, C4-2-PKD1-GFP and C4-2-GFP cells (2×10^6 cells/per mouse) were dispersed in 100 µL 1X PBS and 100 µL Matrigel (BD Biosciences) and injected Subcutaneously directly into the dorsal flank of nude mice. Similarly, for *in vivo* functional effect of ORM C4-2 cells (2×10^6 cells/per mouse) mixed with Matrigel were ectopically implanted into dorsal flank of mouse. The animals were periodically monitored for tumor development and the tumor volume was measured using a digital Vernier caliper. The tumor volume was calculated using the ellipsoid volume formula: tumor volume (mm^3) = $\pi/6 \times L \times W \times H$, wherein L is length, W is width, and H is height. The mice were given Intraperitoneal injection of ORM (100 and 500µg/mice) 3 times a week for 5 weeks. The tumor was regularly monitored and allowed to grow until the tumor burden reached a maximum volume of 2000 mm^3 in control group. At the time of sacrifice, the mice tumors were removed, fixed in formalin, embedded in paraffin, and sliced into 5 micron sections for further processing and analysis.

Intra-tibial Bone Metastasis Model

Athymic nude mice (Cancer Research Animal Core, UTHSC, Memphis, TN) were used to generate an intra-tibial model of prostate cancer. Briefly, C4-2-PKD1-GFP and C4-2-GFP cells (1×10^5 cells/per mouse) were dispersed in 10 µL 1X PBS and injected intra-tibially directly into the mice. The animals were periodically monitored for tumor development for over 2 months. The tumor was regularly monitored and allowed to grow until the tumor burden reached a maximum volume of 1100 mm^3. At the time of sacrifice, the mice tibiae were removed, fixed in formalin, demineralized and embedded in paraffin, for further processing and analysis.

Statistical Analyses

Student's t test was used for analysis of statistical significance and the significance was determined using a paired t-test. A p value of < 0.05 was considered significant.

Results

PKD1 Overexpression Inhibits MTA1 Expression in Cancer Cells

MTA1 is known to be upregulated (124,236) whereas PKD1 is known to be downregulated in different cancer cells such as prostate and colon cancer (109,239). But the correlation of PKD1 and MTA1 expression in less metastatic and more metastatic cancer cell line is not very well studied or defined. Therefore, we investigated the expression pattern of PKD1 and MTA1 in less metastatic prostate (LNCaP), colon (SW480) and more metastatic prostate (C4-2), colon (SW48) cancer cell line. We investigated this correlation in these cancer cell lines using immunoblotting and confocal microscopy techniques. Representative immunoblot of prostate and colon cancer cell line has been shown in **Figure 3-1A**. PKD1 expression was more in less metastatic prostate (LNCaP) and colon (SW480) cancer cell line as compared to more metastatic prostate (C4-2) and colon (SW48) cancer cell line. Correspondingly, we observed inverse expression of MTA1; less expression in less metastatic prostate (LNCaP) and colon (SW480) and more expression in more metastatic prostate (C4-2) and colon (SW48) cell line. Real-time expression of these proteins in these cells were observed through confocal microscopy as shown in **Figure 3-1B**. Again, we observed inverse correlation between PKD1 and MTA1 in these cancer cell lines. Subsequently, we used C4-2 and SW480 prostate and colon cancer cell line to transfect and exogenously overexpress PKD1. The representative immunoblot for expression of PKD1 and MTA1 in C4-2-PKD1-GFP/C4-2-GFP and SW480-PKD1-GFP/SW480-GFP overexpressing cells has been shown in **Figure 3-1C**. We observed that when PKD1 is overexpressed in C4-2 prostate and SW480 colon cancer cell line, it leads to inhibition of MTA1 at protein level. Consequently, qRT-PCR of PKD1 overexpressing prostate and colon cancer cell line demonstrate inhibition of MTA1 mRNA in PKD1overexpressing C4-2 prostate and SW480 colon cancer cell line. Representative quantitative qRT-PCR results have been shown in **Figure 3-1D**. To further understand this interaction between PKD1 and MTA1 we performed first silenced the expression of PKD1 using specific PKD1 siRNA in LNCaP cells and observed that inhibition of PKD1 leads to increased expression of MTA1. The representative immunoblot is shown in **Figure 3-1E**. Similarly, we silenced expression of MTA1 using specific MTA1 siRNA in C4-2 cells and observed specific inhibition of MTA1 leads to increased expression of PKD1. The representative immunoblot is shown in **Figure 3-1F**. This study overall confirms a negative correlation between PKD1 and MTA1 proteins.

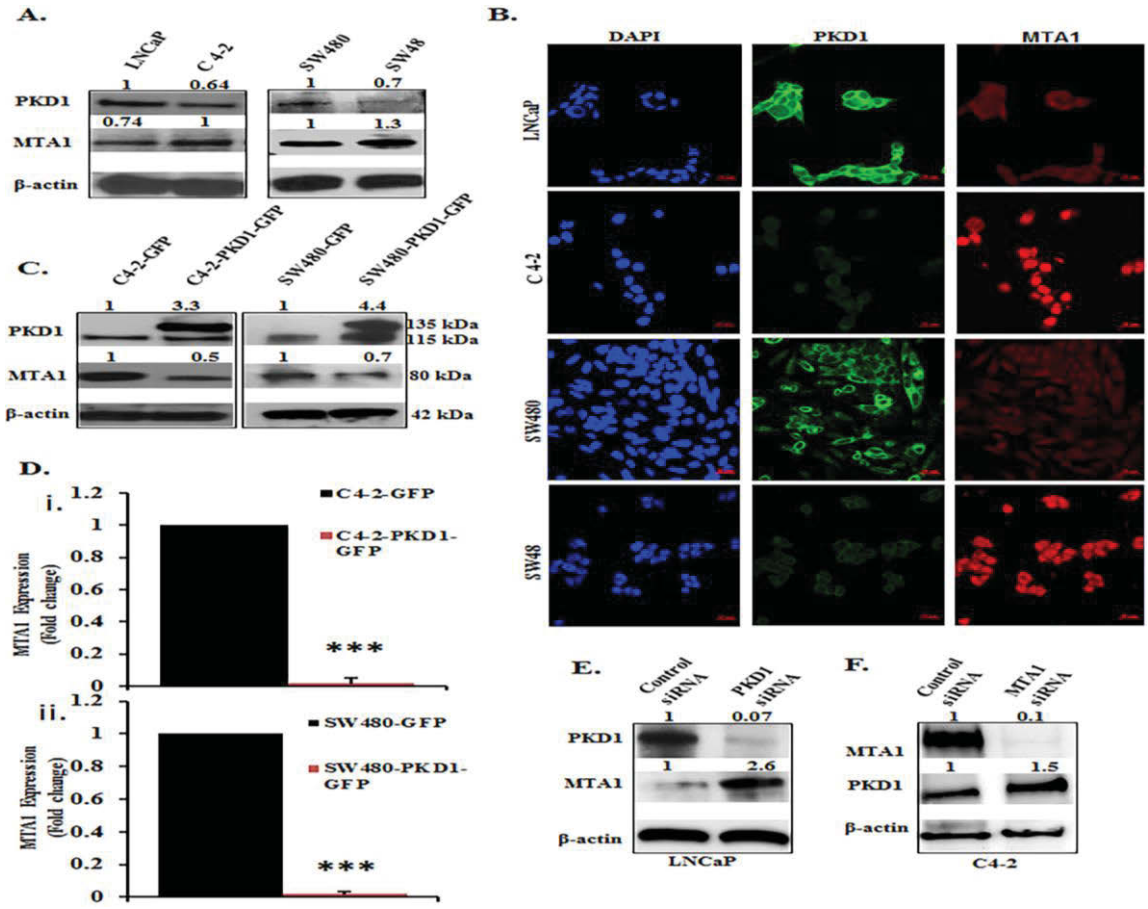

Figure 3-1. PKD1 overexpression inhibits MTA1 expression in cancer cells
A Prostate Cancer (LNCaP, C4-2) and Colon Cancer (SW480, SW48) cells were analyzed for the protein levels of PKD1 and MTA1 by Western blot analysis. **B**. Representative confocal images showing localization of PKD1 (Green) and MTA1 (Red) in LNCaP, C4-2, SW480 and SW48 cells by immunofluorescence. DAPI staining (blue) served as a nuclear marker. **C**. C4-2 and SW480 cells were stably transfected with either PKD1 overexpressing vector (C4-2-PKD1-GFP, SW480-PKD1-GFP) or GFP tagged vector (C4-2-GFP, SW480-GFP) (control). Cell lysates were prepared and subjected to Western blot for examining the protein levels of PKD1 and MTA1. **D**. Effect of PKD1 overexpression on the mRNA expression of MTA1 in PKD1 overexpressing C4-2 and SW480 cells. RNA was isolated and transcribed for cDNA synthesis from control (C4-2-GFP, SW480-GFP) and PKD1 overexpressing (C4-2-PKD1-GFP, SW480-PKD1-GFP) cells. qRT-PCR was performed for mRNA expression of MTA1. **E**. Silencing of PKD1 increases expression of MTA1 in LNCaP cells. LNCaP cells were transiently transfected with control and PKD1 siRNAs for 48 hrs. Lysates were collected for Western blot analysis to determine the protein levels of PKD1 and MTA1. **F**. Silencing of MTA1 increases PKD1 expression in C4-2 cells. Cells were transiently transfected with control and MTA1 siRNA and PKD1 and MTA1 protein levels were examined by Western blot analysis.

PKD1 Interacts with and Phosphorylates MTA1 in Cancer Cells

To investigate the novel association of PKD1 and MTA1 we performed immunoprecipitation assay to confirm whether PKD1 interacts with MTA1 or not. The representative immunoblot of PKD1 immunoprecipitation is shown in **Figure 3-2A**. We observed that there is increased interaction between MTA1 and PKD1 in PKD1 overexpressing cells as compared to GFP control cells in prostate cancer cells. This interaction was further inhibited if the Kinase domain of PKD1 (PKD1.KD) was dead thereby indicating that kinase domain plays a role in PKD1-MTA1 interaction. To further determine if this interaction between PKD1 and MTA1 is a direct interaction we performed Proximity Ligation Assay (PLA). In PLA, we used complementary short DNA sequence which are fluorescently labelled and conjugated to secondary antibody which is raised against primary antibodies from two different species each recognizing a specific epitope on the two different proteins of interest. For both the complimentary DNA sequence to ligate and amplify the distance between two proteins must be less than 30-40 nm. This is an indicator of direct interaction between two different proteins of interest. The representative image of PLA assay is shown in **Figure 3-2B**. We observed that in PKD1 overexpressing cells PKD1-MTA1 interaction is localized to peri-nuclear or cytoplasmic space. This demonstrates that PKD1 mediates MTA1 nuclear export in a very similar manner as it mediates β-catenin nuclear export in prostate cancer cells (120). MUC13 and β-catenin interaction in HPAF cells was used as a negative and positive control. Further, to identify the role of kinase domain in PKD1 and MTA1 interaction we performed kinase assay using phospho-PKD substrate antibody and tried to immunoprecipitate MTA1. We observed that when PKD1 is overexpressed only then MTA1 is immunoprecipitated with phospho-PKD substrate antibody indicating that PKD1 is involved in phosphorylation of MTA1 in PKD1 overexpressing cells. PKD1 which is overexpressed in these cells is modified in such a way that it is constitutively active. In GFP overexpressing cells PKD1 is not constitutively active and hence MTA1 doesn't precipitate out when PKD1 substrate antibody is used. The representative immunoblot is shown in **Figure 3-2C**. Further, to investigate which domain of PKD1 interacts with MTA1 we transiently transfected C4-2 cells with different overexpressing plasmids of PKD1 deletion mutants. Δn corresponds to deletion of N terminal domain of PKD1, ΔAP corresponds to deletion of Alanine proline rich region, ΔC1a and ΔC1b corresponds to deletion of either of the cysteine rich regions a or b. ΔCRD corresponds to deletion of both cysteine rich regions. ΔPH corresponds to deletion of pleckstrin homology domain. We observed that deletion of N terminal domain leads to inhibition of PKD1 and MTA1 interaction indicating that N-terminal domains plays a huge role in interaction of PKD1 and MTA1. Further, we again verified that this interaction was inhibited in case of PKD.KD (kinase dead domain). The representative immunoblot is shown in **Figure 3-2D**.

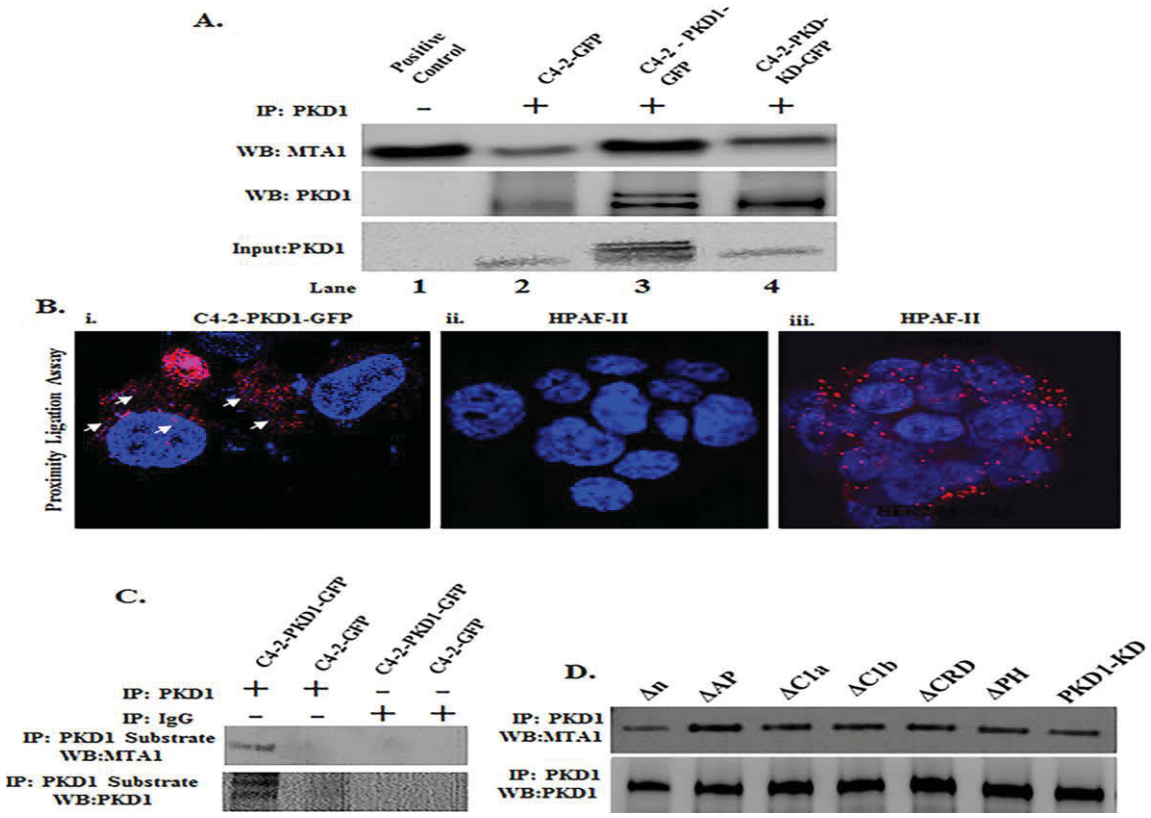

Figure 3-2. PKD1 interacts with and phosphorylates MTA1 in cancer cells
A. C4-2 cells were transiently transfected with GFP tagged PKD1 overexpressing (C4-2-PKD1-GFP) and PKD1 kinase dead (PKD-KD-GFP) plasmid vectors. Cell lysates prepared and subjected to immunoprecipitation (IP) with PKD1 antibody followed by Western blot analysis to detect the interaction of PKD1 and MTA1. Lane 1 is positive control where MB231 cell lysate was used. Lane 2 and lane 3 are IP with PKD1 in C4-2-GFP and C4-2-PKD1-GFP cells, and lane 4 is IP with PKD1 in C4-2-PKD-KD positive control. **B.** Proximity ligation assay (PLA) for interaction of PKD1 with MTA1 in C4-2-PKD1-GFP cells. Representative PLA image showing PKD1-MTA1 interaction localized to peri-nuclear space (red dots) (i). PLA image of MUC13/β-catenin showing no interaction in pancreatic cancer cells (HPAF-II) and serves as negative control (ii). PLA image of HER2/MUC13 showing strong HER2-MUC13 interaction in HPAF-II cells and serves as positive control. **C.** Kinase assay for PKD1 and MTA1 interaction. Lysates from C4-2-PKD1-GFP and C4-2-GFP cells were subjected to IP with phospho-PKD substrate antibody followed by Western blot analysis with MTA1 and PKD1 antibodies to determine phosphorylation of MTA1 by PKD1. IgG was used as negative control. **D.** Interaction of MTA1 with different domains of PKD1 to determine which domain of PKD1 is responsible for interaction of PKD1 with MTA1. C4-2 cells were transiently transfected with different deletion mutants of PKD1 [ΔAC (acidic region deleted), ΔC1a (Cysteine rich region a deleted), ΔC1b (Cysteine rich region b deleted), ΔCRD (Cysteine rich region a & b deleted) ΔPH (pleckstrin homology domain deletion), ΔN (N-terminal domain deletion), PKD1-KD (Kinase dead domain) and full length PKD1. Samples were subjected to IP with PKD1 antibody followed by Western blot analysis for MTA1 and PKD1 proteins.

PKD1 Overexpression Mediated MTA1 Degradation

To investigate the effect of PKD1 overexpression on MTA1 signaling in prostate cancer and colon cell line we performed confocal microscopy experiment to see the localization of MTA1 in PKD1 overexpressing and GFP control cells. The representative confocal image has been shown in **Figure 3-3A** and **3-3B**. We observed that in GFP overexpressing MTA1 was localized to nucleus as it has been known in different cancer cells such as prostate and colon (123,235). But in PKD1 overexpressing cells we observed that MTA1 is not localized to nucleus rather the expression of MTA1 in PKD1 overexpressing cells is dramatically downregulated leading us to believe that MTA1 is degraded in PKD1 overexpressing cells. To determine if this downregulation of MTA1 is a PKD1 dependent phenomenon we performed pulse chase experiment using cycloheximide to inhibit protein translation in both C4-2-GFP and C4-2-PKD1-GFP overexpressing cells. The representative immunoblot has been shown in **Figure 3-3C**. We observed that in GFP control cells there was no change in the expression of MTA1 levels between 2 to 3 hours after addition of cycloheximide, whereas in PKD1 overexpressing cells there is gradual decrease in MTA1 expression levels between 2 and 3 hours after addition of cycloheximide. This demonstrates that MTA1 degradation is a PKD1 dependent phenomenon. Similar results were obtained in SW480-PKD1-GFP and SW480-GFP cells (**data not shown**). To study the molecular mechanism how PKD1 activation is leading to MTA1 degradation we used a known PKD1 modulator Bryostatin-1. Previous work from our lab have shown that PKD1 is activated by small molecular PKD modulator such as Bryostatin-1 (120). We observed that 20 nM and 30 nM concentration of Bryostatin-1 fully activates PKD1 (pPKD1 Ser916). Simultaneously, it also leads to inhibition of MTA1 in a dose dependent mechanism in C4-2 cells. The representative immunoblot is shown in **Figure 3-3D**. To investigate the pathway for PKD1 mediated translocation of MTA1 from Nucleus to peri-nuclear or cytoplasmic space we treated C4-2 cells with 20nM concentration of Bryostatin-1 for different time points and performed confocal microscopy of MTA1 localization with different organelle markers. At 3 hours, post treatment with Bryostatin-1, we observed the localization of MTA1 to be in Golgi apparatus. That means at 3 hours, post activation of PKD1, it phosphorylates and translocate MTA1 to Golgi apparatus as it co-localizes with GM130 a marker for Golgi apparatus. The representative confocal image is shown in **Figure 3-3E**. Again, after 12 hours of post treatment or 12 hours post activation of PKD1, we observed that MTA1 localization to be at trans-Golgi network as it co-localizes with p230 which is a marker for trans-Golgi network. The representative image is shown in **Figure 3-3F**. Further, observation showed us that at 24 hours post treatment or activation of PKD1 the MTA1 protein co-localizes with Lysosomal markers leading to its degradation. This observation is consistent with the fact that with overexpression of PKD1 leads to downregulation of MTA1. The representative image is shown in **Figure 3-3G**.

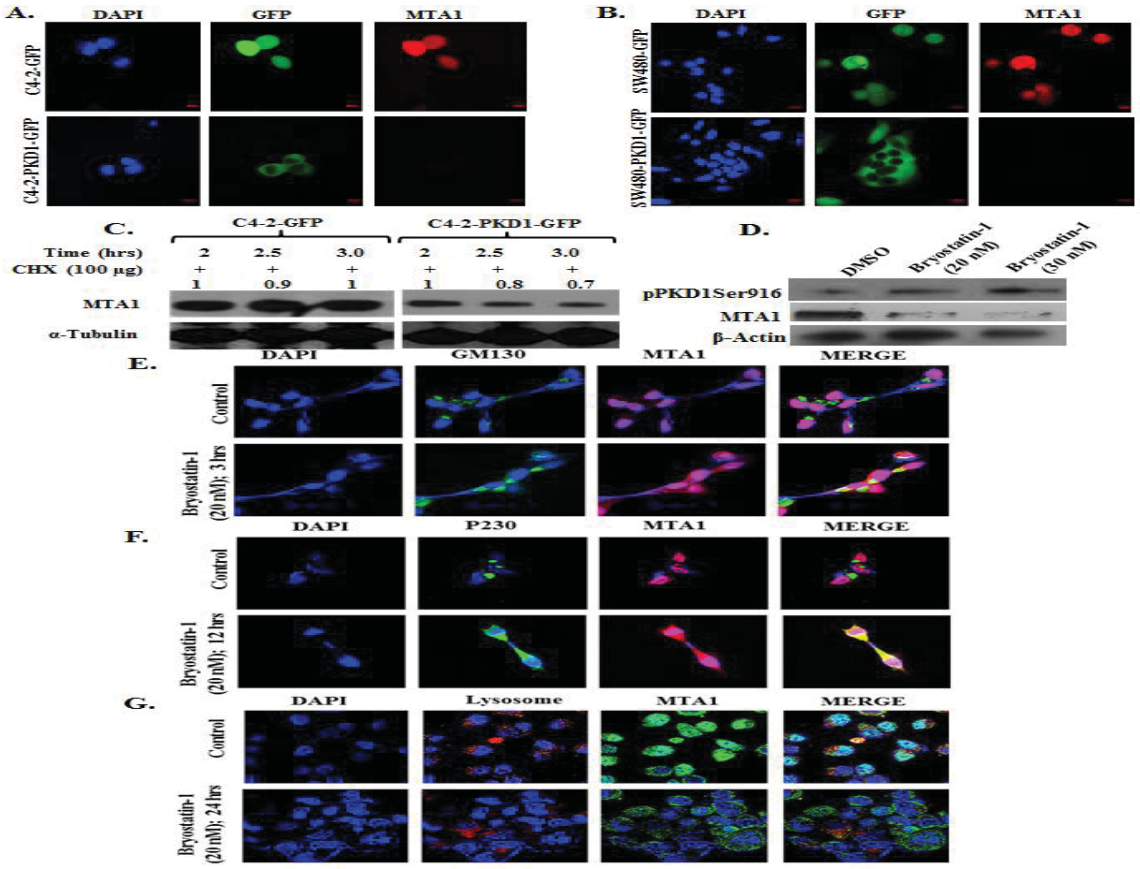

Figure 3-3. PKD1 degrades MTA1 by translocation to lysosome *via* golgi and trans-golgi network

A. Immunofluorescence analysis of PKD1 and MTA1 was performed in GFP tagged control (C4-2-GFP) and PKD1 overexpressing C4-2 (C4-2-PKD1-GFP) cells. Control and PKD1 overexpressing vectors were detected using GFP tag (Green) whereas MTA1 was detected using cy3 labelled secondary antibody (Red). DAPI staining was used as a nuclear marker**. B.** Immunofluorescence analysis of PKD1 and MTA1 was performed in GFP tagged control (SW480-GFP) and PKD1 overexpressing SW480 (SW480-PKD1-GFP) cells **C.** PKD1 overexpression degrades MTA1 protein levels in C4-2 cells. GFP-tagged control and PKD1 overexpressing cells were treated with indicated concentrations of cyclohexamide (CHX) for 2, 2.5 and 3 hrs. **D.** C4-2 cells were treated with indicated concentration of Bryostatin-1 (20 and 30 nM) for 24 hrs. **E.** Representative confocal images. Representative confocal images (lower panel) indicate translocation of MTA1 into golgi. Localization of MTA1 (Red) into golgi was detected by using GM130 (Green) as a marker for golgi in C4-2 cells treated with Bryostatin-1 for 3 hrs**. F.** Representative confocal images (lower panel) indicating translocation of MTA1 into trans-golgi network (TGN). Localization of MTA1 (Red) into TGN was detected by using P230 (Green) as a marker for TGN**. G.** Representative images (lower panel) indicate translocation of MTA1 into lysosome. Localization of MTA1 (Green) into lysosome was detected by using Red lysotracker (Red) as a marker for lysosome.

PKD1 Degrades MTA1 *via* Ubiquitin Dependent Pathway

To further confirm if MTA1 translocation is a ubiquitin mediated translocation, we treated cells with Bryostatin-1 for 24 hours and performed confocal microscopy for co-localization of ubiquitin marker and MTA1 protein. We observed that Ubiquitin marker and MTA1 do co-localize with each other, which indicate that MTA1 translocation although being a PKD1 mediated translocation is a ubiquitin dependent degradation mechanism. The representative image is shown in **Figure 3-4A**. To further verify if this PKD1 mediated MTA1 degradation is a ubiquitin mediated mechanism we used MG132, an inhibitor of ubiquitin mediated proteolysis in presence and absence of Bryostatin-1. The results indicate that MG132 prevents degradation of MTA1 in prostate cancer cells. The representative image is shown in **Figure 3-4B**. Further we performed immunoblot for the expression of MTA1 in Bryostatin-1 treated cells in presence and absence of MG132. The results indicate inhibition of MTA1 in Bryostatin-1 alone treated cells but not in MG132 treated cells. The representative immunoblot is shown in **Figure 3-4C**. Ubiquitin dependent phenomenon is basically of two types - polyubiquitination at lysine 48 site leads proteins to proteosomal degradation (240). To identify if MTA1 degradation is a lysine 48 specific polyubiquitin phenomenon, we immunoprecipitated MTA1 with lysine 48 specific polyubiquitin antibody. We observed that MTA1 immunoprecipitated with lysine 48 specific ubiquitin antibody indicating that MTA1 undergoes both endocytosis and proteosomal degradation at the same time. The representative immunoblot is shown in **Figure 3-4D**.

PKD1 Is Downregulated and MTA1 Is Upregulated in TRAMP Mouse Model

TRAMP mouse mode tissues, RNA and protein samples were acquired from University of Wisconsin, Madison and are a generous gift from Dr. Bilal Hafeez. Immunohistochemistry analysis of 8, 12, 16, 20 and 24 weeks TRAMP tissue shows that PKD1 is downregulated between 8 to 24 weeks TRAMP whereas MTA1 is upregulated in these TRAMP tissues. The representative image is shown in **Figure 3-5A**. Protein analysis of 8 weeks and 24 weeks TRAMP and wildtype tissue shows that PKD1 is expressed in continuously between 8 weeks and 24 weeks wildtype mouse prostate tissues whereas in TRAMP mice model only 8 week TRAMP mice shows PKD1 with no expression at 24 weeks. This is due to the fact at 9 weeks cre proteins start expressing and these mice starts forming tumors. The representative image is shown in **Figure 3-5B**. The RNA analysis of the same samples reveals that PKD1 is expressed in 24 weeks Wiltype prostate tissue but not in 24 weeks TRAMP prostate tissue. Similarly, MTA1 is not expressed in 24 weeks wildtype tissues but highly expressed in 24 weeks TRAMP prostate tissue. The representative qRT-PCR graph is shown in **Figure 3-5C**. qRT-PCR analysis of 8 weeks wildtype and TRAMP show that PKD1 is expressed in 8 week wildtype tissue but not in TRAMP tissue (data not shown).

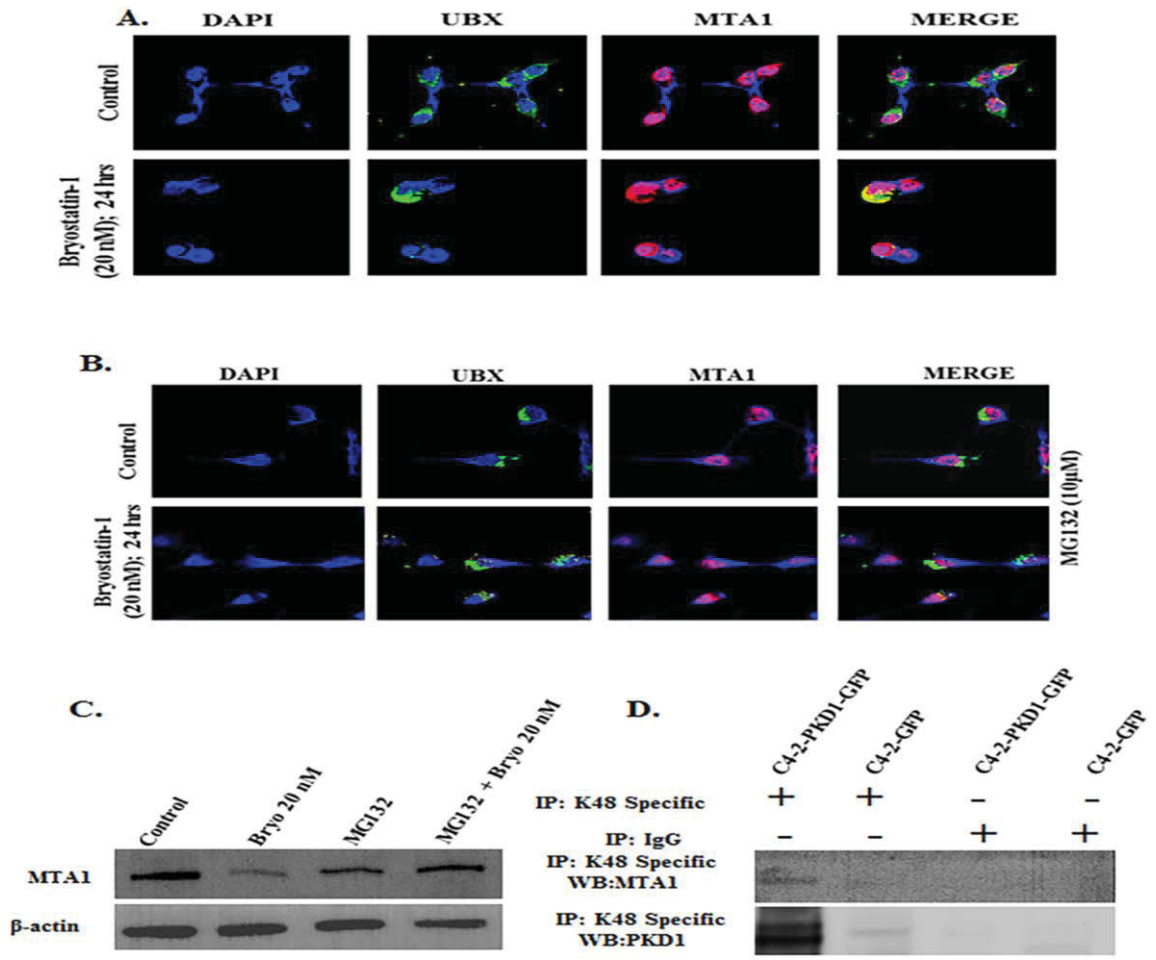

Figure 3-4. PKD1 degrades MTA1 protein *via* ubiquitin mechanism
A. Representative confocal microscopy images (lower panel) indicating co-localization of MTA1 (Red) with Ubiquitin (UBX) marker (Green). Twenty-four hrs post-treatment of Bryostatin-1 activated PKD1 translocates MTA1 to lysosome *via* ubiquitin-dependent mechanism. **B.** Cells were treated with MG132 (10μM) and Bryostatin-1 for 24 hrs and subjected to immunofluorescence analysis for MTA1 and UBX. Representative image indicating co-localization of MTA1 (Red) with Ubiquitin (UBX) marker (Green) in presence of MG132, a proteasome inhibitor in Bryostatin-1 treated cells. **C.** C4-2 cells were treated with Bryostatin-1, MG132 (10μM) and combination of Bryostatin-1 and MG132 for 24 hrs. Lysates were prepared and subjected to Western blot analysis for MTA1 analysis. β-actin was used as a loading control. **D.** Transiently transfected C4-2-PKD1-GFP and C4-2-GFP cells were used and cell lysates prepared. Lysates were subjected to immunoprecipitation in presence of K48 specific polyubiquitin antibody followed by western blotting to determine to detect interaction of MTA1 and K48 specific polyubiquitin antibody. Western blot analysis determines MTA1 being immunoprecipitated with K48 specific polyubiquitin antibody. IgG was used as an internal control.

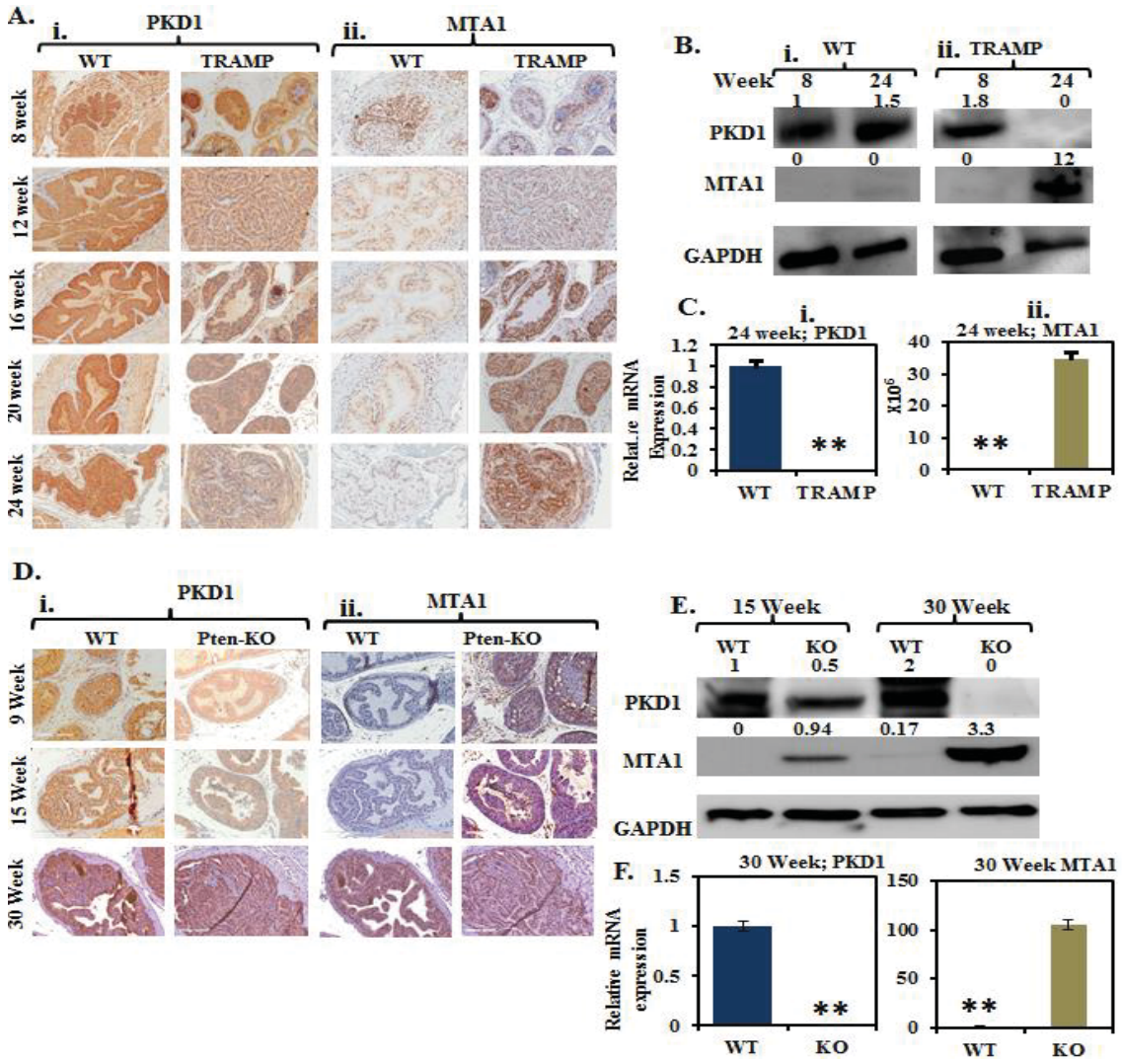

Figure 3-5. PKD1 negatively correlates with MTA1 in prostate tumor tissues of TRAMP and PTEN-knockout (Pten-KO) mice

A. Immunohistochemistry of PKD1 (i) and MTA1 (ii) in the prostate of 8, 12, 16, 20 and 24 weeks old wild type (WT) and TRAMP mice. Result indicate decreased expression of PKD1 and subsequent increased of MTA1 in the prostate tumor of TRAMP mice compared to the respective control (WT). **B**. Different weeks WT and TRAMP mice protein lysates were collected and subjected to Western blot analysis for examine PKD1 and MTA1 protein levels. **C**. mRNA expression of PKD1 and MTA1 in 24 weeks old TRAMP and WT mice. **D**. Immunohistochemistry of PKD1 (i) and MTA1 (ii) in the prostate tumors of 9, 15, and 30 weeks old Pten-KO mice and prostate of WT mice. **E.** Western blot analysis of PKD1 and MTA1 in prostate tissues of 15 and 30 weeks Pten-KO and WT mice. GAPDH was used as a loading control. **F**. mRNA expression of PKD1 and MTA1 expression in prostate tissues of 30 weeks Pten-KO and WT mice. Values in bar graphs are shown as mean ±SD obtained from three experimental replicates. Asterisk (**) indicates statistical significance ($p<0.01$; student's t-test).

PKD1 Is Downregulated in PTEN KO Mice Model

PTEN KO mice model was generated in University of Wisconsin, Madison and the xenograft tissues, RNA and protein samples are a generous gift from Dr. Bilal Hafeez. Analysis PTEN KO xenograft mice tissue sample for PKD1 and MTA1 immunohistochemistry, we observed that in wildtype mice expressing PTEN gene, PKD1 is overexpressed whereas the MTA1 is downregulated at 9 weeks, 15 weeks, and 30 week mice. Whereas, in PTEN KO mice the immunohistochemistry of PKD1 and MTA1 showed that in PTEN KO mice the PKD1 is downregulated whereas MTA1 is upregulated in 9 weeks, 15 weeks, 30 week mice model. The representative images are shown in **Figure 3-5D**. Protein analysis of 15 and 30 weeks wild type and KO mice model shows that PKD1 is abundantly expressed in 15 and 30 weeks wildtype mice model but its expression in inhibited in 15 weeks KO mice model with complete disappearance PKD1 protein expression at 30 weeks KO mice model. Subsequently, in 15 and 30 weeks wildtype mice model no expression of MTA1 is observed. In 15 week PTEN KO mice we observe some expression of MTA1 with abundant expression at 30 weeks. The representative immunoblot for the same is shown in **Figure 3-5E**. Similar effects were observed in qRT-PCR of 15 and 30 weeks wildtype and KO mice model. The representative qRT-PCR graph is shown in **Figure 3-5F**.

***In vitro* Regulation of MTA1**

To understand the functional relevance of PKD1 mediated MTA1 downregulation of cancer cells we performed some *in vitro* functional assays. C4-2 cells overexpressing PKD1 were used to perform invasion and migration assay on xCELLigence system. Overexpression of PKD1 inhibited invasion and migration of cells as compared to GFP control cells. There representative graph for invasion and migration is shown in **Figure 3-6A** and **3-6B**. C4-2 cells were also used to specifically downregulate MTA1 expression by using MTA1 specific siRNA. Downregulation of MTA1 in C4-2 cells inhibited the healing of wound even after 48 hours in a wound healing assay (Data not shown). Further using C4-2 cells transiently transfected with MTA1 siRNA we performed invasion assay. Boyden's chamber coated with matrigel were used and cells were allowed to invade through matrigel for 48 hours. After 48 hours, less number of cells invaded the matrigel column in C4-2 cells transiently transfected with MTA1 siRNA as compared to C4-2 cells transiently transfected with control siRNA (Data not shown). These assays indicate that through activation of PKD1 and subsequent downregulation of MTA1 the prostate cancer cells become less metastastic in nature and hence epithelial to mesenchymal transition in these cells can be inhibited leading to less metastatic cancer cells. C4-2-PKD1-GFP and C4-2-GFP cells were ectopically transplanted on nude mice and the tumor was allowed to form. Over the period of time tumor volume was noted. PKD1 overexpression inhibited tumor formation in nude mice as well as on day 29 after tumor transplantation had significantly lower tumor volume as compared to GFP control cells. The representative mice picture and tumor volume graph is shown **Figure 3-6Ci and 3-6Cii**. Bone metastasis is a very common phenomenon associated with people suffering from prostate cancer (241). Therefore, to observe the effect of PKD1 on prostate cancer

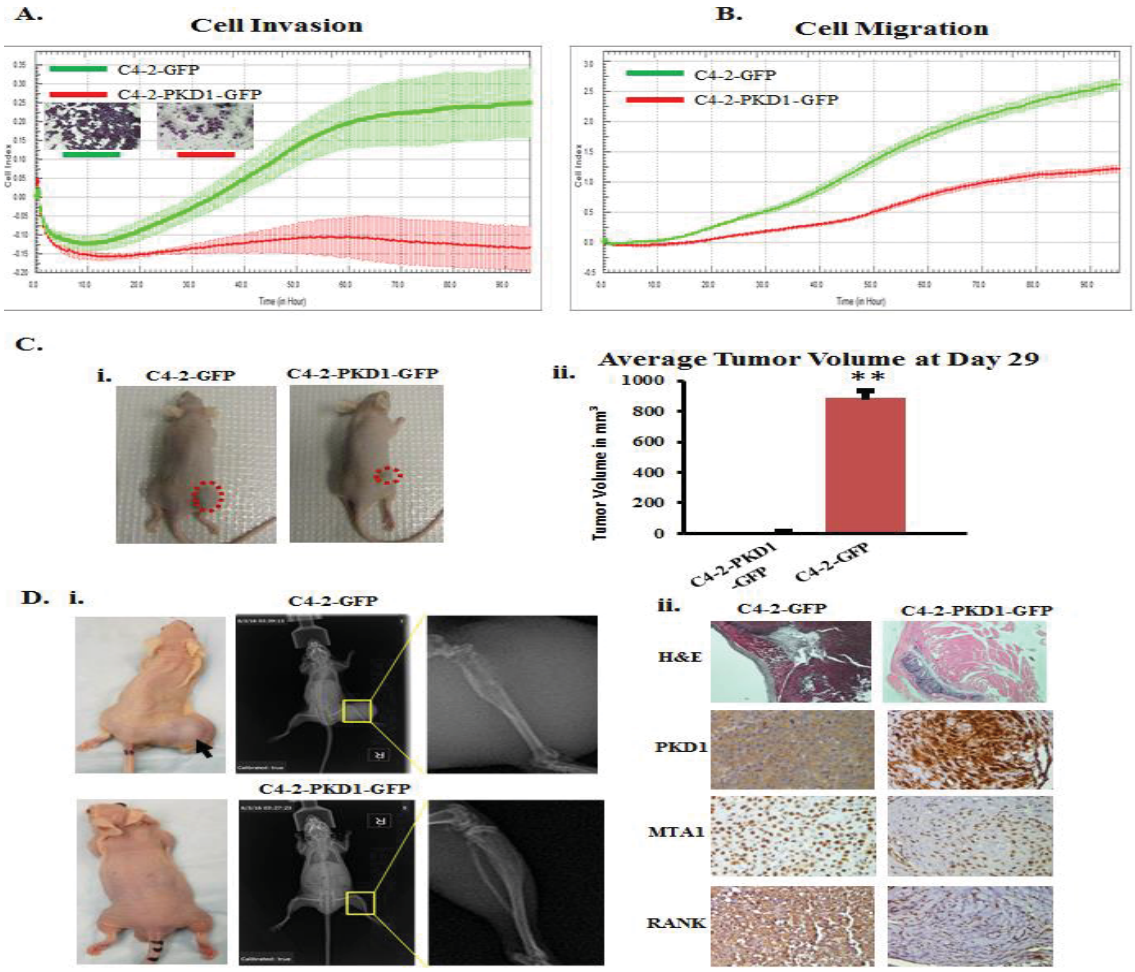

Figure 3-6. PKD1 overexpression inhibits prostate cancer tumor growth and bone metastasis

A. PKD1 overexpression inhibits cell invasion of C4-2 cells. Red bar indicates significantly less invasion of C4-2-PKD1-GFP cells compared to C4-2-GFP. **B.** PKD1 overexpression inhibits cell migration of C4-2 cells. Red bar indicates significantly less migration of C4-2-PKD1-GFP cells compared to C4-2-GFP. **C.** Stably PKD1 overexpressing and GFP control C4-2 cells (2X106) were ectopically transplanted into the dorsal flank of nude mice (n=4). C4-2-PKD1-GFP cells show decreased tumor volume as compared to respective control (C4-2-GFP) indicating PKD1 inhibits prostate cancer tumor growth. Representative tumor bearing mice images (i) and tumor volume (ii) of C4-2-GFP and C4-2-PKD1-GFP implanted cells at day 29. **D.** Overexpression of PKD1 in C4-2 cells inhibits bone metastasis in athymic nude mice. Briefly, nude mice were intra-tibially transplanted with C4-2 cells (1X105) stably transfected with GFP tagged control vector and PKD1 overexpressing vector. Representative images of C4-2-GFP and C4-2-PKD1 cells derived athymic nude mice bearing bone metastasis. X-Ray images showing bone metastasis in C4-2-GFP implanted mice, which did not appear in C4-2-PKD1-GFP implanted mice (i). Histopathological analysis of bone of C4-2-GFP and C4-2-PKD1 implanted mice for the expression of PKD1, MTA1 and RANK proteins as analyzed by immunohistochemistry (ii).

bone metastasis we performed intra-tibial implantation of C4-2-PKD1-GFP and C4-2-GFP cells. After 2 months of transplantation, mice with C4-2-GFP started to show bone metastasis whereas PKD1 overexpressing cells didn't show any bone metastasis indicating PKD1 inhibits prostate cancer bone metastasis. The representative image and mice X-ray is shown in **Figure 3-6Di**. Immunohistochemical analysis of mouse prostate show that expression of RANK1 protein which is marker for osteoclast differentiator receptor and a member of TNF receptor superfamily is highly expressed in C4-2-GFP bone tissues indicating osteoblast to osteoclast formation leading to degradation of bone cells. The representative immunohistochemical analysis is shown in **Figure 3-6Dii**.

PKD1 and MTA1 Expression Is Inversely Correlated in Human Tissue Microarray

To understand the clinical relevance of PKD1 and MTA1 correlation with respect to humans, we performed immunohistochemistry of PKD1 and MTA1 in different Gleason grade Human Tissue Microarray. Gleason grade 7, 8 and 9 tumors and their adjacent normal were stained for PKD1 and MTA1 expression. We observed that PKD1 expression was high in adjacent normal but the expression of PKD1 was inhibited as tumor progressed from Grade 7 to 9. Moreover, the reverse co-relationship was observed for MTA1. There was low or no expression of MTA1 in different adjacent normal but high progressive expression of MTA1 was observed in tumor as they progressed from grade 7 to 9. Similar results were obtained for different stages of Colon and Breast cancer tissues. PKD1 was highly expressed in normal and lower stage tumors but not expressed in higher stage tumors whereas MTA1 was absent in normal and but highly expressed in lower to higher stage tumors tissues. The representative images have been shown in **Figure 3-7A, B, C**. This suggests that MTA1 is upregulated and PKD1 subsequently downregulated as tumors become more aggressive and metastasize to the different parts of the body. Resurgence of PKD1 levels leading to subsequent downregulation of MTA1 may lead cancer to be less aggressive in nature and inhibit cancer cell metastasis.

Ormeloxifene Is a Specific Activator of PKD1 Protein Expression

As a proof of principle to test our hypothesis that activation/overexpression of PKD1 signaling will lead to inhibition of MTA1 activity we wanted to study the effect of pharmacological activation of PKD1 on MTA1 signaling pathway. Our recent studies have shown a potent anti-cancer activity of ormeloxifene in various cancer cell lines such as pancreatic and ovarian cancer cell lines (180-182). Therefore, we investigated the potential of Ormeloxifene as a specific activator on PKD1 activity. Ormeloxifene (ORM) is a non-hormonal, non-steroidal synthetic molecule for human use as an oral contraceptive (176,177). Recently, its anti-cancer activity has been reported against advanced breast cancer (178) and head and neck squamous cell carcinoma (HNSCC) (179). Moreover, ORM is reported to have an excellent therapeutic index and is safe for chronic administration (183). We investigated the anti-cancer efficacy of ORM in C4-2 prostate cancer cells. ORM 5, 10, 15 and 20μM concentrations was used to test its efficacy in C4-2 prostate cancer cells.

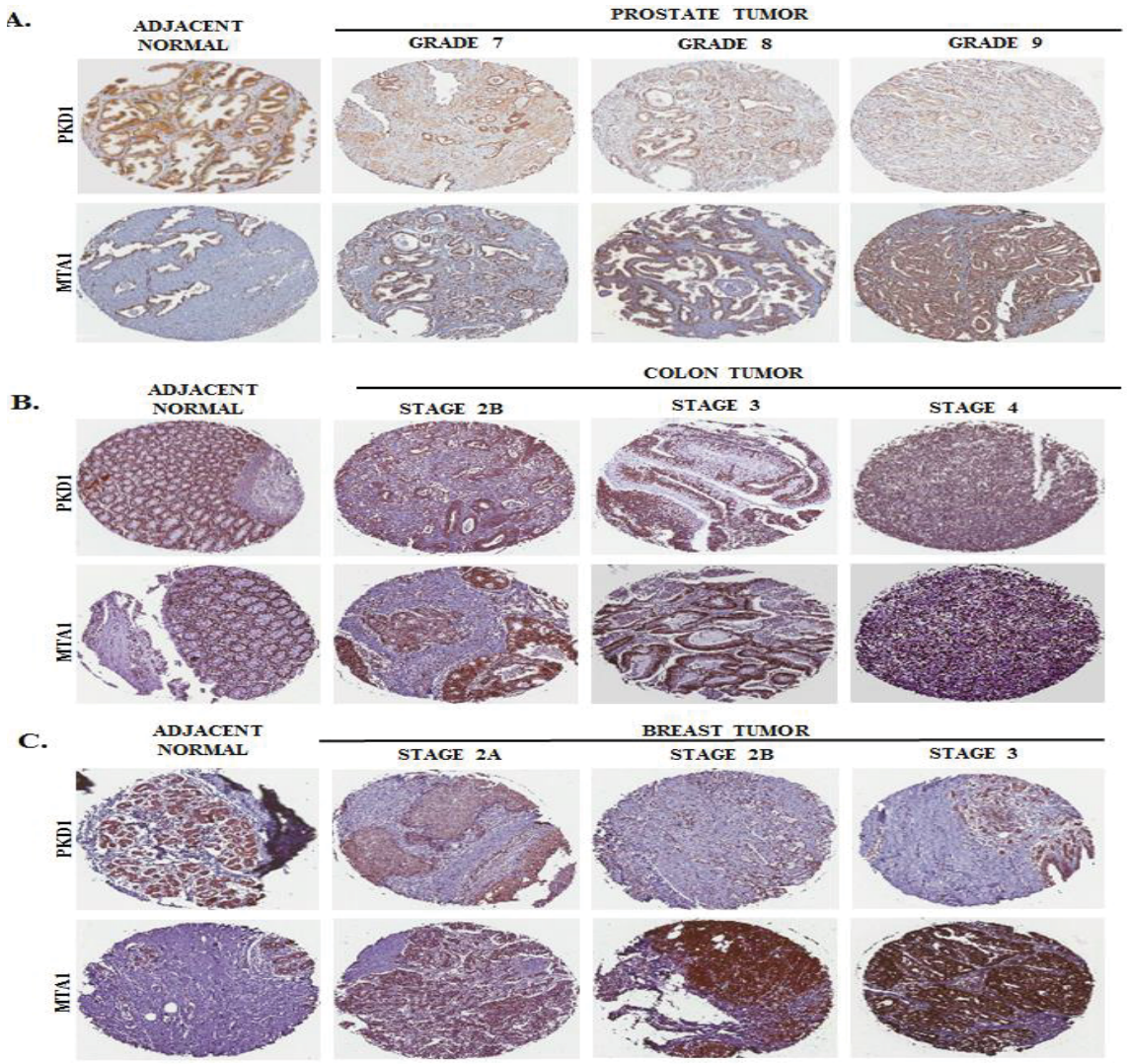

Figure 3-7. PKD1 and MTA1 negatively correlates with the progression of prostate, colon and breast cancers

A. Prostate tissue microarray result indicates the loss of PKD1 and gain of MTA1 with the progression of prostate cancer. Upper panel indicates IHC of PKD1 in grade 7 to 9 prostate tumors vs adjacent normal prostate tissues. Lower panel indicates MTA1 expression in grade 7 to 9 prostate tumor vs adjacent normal prostate tissue as determined by IHC. **B**. Colon tissue microarray result indicates the loss of PKD1 and gain of MTA1 with the progression of colon cancer. Upper panel indicates IHC of PKD1 in stage 2B to 4 colon tumors vs adjacent normal colon tissue. Lower panel indicates MTA1 expression in stage 2B to 4 colon tumors vs adjacent normal colon tissue as determined by IHC. **C.** Breast tissue microarray result indicates the loss of PKD1 and gain of MTA1 with the progression of Breast cancer. Upper panel indicates IHC of PKD1 in stage 2A to 3 breast tumors vs adjacent normal breast tissue. Lower panel indicates MTA1 expression in stage 2A to 3 breast tumors vs adjacent normal breast tissue as determined by IHC.

ORM showed dose dependent effect on C4-2 cell viability as shown in **Figure 3-8A**. The IC50 of ORM was observed at 20 μM concentration. Further, we also observed dose dependent effect on anchorage dependent and independent assay as shown by **Figure 3-8B and 3-8C** respectively. Next, we investigated the effect of ORM on C4-2 cells invasion and we observed that there was dose dependent inhibition of C4-2 invasion potential on treatment with ORM as shown in **Figure 3-8D.** Next, we investigated the effect of ORM on PKD1 and MTA1 protein expression in C4-2 cells at 10μM concentration which is sub toxic (<IC50) concentration. We observed that at 10 μM concentration ORM very specifically activated PKD1 expression, while it had no effect on PKD2 and inhibited PKD3 (PKD isoforms) protein expression which are oncogenic protein as shown in **Figure 3-8E**. At mRNA level ORM increased PKD1 mRNA expression by 4- fold as compared as shown in **Figure 3-8F** while it had no effect on mRNA expression of PKD2 and PKD3 (data not shown).

ORM Inhibits Tumor Growth of Prostate Cancer Cells in Athymic Nude Mice

To investigate the *in vivo* functional effect of ORM on prostate cancer cells, we performed xenograft study using C4-2 cells. A total of 18 mice, were used in the study and were ectopically injected and were divided into three groups (control, ORM 100 μg), and 250 μg). One-week post-cell injection, ORM treatment was started i.p 3 times a week for 5 consecutive weeks. Our results indicated that ORM treatment showed significant ($P<0.01$) dose-dependently inhibition of C4-2 cells derived xenograft tumors in athymic nude when compared with vehicle treated group which was determined by decrease in tumor volume and tumor weight (**Figure 3-9Ai-ii**) and tumor weight **(Figure 3-9Aiii)** compared to control group mice. The average volume of tumors in control mice reached the targeted volume of 1800 mm^3 after 5 weeks. At this time, ORM treated mice average tumor volume was only 700 mm^3 at 100 μg and 350 mm^3 at 500 μg **(Figure 3-9Ai**). There was a significant interaction between treatment and time, so differences were tested over time. The observed differences in tumor development were statistically significant ($P<0.01$) starting at week 3 and continuing until week 5. We isolated the tumor xenograft tissue and performed immunohistochemistry on these mice tissues. We observed that there was dose dependent decrease in PCNA and MTA1 expression whereas dose dependent increase in PKD1 expression with highest effect at 500 μg (**Figure 3-9B).**

Discussion

MTA1 is an integral member of the nucleosome remodeling and histone deacetylase (NuRD) complex and multifunctional DNA damage response protein (121). MTA1 acts as both co-activator and co-repressor of various genes. MTA1 is highly overexpressed in prostate cancer (122). It has been shown that nuclear expression of MTA1 correlates with progression and metastasis of prostate cancer (123) and up-regulation of MTA1 increases EMT (124). Therefore, it is essential to understand the molecular mechanism leading to upregulation of MTA1 expression and

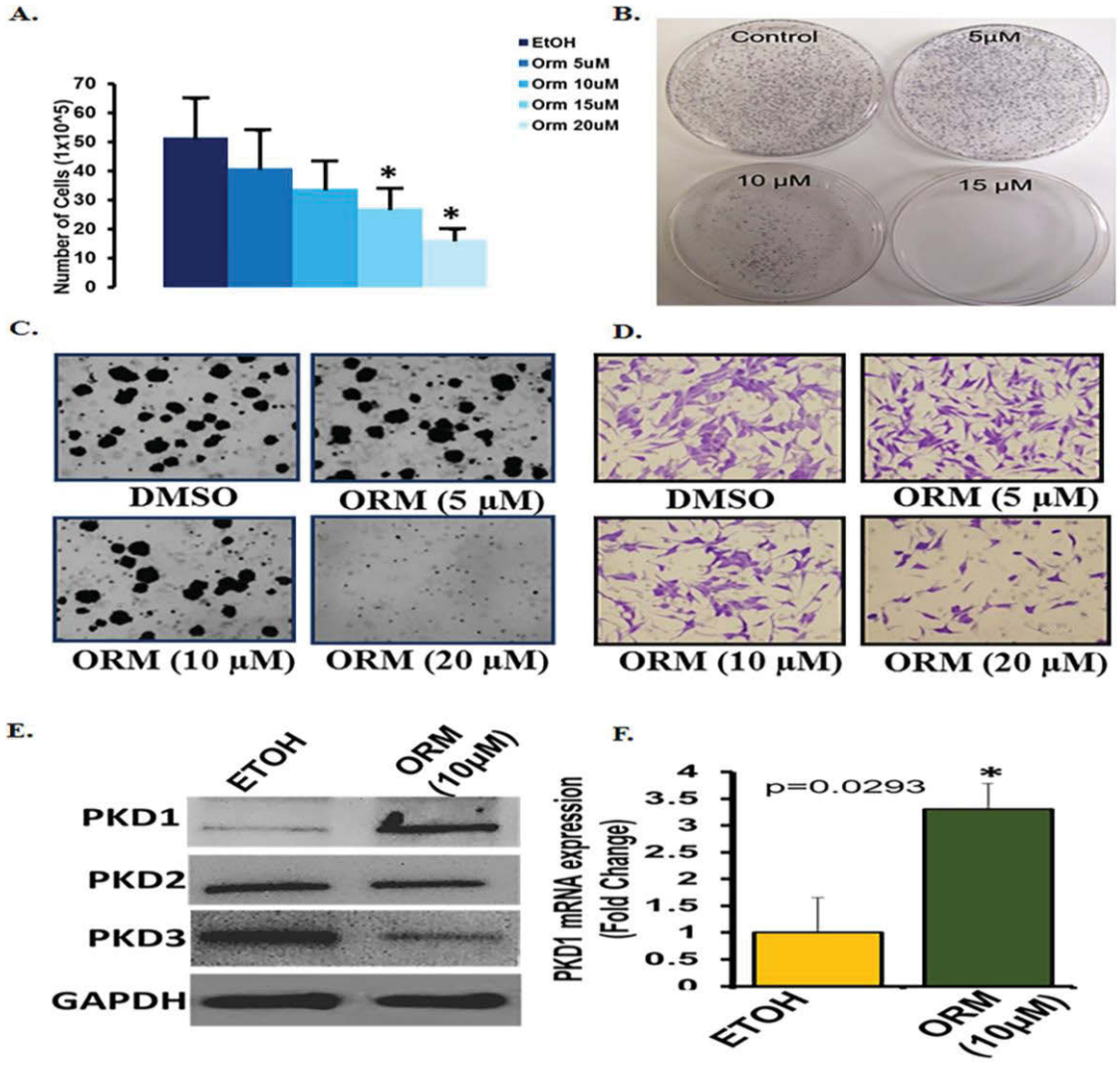

Figure 3-8. Ormeloxifene specific pharmacological activator PKD1 expression in C4-2 cells

A. C4-2 cells were treated with ORM 5, 10, 15 and 20µM concentration and cell viability was determined by the number of viable cells. IC50 concentration of ORM was observed at 20 µM. **B**. ORM inhibited anchorage dependent growth of C4-2 prostate cancer cells. ORM 5, 10 and 15µM concentration was used to determine the effect of ORM on anchorage dependent colony formation assay of C4-2 cells. ORM inhibited anchorage dependent colony formation in a dose dependent manner. **C**. ORM inhibits anchorage independent growth of C4-2 prostate cancer cells. ORM inhibited anchorage independent growth of prostate cancer cells in a dose dependent manner. **D**. ORM inhibited invasion capability of C4-2 prostate cancer cells. C42 cells were treated with different doses of ORM and it inhibited invasive capability of C4-2 cells in a dose dependent manner. **E**. ORM 10µM concentration specifically activated PKD1 whereas on other PKD isoforms it had no effect on PKD2 expression and inhibited PKD3 expression which are oncogenic proteins. **F**. ORM increased mRNA expression of PKD1. ORM 10µM concentration increased PKD1 mRNA expression by four-fold as compared to control treated cells.

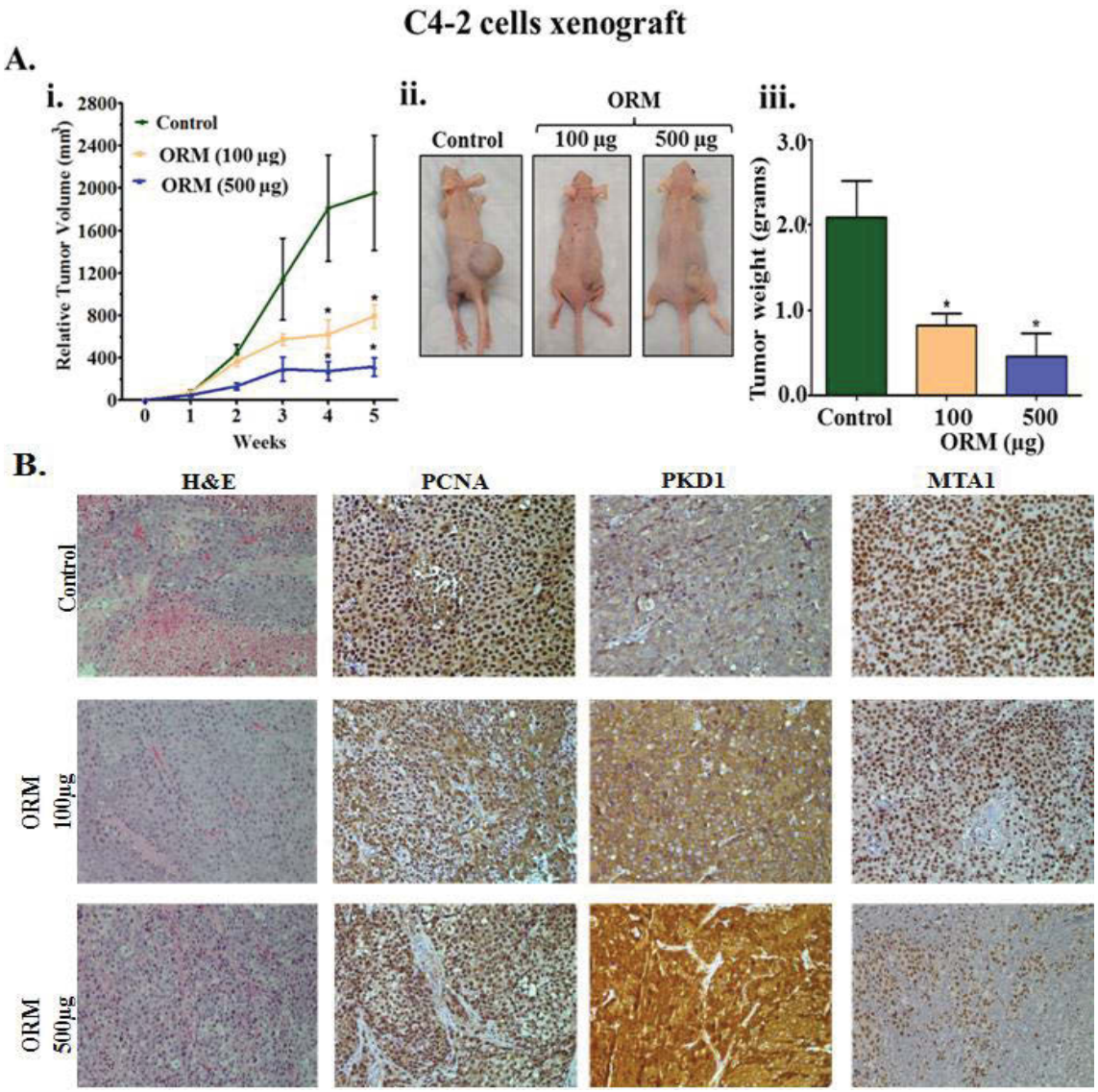

Figure 3-9. Ormeloxifene inhibits C4-2 tumor growth by activating PKD1 and inhibiting MTA1 expression

A. Effect of ORM on C4-2 xenograft tumors in athymic nude mice. Briefly, $2X10^6$ cells were injected ectopically in each athymic nude mouse of indicated groups. A total of 18 mice were used containing 6 mice in each group. ORM treatment (100 and 500 µg) i.p was started at week 1 and continued till 5 weeks. Treatment was given three times/week. **Ai** Line graph is showing mean tumor volume of 4 mice in each group at 1-5 weeks**. Aii.** Representative C4-2 xenograft tumor bear mouse in each group**. Aiii.** Bar graph representing tumor weight of each group mice. Value in graph represents Mean±SE of 4 mice in each group. **B.** Immunohistochemistry of mouse Xenograft tissue. C4-2 mouse xenograft tissues were isolated, fixed and paraffin embedded and analysed for expression of PCNA, MTA1 and PKD1. Dose dependent effect of ORM on MTA1 and PKD1 expression was observed. First column represents subsequent tumor tissue H&E staining**.**

progression of cancer from benign to metastatic state.

PKD1 is a serine threonine kinase which is downregulated in Prostate, Breast and Colon cancer cells. It acts as a tumor suppressor and has emerged as an important modulator of several kinase signal transduction pathways (133). PKD1 functions as regulator of signal trafficking by growth-factor receptors and also regulates cell shape and tumor cell invasion (133). PKD1 expression negatively correlates with the aggressiveness of the cancer and as the cancer becomes metastatic in nature PKD1 expression is completely inhibited. Expression of both PKD1 and MTA1 is inversely correlated in many of the cancers. However, there has been no investigation done to study the link between PKD1 and MTA1 in metastatic cancers. We have for the first time identified a novel molecular interaction between PKD1 and MTA1 leading to cancer acquiring more metastatic phenotype **(Figure 3-1** and **3-2)**. This molecular mechanism of PKD1 and MTA1 is linked to the induction and progression of various types of cancer.

Metastatic and non-metastatic prostate and colon cancer cells were used to identify the protein expression of PKD1 and MTA1. The result of both western blotting and confocal microscopy indicate negative correlation of PKD1 and MTA1 as the cancer progressed from metastatic to non-metastatic in nature and this interaction is not cancer specific but global in nature. Overexpression of PKD1 in prostate and colon cancer cell line inhibited protein and mRNA expression of MTA1. Further silencing of PKD1 upregulated the expression of MTA1 and MTA1 inhibition lead to PKD1 upregulation indicating there is interaction between these two proteins. Immunoprecipitation and Proximity ligation assay indicated direct interaction between MTA1 and PKD1 which leads to MTA1 being phosphorylated and translocation out of the nucleus. Translocation of MTA1 out of the nucleus has a significant impact on inhibition of metastasis as it inhibits its oncogenic function. The N-terminal domain and Kinase domain play a significant role in this interaction. Moreover, translocation of MTA1 by PKD1 is mediated through Golgi to trans-Golgi into lysosomal complex. Lysosomal degradation of MTA1 is a ubiquitin dependent phenomenon whereby MTA1 is polyubiquitinated at lysine 48 amino acid for proteosomal degradation. This phenomenon was further inhibited by polyubiquitin inhibitor MG132. PKD1 overexpression showed inhibition of invasion and migratory capacity of prostate cancer cells and inhibition of prostate cancer tumor growth and bone metastasis in athymic nude mouse model. These results indicate progressive loss of PKD1 leads to tumor growth and bone metastasis in prostate cancer patients.

Further investigation revealed that PKD1 and MTA1 negative regulation is observed in PTEN-KO and TRAMP mouse model (**Figure 3-5A-C** and **3-5D-F)**. There was progressive loss of PKD1 and gain of MTA1 in PTEN-KO and TRAMP mouse model as compared to Wildtype mouse over different weeks. This result indicates that progressive inhibition of PKD1 and upregulation of MTA1 is involved in spontaneous development of prostate cancer. In our study, we have shown that there is progressive loss of PKD1 and progressive gain of MTA1 as tumor progresses from low grade to high grade tumor in human tissue microarray correlating with our findings in mouse model.

Specific pharmacological activator of PKD1 will be able to inhibit MTA1 expression and revert metastatic phenotype of cancer cells. Therefore, we investigated the potential effect of ORM as a novel pharmacological activator of PKD1. Our study revealed ORM specifically activated PKD1 expression and had no effect of PKD2 isoform whereas it inhibited PKD3 isoform. PKD2 and PKD3 have both been shown to be oncogenic in nature. *In vivo* tumor growth analysis revealed inhibition of tumor growth by ORM by activating PKD1 and inhibiting MTA1 expression.

In summary, MTA1 is overexpressed in prostate, breast and colon cancer (122,236,242). Overexpression of PKD1 inhibits MTA1 expression and reverts metastatic phenotype of cancer cells. PKD1 levels negatively correlates and MTA1 levels positively correlates with aggressiveness of prostate, breast and colon cancer. Pharmacological activator of PKD1 leading to inhibition of MTA1 signaling pathway could be a potential therapeutic modality for the treatment of metastatic cancers. Therefore, ORM could be potentially be a novel therapeutic modality for treatment of metastatic cancer as it targets PKD1 and MTA1 signaling cascade. Having showed ORM could potentially be a treatment modality for metastatic cancer, we now wanted to study the effect of ORM on metastatic cancers.

CHAPTER 4. ORMELOXIFENE INHIBITS PROSTATE CANCER METASTASIS BY MODULATING CELL CYCLE REGULATORY PROTEINS AND EMT SIGNALING PATHWAY

Introduction

Prostate Cancer is the second most common and leading cause of death among American men. 180,890 new prostate cancer cases will be diagnosed within the year 2016, and of those cases approximately 26,120 men will die (1). Prostate Cancer in the initial stages is androgen (AR) sensitive and it can be treated with either an androgen-receptor antagonist or chemical castration but as the cancer progresses prostate cancer cells become androgen-resistant and do not respond to Androgen ablation therapy leading to high rates of mortality and morbidity (232). Therefore, effective treatment modality for metastatic prostate cancer is an unmet need.

Activation of Wnt signaling leads to inhibition of β-catenin degradation, resulting in the accumulation of free cytoplasmic β-catenin. This translocates to the nucleus and, in conjunction with TCF4, upregulates the production of various oncogenic signaling components like c-Myc, cyclin-D1, MMP-7, and AR (109). AR mediated signaling plays a critical role in the development and progression of prostate cancer. Gene amplification and mutations in AR are frequently observed in recurrent prostate cancer, which may account for the hypersensitivity of AR to low castrate levels of androgens and altered ligand specificity. Several mechanisms are proposed for androgen-independent (AI) activation of AR in prostate cancer (1,110-114). One of the mechanisms for androgen-independent activation of AR is through β-catenin (115). We have previously reported that β-catenin enhances transactivation of AR in prostate cancer cell (109). Accumulation of nuclear β-catenin and AR, has been reported in advanced stage metastatic prostate cancer (116,117). It has been reported that expression of β-catenin and AR correlates with an increasing prostate tumor grade (117-119) and higher nuclear staining was observed in high Gleason grade metastatic prostate cancer, suggesting an involvement of β-catenin and AR signaling pathways in prostate cancer metastasis. Therefore, drug molecule which can directly targets β-catenin activity leading to suppression of prostate cancer metastasis can be a potential therapeutic modality for treatment of metastatic prostate cancer.

Ormeloxifene (ORM) is a non-hormonal, non-steroidal synthetic molecule for human use as an oral contraceptive (176,177). Recently, its anti-cancer activity has been reported against advanced breast cancer (178) and head and neck squamous cell carcinoma (HNSCC) (179). Moreover, ORM is reported to have an excellent therapeutic index and is safe for chronic administration (183). Herein, we show that ORM shows excellent anti-cancer potential against metastatic prostate cancer. Moreover, it targets cell cycle regulatory proteins leading to cell arrest at G_0/G_1 phase. ORM inhibits key EMT markers and MMPs leading to inhibition of invasion and migration of prostate cancer cells. Further, ORM treatment also inhibits tumor growth of metastatic prostate tumors in athymic nude mice.

Materials and Methods

Cell Lines and Other Materials

Prostate Cancer cells PC3 and DU145 were purchased from ATCC (ATCC, Manassas, Virginia). These cell lines were propagated in RPMI media supplemented with 10% fetal bovine serum (FBS) and 1X antibiotic and antimycotic solution. The media components were purchased from Lonza (Lonza, Walkersville, MD). Ormeloxifene was a generous gift from Dr. Fathi Halaweish lab in South Dakota State University, Brookings, SD. All other chemicals were purchased from Sigma (Sigma-Aldrich, St. Louis, MO) unless mentioned otherwise.

Cell Proliferation

Cell proliferation was determined by either using 3-(4,5-dimethylthiazol-2-yl)-2,5-diphenyltetrazolium bromide (MTT) assay. Briefly, $5x10^3$ cells of PC3 or DU145 were plated in 96-well plates and incubated for 24h in a humidified incubator at 37°C/5% CO_2. After 24h different drug concentration of ORM was added and the cells were grown for 48h. After 48h 20µl/ well of 5mg/ml of MTT was added to the 100µl media containing cells. The cells were allowed to incubate for 6 hours in humidified incubator. After 6h the media was removed and 150µl of DMSO was added and the cells were vigorously shake for 15 minutes. After 15 minutes absorbance was taken at 570nm on microplate reader (Cytation 3, BioTek, Winooski, VT, USA).

Real-Time Cell Proliferation, Migration, and Invasion Assays Through xCELLigence System

To further confirm effects of ORM on cellular growth and motility and invasiveness, real-time migration, invasion, and proliferation assays were performed using the xCELLigence system, as described earlier (180). xCELLigence system is an electrical impedance-based method that allows for the measurement of cell migration, invasion, and proliferation in real time. Briefly, cells (PC3, DU145) were seeded per chamber of cell proliferation (5×10^3) or invasion and migration (7×10^4) plates, and the cells after treatment with ORM were analyzed in xCELLigence instrument at 37 °C, 5 % CO2 for real-time cell proliferation, migration, and invasion assays.

Cell Cycle Analysis

Cell cycle arrest was analyzed by the Telford method. PC3 prostate cancer cells (1×10^6) were plated in a 100-mm dish and allowed to attach overnight. The following day, cells were exposed to either 10, 15 and 20 µM ORM for 24 hrs, trypsinized, washed, fixed with 70% ethanol, stored at 4 °C for an hour, stained with propidium iodide (Sigma-

Aldrich, St. Louis, MO; 50 µg in 1 mL Telford reagent) in the dark for 4 hrs at 4 °C and analyzed by an Accuri C6 Flow Cytometer in FL2 channel.

Western Blotting

Actively growing prostate cancer cells were used for immunoblot analysis as described earlier (120). Briefly, cells (70-80% confluent) were washed with ice-cold phosphate buffer saline (PBS) and lysed in 2X SDS lysis buffer. Equivalent amounts of protein samples were electrophoretically resolved on 4-20% SDS-PAGE gels, blotted onto PVDF membrane (Bio-Rad Laboratories, Hercules, CA), blocked with 10% bovine serum albumin (BSA; 5 ml for one hour) and probed for various proteins using specific primary antibodies. The western blots were incubated with HRP-labeled secondary antibody and the protein bands were developed using Millipore Immobilon western chemiluminescent HRP substrate.

Cell Invasion Assay

Cell invasion assay was performed to investigate the effect of ORM on the cells using BD Biocoat Matrigel Invasion Chambers (BD Biosciences), as per manufacturer's protocol. After 48 h incubation, the invading cells were fixed with methanol and stained with crystal violet and compared to control.

Cell Migration Assay

Cell invasion assay was performed to investigate the effect of ORM on the cells using Boyden's Chambers (BD Biosciences), as per manufacturer's protocol. After 48 h incubation, the migrating cells were fixed with methanol and stained with crystal violet and compared with control.

Molecular Docking

Molecular Docking studies were performed using autodock 4.2 suit by employing Lamarckian genetic algorithm (243). The grid map illustrating the active site pocket for ligands were calculated by autogrid. Docking was accomplished by each cycle with an initial population of 150 individuals and the remaining parameter set as default. Ten conformational docking poses were created and the best docked conformation was selected based on the autodock binding energy (244).The confirmations with the most favorable free binding energy were selected for analyzing the interactions between the target receptor and ligands by visualization with Discovery Studio software (version 3.5). Auto docking 4.2 was used to determine the orientation of inhibitor bound in the active site of the different proteins and the conformation with the highest binding energy value for each protein was chosen for further analysis.

Animal Studies

Athymic nude male mice were used for these experiments. The mice were maintained in a pathogen-free environment and all were carried out as approved by the UTHSC Institutional Animal Care and Use Committee (UTHSC-IACUC). Athymic nude mice (5 per group) were injected Subcutaneously with PC3 cells. Briefly, PC3 cells (2×10^6 cells/per mouse) were dispersed in 100 µL 1X PBS and 100 µL Matrigel (BD Biosciences) and injected Subcutaneously directly into the dorsal flank of nude mice. The animals were periodically monitored for tumor development and the tumor volume was measured using a digital Vernier caliper. The tumor volume was calculated using the ellipsoid volume formula: tumor volume (mm^3) = $\pi/6 \times L \times W \times H$, wherein L is length, W is width, and H is height. The mice were given intraperitoneal injection of ORM (250µg/mice) 3 times a week for 5 weeks. The tumor was regularly monitored and allowed to grow until the tumor burden reached a maximum volume of 1100 mm^3. At the time of sacrifice, the mice tumors were removed, fixed in formalin, embedded in paraffin, and sliced into 5 micron sections for further processing and analysis.

Statistical Analyses

Student's t test was used for analysis of statistical significance and the significance was determined using a paired t-test. A p value of < 0.05 was considered significant.

Results

ORM Treatment Inhibits the Growth of Metastatic Prostate Cancer Cells

Prostate Cancer metastasis is the major cause of mortality and morbidity in prostate cancer patients (1). Thus, we were interested to examine the effect of ORM on metastatic human prostate cancer cells. For this experiment, we used two metastatic prostate cancer cells (PC3 and DU145) and investigated first, the effect of ORM on growth of these cells by MTS assay. We observed that ORM treatment (10-40µM) dose-dependently inhibited viability of both PC3 and DU145 cells. IC50 of ORM was 22µM and 17µM in PC3 (**Figure 4-1Ai**) and DU145 (**Figure 4-1Aii**) cells, respectively, after 24 h treatment, while IC50 of ORM 48 h post-treatment was 20µM in PC3 cells and 15µM in DU145 cells. We next evaluated the effect of ORM treatment on prostate cancer cell proliferation using xCELLigence where we measured the growth of prostate cancer cells in real time for duration of 80 hours using the xCELLigence system (**Figure 4-1Bi-ii**). This assay monitors cell growth in real time by measuring changes in electric impedance between two golden electrodes embedded in the bottom of the cell culture wells. the impedance, which is converted to a cell index value, is directly proportional to the number of cells and also reflects the cells' viability, morphology, and adhesion strength (245). The growth curve, which is presented as a baseline cell index, showed that ORM

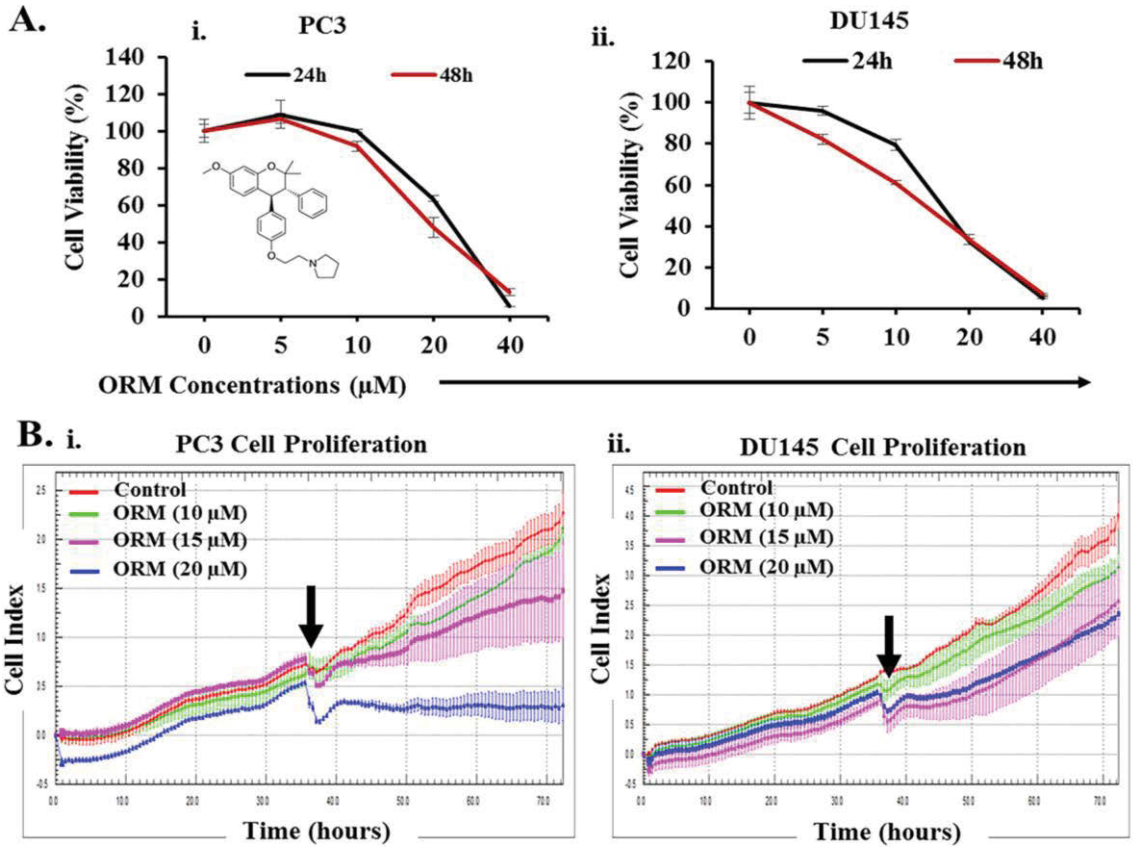

Figure 4-1. ORM inhibits the growth of metastatic prostate cancer cells
A. Effect of ORM on cell viability of PC3 (i) and DU145 (ii) cells. Briefly, cells (2,500) were seeded in each well of 96-well plate and after overnight incubation, cells were treated with the indicated concentrations of ORM for 24 and 48 h. Cell viability was assessed by MTS assay. The line graph represents the percent viable cells compared to the vehicle-treated group cells. Each concentration value is the mean±SE of triplicate wells of each group. **Bi-ii**. Effect of ORM on prostate cancer cells proliferation. Briefly, prostate cancer cells (5,000 cells/well) were seeded in E-plate (xCELLigence) following the xCELLigence Real Time Cell Analyzer (RTCA) DP instrument manual as provided by the manufacturer. After 38 h, ORM or the vehicle control was added and the experiment was allowed to run for 80 h. Average baseline cell index for ORM-treated PC3 (Bi) and DU145 (Bii) cells was compared to vehicle treated group.

significantly reduced the baseline cell index in PC3 (**Figure 4-1Bi**) and DU145 cells compared to vehicle treated cells (**Figure 4-1Bii**).

ORM Treatment Arrests Cell Cycle in G0/G1 Phase

Since, we observed ORM inhibits the growth of prostate cancer cells, therefore, we wanted to further determine the effect of ORM on cell cycle distribution. In this experiment, we synchronized the PC3 cell by starving them in FBS free media for overnight and then treated with ORM (10-50 μM) concentrations for 24 h. Cell cycle analysis was done by flow cytometry. Our results demonstrated that ORM treatment dose-dependently arrests cell cycle in G0-G1 phase of cell cycle in PC3 cells **(Figure 4-2Ai-ii)**. ORM treatment was resulted 60%, 75% and 75% cell cycle arrest in G0-G1 phase at 10, 15 and 20 μM dose respectively compared to vehicle treated cells **(Table in Figure 4-2ii).** Subsequently, we also observed dose dependent increase in sub-G0 or apoptotic cells after ORM treatment **(Figure 4-2B)**.

ORM Treatments Modulates Cell Cycle Regulatory Proteins in Prostate Cancer Cells

We evaluated the effect of ORM on the cell cycle regulatory proteins in prostate cancer cells. ORM treatment inhibited expression of MCL1, cyclin D1, and CDK4 in both PC3 and DU145 cells **(Figure 4-3)** as determined by Western blot analysis. ORM treatment was resulted in the expressions of cell cycle inhibitory proteins (p21 and p27) in both PC3 and DU145 cells **(Figure 4-3)**.

ORM Treatment Inhibits EMT, MMPs, Invasion, and Migration of Prostate Cancer Cells

Epithelial to mesenchymal transition (EMT) is the basic characteristic of metastatic cancer cell in which epithelial cells undergo morphological changes to a motile mesenchymal phenotype, a phenomenon implicated in cancer metastasis but also therapeutic resistance. Therapeutic targeting of EMT has the potential to open a new avenue in the treatment paradigm of metastatic prostate cancer through the reversion of the invasive mesenchymal phenotype to the well differentiated tumor epithelial tumor phenotype (246). Thus, we were interested to investigate whether ORM can inhibit EMT of prostate cancer cells. We evaluated the effect of ORM treatment on various EMT markers in prostate cancer cells. ORM treatment of PC3 and DU145 cells **(Figure 4-4i-ii)** revealed marked inhibition of N-Cadherin, Slug, Snail, and vimentin expressions as determined by Western blot analysis.

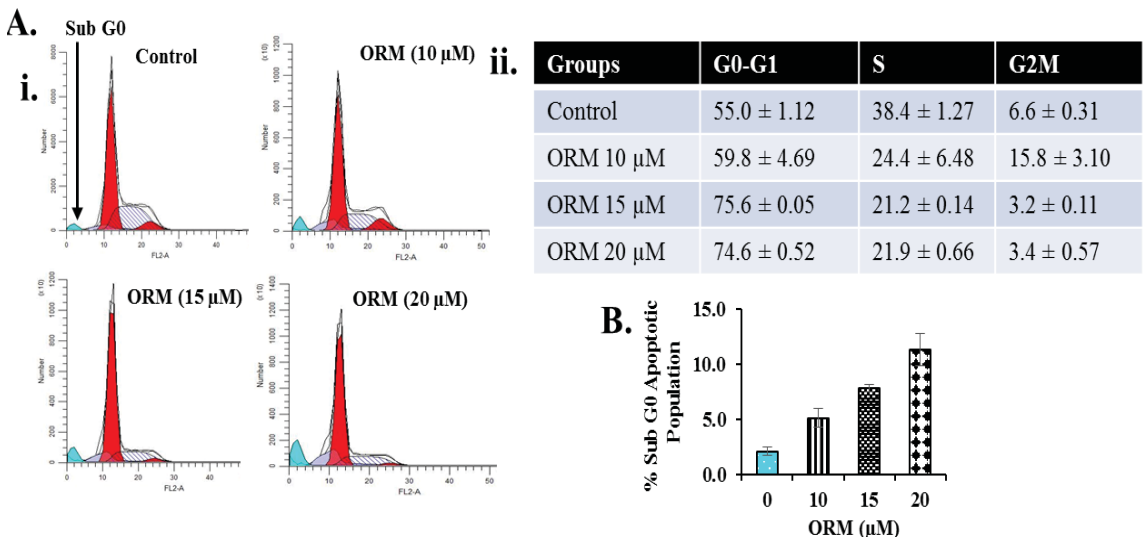

Groups	G0-G1	S	G2M
Control	55.0 ± 1.12	38.4 ± 1.27	6.6 ± 0.31
ORM 10 µM	59.8 ± 4.69	24.4 ± 6.48	15.8 ± 3.10
ORM 15 µM	75.6 ± 0.05	21.2 ± 0.14	3.2 ± 0.11
ORM 20 µM	74.6 ± 0.52	21.9 ± 0.66	3.4 ± 0.57

Figure 4-2. Effect of ORM on cell cycle progression of prostate cancer cells
ORM arrests PC3 cell cycle in G0/G1 phase as determined by flow cytometry. **A**. Histogram (i) and table (ii) represent the cell cycle distribution in PC3 cells. **B**. Bar graph represents the % apoptotic population in vehicle and ORM treated groups.

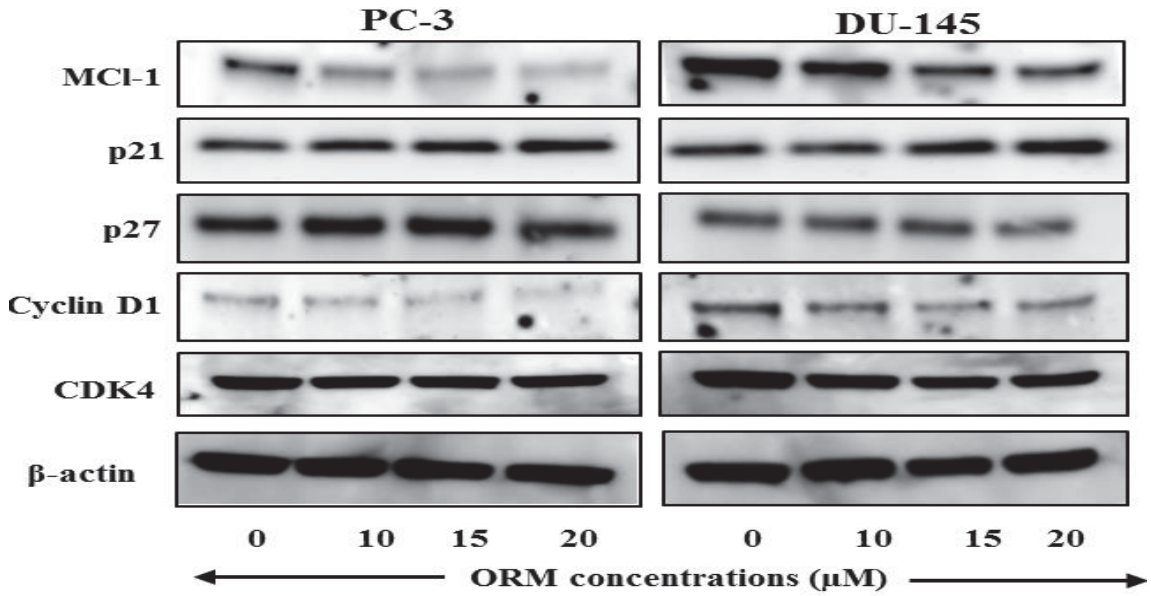

Figure 4-3. Effect of ORM on cell cycle regulatory proteins
Briefly, approximately 70% confluent prostate cancer cells were treated with ORM at indicated concentrations and subjected for Western blot analysis. Results indicated that ORM inhibits the expression of MCl-1, cyclin D1, CDK4 and induced the expression of p21 and p27 in PC3 (i) and DU145 (ii) cells.

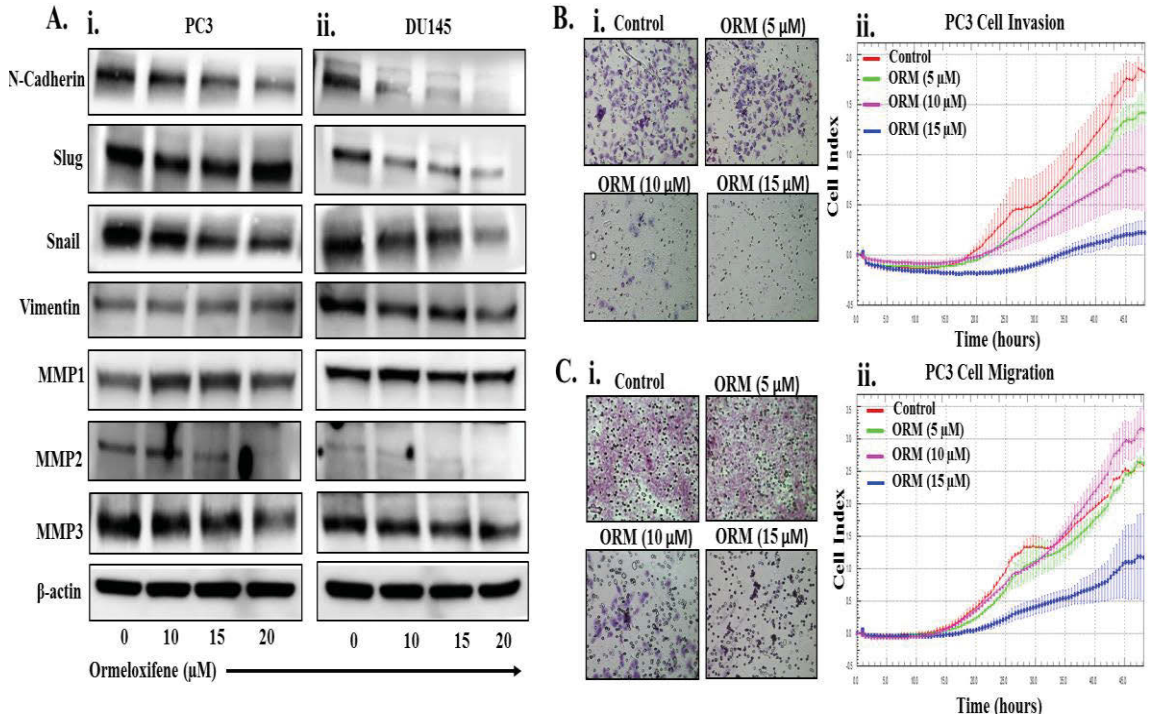

Figure 4-4. Effect of ORM on cell invasion, migration and EMT markers
Briefly, approximately 70% confluent prostate cancer cells were treated with ORM (10-20 μM) for 24 hrs. Cell lysates were prepared and subjected for Western blot analysis for EMT markers and MMPs analysis. **A**. Effect of ORM on indicated EMT markers and MMPs. **B**. Effect of ORM on invasion of PC3 cells as determined by Boyden chamber. **C (i)**. Effect of ORM on invasion of PC3 cells. Arrows in the line graphs indicate time of ORM treatment. Briefly, PC3 cells ($7X10^4$) were seeded in invasion plate and invasion potential of these cells was determined by xCELLigence instrument at 37 °C and 5% CO2 for real time invasion assay. Results indicate that ORM treatment inhibits invasion of PC3 cells as shown. **C (ii)**. ORM treatment inhibits cell migration of PC3 cells. Briefly, PC3 cells ($7X10^4$) were seeded in migration plate and migration potential of these cells was determined by xCELLigence instrument at 37 °C and 5% CO2 for real time migration assay. Results indicate significant decrease in migratory potential of ORM treated PC3 cells compared to control cells.

Activation of MMPs are involved matrix degradation and provide safe environment to cancer cells to invade. The expression of MMP2 and MMP9 play an important role in the metastasis, prognosis and progression of prostate cancer (247-250). Therefore, we investigated the effects of ORM on various MMPs in prostate cancer cells. Our results indicate that ORM treatment inhibited the expression of MMP2 and MMP3 not on MMP1 **(Figure 4-4Ai-ii).** Because we observed that ORM treatment inhibits the EMT markers, therefore, we determined the effect of ORM on invasion and migration of PrC cells *in vitro.* Our results revealed that ORM treatment effectively inhibited both invasion **(Figure 4-4Bi-ii)** and migration **(Figure 4-4Ci-ii)** of PC3 cells.

ORM Docks with β-catenin, GSK3β, and AR/ER

We performed molecular docking using ORM as ligand with androgen receptor (PDB ID: 1E3G) (251) estrogen receptor α (PDB ID:1SJ0) (252), estrogen receptor β (PDB Id: 2NV7) (253), β-catenin (PDB ID: 4DJS) (254) and Glycogen synthase kinase-3β (GSK3 β) (PDB ID: 4ACH) (255) using autodock 4.2 suit by employing Lamarckian genetic algorithm (243). The grid map illustrating the active site pocket for ligands were calculated by autogrid and the dimension of the grid for 1E3G, 1SJ0, 2NV7, 4DJS and 4ACH were 52x40x48, 40x44x56, 50x40x60, 56x50x90 and 60x62x70 grid points respectively with a spacing of 0.375 Aº between the grid points and centered on the ligand. Docking was accomplished by each cycle with an initial population of 150 individuals and the remaining parameter set as default. Ten conformational docking poses were created and the best docked conformation was selected based on the autodock binding energy (244).The confirmations with the most favorable free binding energy were selected for analyzing the interactions between the target receptor and ligands by visualization with Discovery Studio software (version 3.5). Auto docking 4.2 was used to determine the orientation of inhibitor bound in the active site of the different proteins and the conformation with the highest binding energy value for each protein was chosen for further analysis**.** We investigated the binding modes of target proteins with drug using Discovery Studio software (version 3.5). The binding site of target proteins has been used to elucidate the interactions as reported earlier (251-255). Our docking results revealed that ORM binds into the active site of AR (1E3G), ERα (1SJ0), ERβ (2NV7), β-catenin (4DJS) and GSK3 β (4ACH) with minimum binding energy (ΔG) -8.0 kcal/mol, -8.3 kcal/mol, -8.0 kcal/mol, -6.7 kcal/mol and -8.7 kcal/mol respectively **(**Table inset**).** ORM showed interaction with one or more amino acid residue of the protein. The docking results showed that ORM strongly binds with amino acid residue of AR at SER A:865, LYS A:861 **(Figure 4-5Ai-ii)**, β catenin at ASN A:516 **(Figure 4-5Bi-ii),** and GSK3 β at LYS A:85, TYR A:134 **(Figure 4-5Ci-ii)**. These amino acids residues actively participate in forming hydrophobic and hydrophilic interaction. The aromatic ring of ORM are stabilized with π–π interaction of LYS A: 861 of AR and ARG A: 469, ARG A: 515 of β catenin and with aromatic amino acid TYR A134 of GSK3 β. However, molecular docking result shows a quite different orientation of ORM at the active site of different target proteins due to changing of active amino acid residue. ORM shows excellent binding energy and bond distance for AR and β catenin. Overall, these results suggest that ORM may be a potent inhibitor of the AR and β-catenin signaling pathway.

S.N.	Protein Name	Binding Energy (Kcal/mol)	Protein Ligand Interaction			
			No of H Bonds	Pi-Interaction	Amino Acid Residue	Distance (A°)
1.	Androgen receptor (1E3G)	-8.0	1	1	SER865, LYS861	3.4
2.	ER-α (1SJ0)	-8.3	2	-	ARG394, CYS530	2.7, 3.4
3.	ER-β (1SJ0)	-8.0	2	-	ARG466, LY471	3.1, 3.1
4.	β-catenin (4DJS)	-6.7	1	2	ASN 516, ARG515	3.3
5.	GSK3β (4ACH)	-8.7	1	1	LY 85, Val135	3.4, 3.1

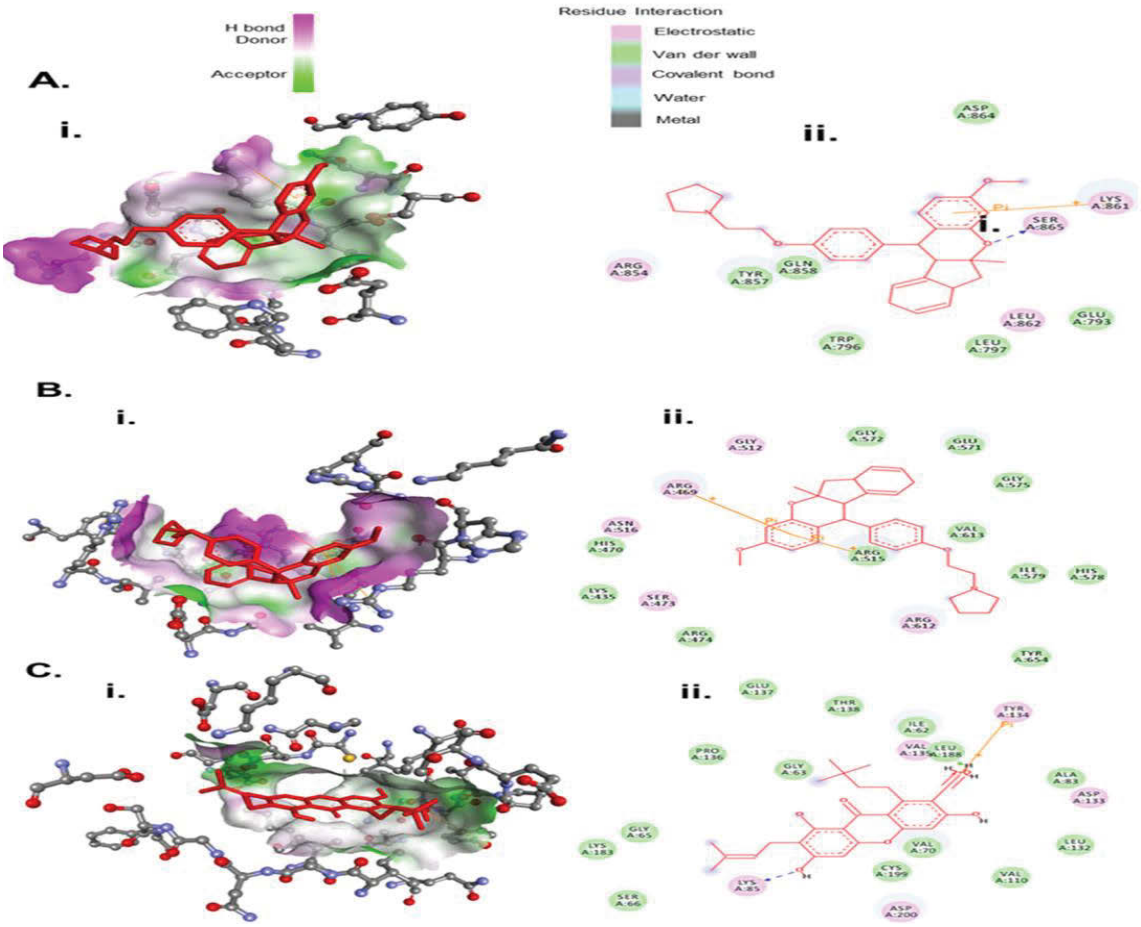

Figure 4-5. Molecular modelling of ORM with AR, GSK3-beta, and β-catenin
Docking study of ORM with androgen receptor (PDBID:1E3G) **(Ai, ii)**, β-catenin (PDBID:4DJS) **(Bi, ii)** and GSK3β (PDBID:4ACH) **(Ci-ii)**. Data generated by Dr. Zubair Hafeez.

ORM Treatment Inhibits the Growth of Metastatic Prostate Cancer Cells Derived Xenograft Tumors in Athymic Nude Mice

We also performed xenograft study using PC3 cells. Results indicate that ORM treatment also inhibited PC3 xenograft tumors at 250 μg dose of ORM as determined by decrease in tumor volume **(Figure 4-6Ai)** and tumor weight **(Figure 4-6Aiii)** when compared with vehicle treated group. Over all these results suggest that ORM is a potent chemotherapeutic agent against prostate cancer. We performed immunohistochemistry analysis of PCNA in excised xenograft tumor tissues. Results revealed a marked decrease nuclear PCNA staining in ORM treated mice xenograft tumors compared to vehicle treated mice (**Figure 4-6B**). Because ORM treatment showed inhibition of β-catenin and MTA1 in vitro, therefore, we also examined the effect of ORM on the expression of these proteins in xenograft tumor tissues. ORM treatment also showed a significant inhibition of β-catenin expression in xenograft tumors as determined by immunohistochemistry (**Figure 4-6B**) and immunofluorescence (**Figure 4-6C**). ORM treatment also inhibited expression of MTA1 protein in xenograft tumors compared to vehicle treatment group (**Figure 4-6B**). ORM treatment also showed a significant inhibition of expression mesenchymal markers such as Snail, Slug, Vimentin and increased expression of epithelial marker such as E-cadherin. This indicates that ORM treatment is reverting the process of EMT in prostate cancer cells (**Figure 4-6B)**. These results suggest that ORM has the ability to inhibit these oncoproteins in prostate cancer cells *in vitro* and *in vivo*.

Discussion

Prostate Cancer metastasis is the major cause of mortality and morbidity in prostate cancer patients (1). Hormone therapy or androgen deprivation therapy (ADT) as it is commonly known is a standard treatment option for advanced and recurrent prostate cancer where the hormones required for the cancer cells to grow is gradually depleted (85). Cancer cells progress to become castration resistant prostate cancer cells within couple of years of ADT. Hence, in depth understanding of ADT-driven molecular changes may yield information about progression to castration resistant prostate cancer. Overexpression of β-catenin has been identified as one of the many ADT regulated signaling pathways. β-catenin enhances transactivation of AR in prostate cancer cell (109). Accumulation of nuclear β-catenin and AR, has been reported in advanced stage metastatic prostate cancer (116,117). It has been reported that expression of β-catenin and AR correlates with an increasing prostate tumor grade (117-119) and higher nuclear staining was observed in high Gleason grade metastatic prostate cancer, suggesting an involvement of β-catenin and AR signaling pathways in prostate cancer metastasis. Therefore, we identified ORM, a non-steroidal triphenylethylene compound that shows excellent anti-cancer efficacy.

Ormeloxifene a non-steroidal Selective estrogen receptor modulator shows

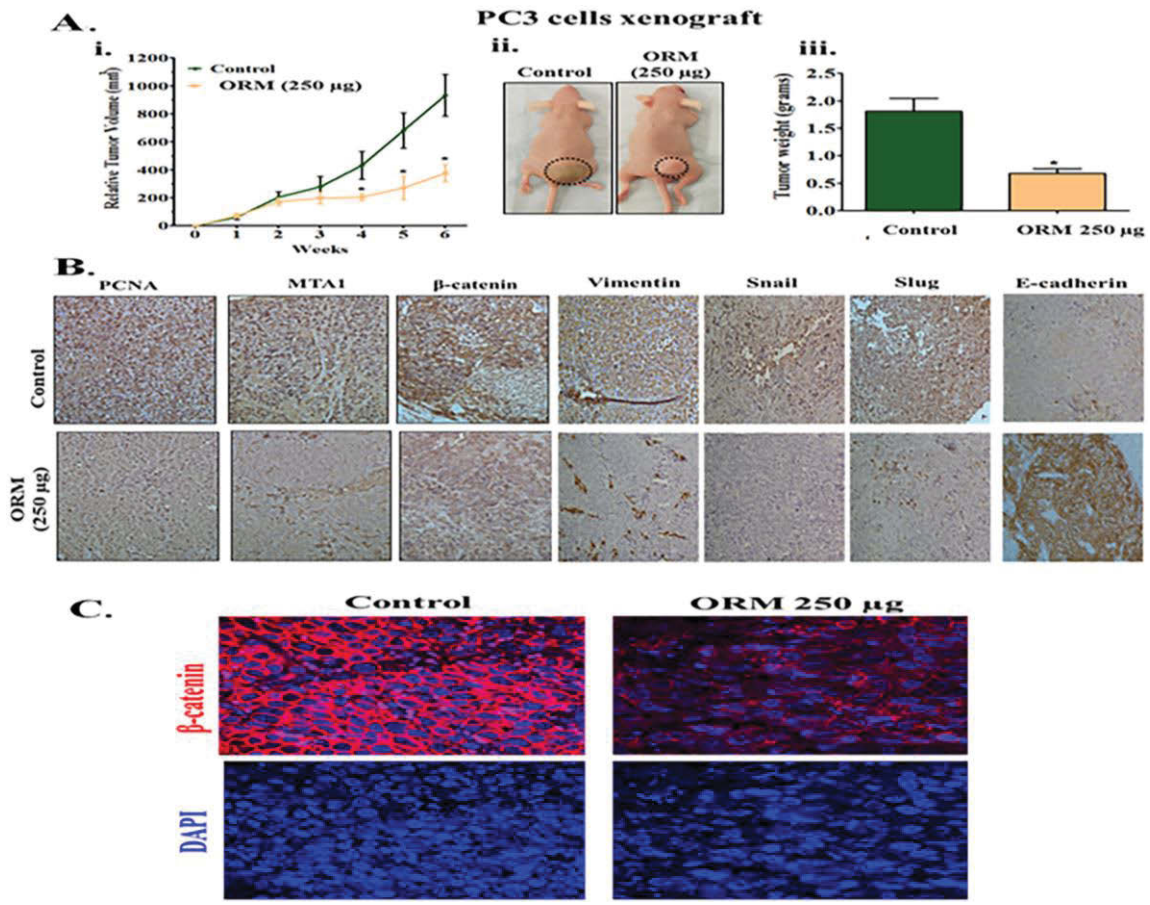

Figure 4-6. ORM inhibits tumor growth of metastatic prostate cancer cells in athymic nude mice

A. Effect of ORM on PC3 xenograft tumors in athymic nude mice. A total of 10 mice were used in this experiment and were divided into two groups (n=5). $2X10^6$ PC3 cells were injected subcutaneously and ORM treatment (250 µg) was administered 3 times a week till 6 weeks. Mice of both the group were sacrificed when control mice showed a targeted tumor volume 1000 mm^3. **Ai.** Average tumor volume of each group mice at different weeks. **Aii.** Representative mouse picture of control and ORM treated tumor bearing mouse. **Aiii**. Bar graph representing tumor weight of each group mice. Value in graph represents Mean±SE of 5 mice in each group. **B.** Effect of ORM on the expression of PCNA, β-catenin, MTA1, Vimentin, Snail, Slug and E-cadherin as determined by Immunohistochemistry analysis. **C**. Effect of ORM on the expression of β-catenin as determined by immunofluorescence.

excellent anti-cancer activity against metastatic prostate cancer cells. Moreover, it targets cell cycle regulatory proteins such as Mcl-1, p21, p27 and Cyclin D1. Investigations of the mechanism of ORM-induced cell death showed the induction of cell cycle arrest at G0-G1 phase, suggesting that ORM may induce apoptosis. These results indicate that in the presence of ORM induces higher apoptotic cell death that might be triggered through the mitochondrial pathway or death receptor mediated cell death.

EMT is a common phenomenon associated with loss of epithelial characteristics and gain of mesenchymal characteristics rendering cells more motile and metastatic in nature. Conversion from epithelial to mesenchymal characteristic is accompanied by loss of epithelial markers such as E-cadherin and gain of mesenchymal markers such as N-cadherin, Snail, Slug, Vimentin. Matrix metalloproteases or MMPs are secreted by cancer cells to help them invade through basal lamina by degrading extracellular matrix. MMP2 and MMP9 play an important role in the metastasis, prognosis and progression of prostate cancer (247-250). Experimental investigations indicate that ORM inhibits mesenchymal markers such as N-cadherin, Snail, Slug, Vimentin and MMPs such as MMP-2 and 9 to inhibit prostate cancer metastasis. All these results confirm that ORM inhibits EMT signaling and prostate cancer metastasis.

The enhanced anti-tumor effect of ORM treatment was observed in xenograft mouse models when compared to control alone**.** Less tumor volume and tumor weight were observed in the ORM treated tumor tissues and less metastatic phenotype as indicated by reduced expression of β-catenin, MTA1, Vimentin, Snail, Slug and increased expression of E-cadherin. This facilitates the anti-cancer effects of ORM and our results have important implications towards the development of effective therapy for metastatic prostate cancer.

CHAPTER 5. CONCLUSION

Protein Kinase D1 (PKD1) and Metastasis associated Protein1 (MTA1) are key regulator of cancer cell progression and metastasis. My work for over 5 years have been focused on identifying the novel relationship between these two proteins and how they regulate each other expression while cancer progresses from benign to metastatic state. Further, I am also involved in identifying potential drug molecules which can target this pathway in such a way that it inhibits cancer progression and metastasis. These compounds have potential to develop as a potential anti-cancer drug molecule.

Protein Kinase D1 (PKD1) is a serine threonine kinase which is downregulated in many of the cancers such as prostate and colon cancer. PKD1 acts as a tumor suppressor in many of the cancers. PKD1 is involved in number of cellular function ranging from cell proliferation to cellular trafficking to epithelial mesenchymal transition. Evidence points toward progressive loss of PKD1 expression as the cancer progresses from non-metastatic to metastatic state. Our previous published results have shown that PKD1 regulated β-catenin signaling in prostate cancer cells by interacting and phosphorylating it. Further, it translocates nuclear β-catenin from nucleus to membrane where it interacts with E-cadherin leading to it activation and cell-cell aggregation and communication. Further our other published results showed that PKD1- β-catenin interaction is not cancer specific and this interaction plays a role in tumorigenesis of colon cancer as well.

In chapter 2, we investigated the role of PKD1 in modulating β-catenin signaling pathway in colon cancer. PKD1 was downregulated and β-catenin was upregulated in different tumor grades of colon cancer as well as different colon cancer cells. Overexpression of PKD1 in different colon cancer cells showed inhibition of cell proliferation, anchorage dependent and independent colony formation as well as β-catenin activity. This effect of PKD1 is induced by nuclear localized PKD1 which interacts with β-catenin and increases its membrane localization. PKD1 overexpression inhibits cellular motility by phosphorylation of cofilin which is critical for de-polymerization of actin filament. Moreover, *in vivo* colon tumorigenesis was influenced by PKD1 overexpression. PKD1 overexpressing colon cancer cells were able to inhibit tumor growth regulating cellular localization of β-catenin. These tumors showed higher necrotic cells but on closer evaluation these cells had higher vasculature and Glut1 expression indicating PKD1 is involved in tumor necrosis.

Metastasis associated Protein 1(MTA1) is upregulated in many cancer cells and involved in initiation of metastasis by inducing epithelial to mesenchymal transition. Progressive gain of MTA1 is known to correlate with aggressiveness of the cancer leading to it acquiring metastatic phenotype. MTA1 is well known to be regulated by β-catenin signaling. MTA1 and PKD1 show negative co-relationship in terms of aggressiveness of the cancer. Therefore, we believe that there could be a co-relationship between MTA1 and PKD1 leading to a novel regulatory signaling pathway which has not been studied yet.

In chapter 3, we observed that PKD1 and MTA1 negatively correlate each other's expression in not only prostate cancer but also colon cancer cells. Overexpression of PKD1 exogenously in prostate cancer cell line which have low PKD1 expression leads to inhibition of MTA1 expression at both protein and mRNA level. This negative relationship was further explored using a specific siRNA's which inhibit the expression of either PKD1 or MTA1 leading to upregulation of the other. This evidence shows there might a possible interaction of PKD1 and MTA1 in cancer cells. To understand this interaction, we performed immunoprecipitation and Proximity ligation assay to confirm that PKD1 and MTA1 do indeed interact with each other leading to regulation of MTA1 signaling pathway. Further, investigation into this pathway revealed that PKD1 being a kinase phosphorylate MTA1 leading to its translocation from nucleus to peri-nuclear space. The regulatory domain and the kinase domain of PKD1 play a significant role in interaction with MTA1. PKD1 overexpression is involved in degradation of MTA1 signaling. To understand if this degradation is PKD1 mediated pulse chase assay was performed using cycloheximide which revealed that MTA1 degradation is expedited by PKD1. To study the mechanism of this degradation pharmacological activator of PKD1 (Bryostatin-1) was used and translocation of MTA1 from nucleus to cytoplasm was tracked using specific markers for different organelles such as Golgi, trans-Golgi and lysosomes. At 3-hour post PKD1 activation MTA1 translocated to Golgi, whereas at 12-hour post activation it translocated to trans-Golgi network. Finally, at 24-hour post activation, MTA1 translocated to lysosome. To understand this PKD1 mediated lysosomal is ubiquitin dependent or ubiquitin independent, we used ubiquitin marker to determine co-localization of MTA1 with ubiquitin. MTA1 indeed co-localized with ubiquitin post Bryostatin-1 treatment. To confirm these findings, we used MG132 an inhibitor of ubiquitin to determine interaction of MTA1 and ubiquitin and MG132 inhibited co-localization of MTA1 and ubiquitin and rescued expression of MTA1 at protein levels. We confirmed that this ubiquitin mediated degradation of MTA1 is lysine 48 dependent mechanism through immunoprecipitation with lysine 48 specific antibody and immunoblotted for MTA1. MTA1 was immunoprecipitated with lysine 48 specific antibody indicating ubiquitin mediated degradation of MTA1.

Having shown interaction of PKD1 and MTA1 is not cancer cell line specific we also investigated the expression of PKD1 and MTA1 in TRAMP and PTEN-KO mouse model. We observed that PKD1 expression was present in abundance in different WT mouse samples but showed progressive loss of PKD1 expression in TRAMP and PTEN-KO mouse model which was further confirmed by protein and mRNA expression. Similarly, WT mouse showed basal level of MTA1 expression whereas TRAMP and PTEN-KO showed progressive increase in MTA1 expression further confirmed by protein and mRNA expression. PKD1 overexpression inhibited cellular invasion and migration as well as tumor growth in ectopic and intra-tibial mouse model. PKD1 overexpressing cells showed low amount of osteoblast to osteoclast transformation as compared to GFP control indicating PKD1 promotes bone formation. Finally, PKD1 and MTA1 inverse correlation had clinical relevance as well as investigation of PKD1 and MTA1 expression showed inverse correlation in human tissue microarray. This indicates progressive loss of PKD1 and progressive gain of MTA1 is responsible for cancer attaining metastatic characteristics. Further, we showed ormeloxifene inhibits prostate

tumor growth and metastasis by inhibiting MTA1 and activating PKD1 expression in mouse xenograft tissue.

In chapter 4, we identified the role of ormeloxifene in inhibiting tumor growth in metastatic prostate cancer. β-catenin is a main player in transformation of hormone sensitive prostate cancer to castration resistant metastatic prostate cancer cells as it regulates Androgen Receptor signaling. It along with MTA1 are major players of metastasis of prostate cancer cells. Therefore, we investigated the anti-cancer potential of ormeloxifene in inhibiting metastatic prostate cancer. Ormeloxifene was able to efficiently inhibit metastatic prostate cancer at 24-hours and 48-hours post treatment as analyzed by MTT and xCelligence analysis. Moreover, it initiated cell cycle arrest at G0/G1 phase in prostate cancer cells by regulating cell cycle proteins such as the expression of MCL-1, p21, p27 and cyclin D1. Further, ormeloxifene is able to inhibit invasion and migration of metastatic prostate cancer cells by targeting EMT markers such as N-cadherin, vimentin, snail and slug, MMP2 and MMP3. *In vivo* functional analysis of the efficacy of ormeloxifene showed that 250µg per mice dose of ormeloxifene 3 times a week given through intraperitoneal route inhibits tumor growth in xenograft mouse model. Immunohistochemistry analysis of xenograft tissue showed inhibition of metastatic markers such as Vimentin, snail, slug, MTA1, β-catenin and activation of epithelial markers such as E-cadherin.

Therefore, PKD1 and β-catenin/MTA1 pathway is a global regulatory pathway which plays a significant role in tumor progression and metastasis. Activation/overexpression of PKD1 can lead to inhibition of tumor growth and metastasis. Pharmacological drug/ PKD1 modulator (Ormeloxifene) induced activation of PKD1 leading to inhibition of β-catenin/MTA1 signaling cascade can be a potent therapeutic modality to treatment of metastatic cancers **(Figure 5-1)**.

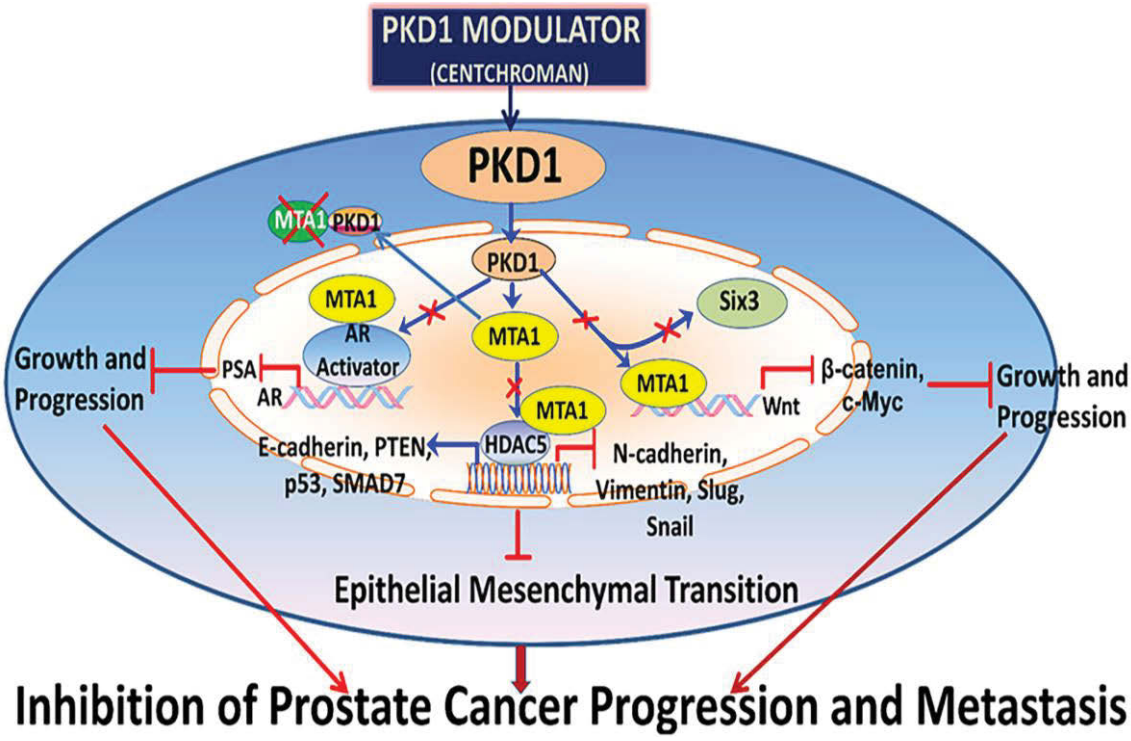

Figure 5-1. Schematic diagram depicting PKD1 modulator induced activation of PKD1 leading to inhibition of β-catenin/MTA1 signaling pathway and cancer metastasis.

LIST OF REFERENCES

1. Siegel RL, Miller KD, Jemal A. Cancer statistics, 2016. CA: a cancer journal for clinicians 2016;66(1):7-30.
2. Mayer RJ. Gastrointestinal Tract Cancer. In: Fauci AS, Braunwald E, Kasper DL, Hauser SL, Longo DL, Jameson JL, et al., editors. Harrison's Princples of Internal Medicine. New York: McGraw Hill; 2008.
3. Edwards B, Ward E, Kohler B, Eheman C, Zauber A. Annual Report to the Nation on the Status of Cancer, 1975-2006, Featuring Colorectal Cancer Trends and Impact of Interventions (Risk Factors, Screening, and Treatment) to Reduce Future Rates. Public Health Resources; 2010. Report nr Paper 244.
4. Kohler B, Ward E, McCarthy B. Annual Report to the Nation on the Status of Cancer, 1975-2007, Featuring tumors of the Brain and other Nervous System. Journal of the National Cancer Institute 2011 May 4:714-36.
5. Colorectal Cancer Facts & Figures 2011-2013. Atlanta: American Cancer Society; 2011.
6. Siegel R, Jemal A, Ward E. Increase in Incidence of Colorectal Cancer Among Young Men and Women in the United States. Cancer Epidemiology Biomarkers Prevention 2009 June:1695-98.
7. Howlader N, Noone A, Krapcho M, Garshell J, Neyman N, Altekruse S, et al. SEER Cancer Statistics Review, 1975-2013. 2016.
8. Baroudi O, Benammar-Elgaaied A. Involvement of genetic factors and lifestyle on the occurrence of colorectal and gastric cancer. Critical reviews in oncology/hematology 2016;107:72-81.
9. Valle L. Recent Discoveries in the Genetics of Familial Colorectal Cancer and Polyposis. Clinical gastroenterology and hepatology : the official clinical practice journal of the American Gastroenterological Association 2016.
10. TNM Classification of Malignant Tumours. Sobin LH, Gospodarowics MK, Wittekind C, editors. New York: Wiley-Blackwell; 2009.
11. Ueno H, Mochizuki H, Hashiguchi Y, Ishiguro M, Kajiwara Y, Sato T, et al. Histological Grading of Colorectal Cancer: A Simpe and Objective Method. Annals of Surgery 2008.
12. Greene FL, Stewart AK, Norton HJ. A new TNM staging strategy for node-positive (Stage III) colon cancer: an analysis of 50,042 patients. Annals of Surgery 2002.
13. Compton CC, Fielding LP, Burgart LJ, Conley B, Cooper HS, Hamilton SR, et al. Prognostic Factors in Colorectal Cancer: College of American Pathologist Consensus Statement 1999. Archives of Pathology & Laboratory Medicine 2000.
14. O'Connell JB, Maggard MA, Ko CY. Colon Cancer Survival Rates With the New American Joint Committee on Cancer Sixth Edition Staging. Journal of the Nation Cancer Institute 2004.
15. Ueno H, Kajiwara Y, Shimazaki H, Shinto E, Hashiguchi Y, Nakanishi K, et al. New Criteria for Histologic Grading of Colorectal Cancer. American Journal of Surgical Pathology 2012.

16. Denoix P. Enquete permanent dans les centres anticancereaux. Bulletin Institut National d'Hygiene 1946:70-75.
17. Edge S, Compton C. The American Joint Committee on Cancer: the 7th edition of the AJCC cancer staging manual and the future of TNM. Annals of Surgical Oncology 2010.
18. Hashiguci Y, Hase K, Ueno H, Shinto E, Mochizuki H, Yamamoto J, et al. Evaluation of the seventh edition of the tumour, node, metastasis (TNM) classification for colon cancer in two nationwide registries of the United States and Japan. Colorectal Disease 2012.
19. Rosenfeld GC, Loose DS. Pharmacology. Baltimore: Lippincott Williams & Wilkins; 2007.
20. Mutch R, Hutson P. Levamisole in the adjuvant treatment of colon cancer. Clinical Pharmacy 1991.
21. Benson AB, 3rd, Venook AP, Bekaii-Saab T, Chan E, Chen YJ, Cooper HS, et al. Colon cancer, version 3.2014. Journal of the National Comprehensive Cancer Network : JNCCN 2014;12(7):1028-59.
22. National Cancer Institute: PDQ Colon Cancer Treatment. 2013.
23. Nelson S, Nathke IS. Interactions and functions of the adenomatous polyposis coli (APC) protein at a glance. Journal of Cell Science 2013;126(4):873-77.
24. Bienz M. The Subcellular Destinations of APC Proteins. Nature reviews Molecular Cell Biology 2002.
25. Powell S, Zilz N, Beazer-Barclay Y, TM B, Hamilton S, Thibodeau S, et al. APC mutations occur early in colorectal tumorigenesis. Nature 1992.
26. Marin O, Bustos VH, Cesaro L, Meggio F, Pagano MA, Antonelli M, et al. A noncanonical sequence phosphorylated by casein kinase 1 in β-catenin may play a role in casein kinase 1 targeting of important signaling proteins. Proceedings of the National Academy of Sciences 2003.
27. Aoki K, Taketo MM. Adenomatous polyposis coli (APC): A multi-functional tumor suppressor gene. Journal of Cell Science 2007.
28. Schneikert J, Brauburger K, Behrens J. APC mutations in colorectal tumours from FAP patients are selected for CtBP-mediated oligomerization of truncated APC. Human Molecular Genetics 2011.
29. Schneikert J, Grohmann A, Behrens J. Truncated APC regulates the transcriptional activity of β-catenin in a cell cycle dependent manner. Human Molecular Genetics 2006.
30. Liu J, Stevens J, Rote CA, Yost HJ, Hu Y, Neufeld KL, et al. Siah-1 Mediates a Novel Beta-catenin Degradation Pathway Linking p53 to the Adenomatous Polyposis Coli Protein. Molecular Cell 2001.
31. Xu W, Kimelman D. Mechanistic insights from structural studies of β-catenin and its binding partners. Journal of Cell Science 2007.
32. Clevers H. Wnt/β-catenin Signaling in Development and Disease. Cell 2006.
33. Polakis P. Wnt signaling in cancer. Cold Spring Harbor Perspectives in Biology 2012.
34. Hierholzer A, Kemler R. Beta-catenin-mediated signaling and cell adhesion in postgastrulation mouse embryos. Developmental Dynamics 2010.

35. Wetering M, Sancho E, Verweij C, Lau W, Oving I, Hurlstone A, et al. The β-catenin/TCF-4 Complex Imposes a Crypt Progenitor Phenotype on Colorectal Cancer Cells. Cell 2002.
36. Kim T, Xiong H, Zhang Z, Ren B. beta-Catenin activates the growth factor endothelin-1 in colon cancer cells. Oncogene 2005.
37. Boon E, Neut R, Wetering M, Clevers H, Pals S. Wnt Signaling Regulates Expression of the Receptor Tyrosine Kinase Met in Colorectal Cancer. The Journal of Cancer Research 2002.
38. Filali M, Cheng N, Abbott D, Leontiev V, Engelhardt J. Wnt-3A/beta-catenin signaling induces transcription from the LEF-1 promoter. Journal of Biological Chemistry 2002.
39. Mann B, Gelos S, Siedow A, Hanski M, Gratchev A, Llyas M, et al. Target genes of beta-catenin-T-cell-factor/lymphoid-enhancer-factor signaling in human colorectal carcinomas. Proceedings of the Nation Academy of Sciences 1999.
40. Roose J, Huls G, Beest M, Moerer P, Horn K, Goldschmeding R, et al. Synergy Between Tumor Suppressor APC and the β-catenin-Tcf4 Target Tcf1. Science 1999.
41. He T, Chan T, Vogelstein B, Kinzler K. PPARdelta is an APC-regulated target of nonsteroidal anti-inflammatory drugs. Cell 1999.
42. Crawford H, Fingleton B, Rudolph-Owen L, Goss K, Rubinfeld B, Polakis P, et al. The metalloproteinase matrilysin is a target of beta-catenin transactivation in intestinal tumors. Oncogene 1999.
43. Jho E, Zhang T, Domon C, Joo C, Freund J, Costantini F. Wnt/beta-catenin/TCF signaling induces the transcription of Axin2, a negative regulator of the signaling pathway. Molecular and Cellular Biology 2002.
44. Conacci-Sorrell M, Ben-Yedidia T, Shtutman M, Feinstein E, Einat P, Ben-Ze'ev A. Nr-CAM is a target gene of the beta-catenin/LEF-1 pathway in melanoma and colon cancer and its expression enhances motility and confers tumorigensis. Genes & Development 2002.
45. Kolligs F, Nieman M, Winer I, Hu G, Van Mater D, Feng Y, et al. ITF-2, a downstream target of the Wnt/TCF pathway, is activated in human cancers with beta-catenin defects and promotes neoplastic transformation. Cancer Cell 2002.
46. Koh T, Bulitta C, Fleming J, Dockray G, Varro A, Wang T. Gastrin is a target of the beta-catenin/TCF-4 growth-signaling pathway in a model of intestinal polyposis. Journal of Clinical Investigation 2000.
47. Wielenga V, Smits R, Korinek V, Smit L, Kielman M, Fodde R, et al. Expression of CD44 in Apc Tcf mutant mice implies regulation by the WNT pathway. The American Journal of Pathology 1999.
48. Batlle E, Henderson J, Beghtel H, van den Born M, Sancho E, Huls G, et al. Beta-catenin and TCF mediate cell positioning in the initestinal epithelium by controling the expression of EphB/ephrinB. Cell 2002.
49. Kim J, Crooks H, Dracheva T, Nishanian T, Singh B, Jen J, et al. Oncogenic beta-catenin is required for bone morphogenetic protein 4 expression in human cancer cells. Cancer Research 2002.

50. Milwa N, Furuse M, Tsukita S, Niikawa N, Nakamura Y, Furukawa Y. Involvement of claudin-1 in the beta-catenin/Tcf signaling pathway and its frequent upregulation in human colorectal cancers. Oncology Research 2001.
51. Zhang T, Otevrel T, Gao Z, Gao Z, Ehrlich S, Fields J, et al. Evidence that APC regulates survivin expressionL a possible mechanism contributing to the stem cell origin of colon cancer. Cancer Research 2001.
52. Zhang X, Gaspard J, Chung D. Regulation of vascular endothelial growth factor by the Wnt and K-ras pathways in colonic neoplasia. Cancer Research 2001.
53. Shimokawa T, Furukawa Y, Sakai M, Li M, Miwa N, Lin Y, et al. Involvement of the FGF18 gene in colorectal carcinogenesis, as a novel downstream target of the beta-catenin/T-cell factor complex. Cancer Research 2003.
54. Jung H, Kim K. Identification of MYCBP as a beta-catenin/LEF-1 target using DNA microarray analysis. Life Sciences 2005.
55. Gavert N, Conacci-Sorrell M, Gast D, Schneider A, Altevogt P, Brabletz T, et al. L1, a novel target of beta-catenin signaling, transforms cells and is expressed at the invasive front of colon cancers. The Journal of Cell Biology 2005.
56. Willert J, Epping M, Pollack JR, Brown PO, Nusse R. A transcriptional response to Wnt protein in human embryonic carcinoma cells. BMC Developmental Biology 2002.
57. Rodilla V, Villanueva A, Obrador-Hevia A, Robert-Moreno A, Fernandez-Majada V, Grilli A, et al. Jagged1 is the pathological link between Wnt and Notch pathways in colorectal cancer. Proceedings of the National Academy of Sciences 2009.
58. Fuchs SY, Spiegelman VS, Kumar KS. The many faces of β-TrCP E3 ubiquitin ligases: reflections in the magic mirror of cancer. Oncogene 2004.
59. Cortina C, Palomo-Ponce S, Iglesias M, Fernandez-Masip J, Vivancos A, Whissell G, et al. EpthB-ephrin-B interactions suppress colorectal cancer progression by compartmentalizing tumor cells. Nature Genetics 2007.
60. Lombardo Y, Scopelliti A, Cammareri P, Todaro M, Iovino F, Ricci-Vitiani L, et al. Bone morphogenetic protein 4 induces differentiation of colorectal cancer stem cells and increases their response to chemotherapy in mice. Gastroenterology 2011.
61. Leow CC, Romero MS, Ross S, Polakis P, Gao W-Q. Hath1, Down-Regulated in Colon Adenocarcinoma, Inhibits Proliferation and Tumorigenesis of Colon Cancer Cells. Cancer Research 2004.
62. Niehrs C. The complex world of WNT receptor signalling. Nature Reviews 2012.
63. Rosen-Arbesfeld R, Townsley F, Bienz M. The APC tumor Suppressor has a nuclear export function. Nature 2000:1009-12.
64. Krieghoff E, Behrens J, Mayr B. Nucleo-cytoplasmic distribution of β-catenin is regulated by retention. Journal of Cell Science 2006.
65. Henderson BR. Nuclear-cytoplasmic shuttling of APC regulates β-catenin subcellular localization and turnover. Nature Cell Biology 2000.
66. Sierra J, Yoshida T, Joazeiro C, Jones K. The APC tumor suppressor counteracts β-catenin activation and H3K4 methylation at WNT target genes. Genes & Development 2006.

67. Miller KD, Siegel RL, Lin CC, Mariotto AB, Kramer JL, Rowland JH, et al. Cancer treatment and survivorship statistics, 2016. CA: a cancer journal for clinicians 2016;66(4):271-89.
68. Torre LA, Bray F, Siegel RL, Ferlay J, Lortet-Tieulent J, Jemal A. Global cancer statistics, 2012. CA: a cancer journal for clinicians 2015;65(2):87-108.
69. Draisma G, Etzioni R, Tsodikov A, Mariotto A, Wever E, Gulati R, et al. Lead time and overdiagnosis in prostate-specific antigen screening: importance of methods and context. Journal of the National Cancer Institute 2009;101(6):374-83.
70. Howlader N NA, Krapcho M, Garshell J, Miller D, Altekruse SF, Kosary CL, Yu M, Ruhl J, Tatalovich Z,Mariotto A, Lewis DR, Chen HS, Feuer EJ, Cronin KA (eds). SEER Cancer Statistics Review, 1975-2012, National Cancer Institute 2014.
71. Rebbeck TR, Devesa SS, Chang BL, Bunker CH, Cheng I, Cooney K, et al. Global patterns of prostate cancer incidence, aggressiveness, and mortality in men of african descent. Prostate cancer 2013;2013:560857.
72. Moller H, Roswall N, Van Hemelrijck M, Larsen SB, Cuzick J, Holmberg L, et al. Prostate cancer incidence, clinical stage and survival in relation to obesity: a prospective cohort study in Denmark. International journal of cancer 2015;136(8):1940-7.
73. Cao Y, Ma J. Body mass index, prostate cancer-specific mortality, and biochemical recurrence: a systematic review and meta-analysis. Cancer prevention research (Philadelphia, Pa) 2011;4(4):486-501.
74. MacInnis RJ, English DR. Body size and composition and prostate cancer risk: systematic review and meta-regression analysis. Cancer causes & control : CCC 2006;17(8):989-1003.
75. Wright ME, Chang SC, Schatzkin A, Albanes D, Kipnis V, Mouw T, et al. Prospective study of adiposity and weight change in relation to prostate cancer incidence and mortality. Cancer 2007;109(4):675-84.
76. Rodriguez C, Patel AV, Calle EE, Jacobs EJ, Chao A, Thun MJ. Body mass index, height, and prostate cancer mortality in two large cohorts of adult men in the United States. Cancer epidemiology, biomarkers & prevention : a publication of the American Association for Cancer Research, cosponsored by the American Society of Preventive Oncology 2001;10(4):345-53.
77. Discacciati A, Orsini N, Andersson SO, Andren O, Johansson JE, Wolk A. Body mass index in early and middle-late adulthood and risk of localised, advanced and fatal prostate cancer: a population-based prospective study. British journal of cancer 2011;105(7):1061-8.
78. Lewis SJ, Murad A, Chen L, Davey Smith G, Donovan J, Palmer T, et al. Associations between an obesity related genetic variant (FTO rs9939609) and prostate cancer risk. PLoS One 2010;5(10):e13485.
79. Steinberger AE, Cotogno P, Ledet EM, Lewis B, Sartor O. Exceptional Duration of Radium-223 in Prostate Cancer With a BRCA2 Mutation. Clinical genitourinary cancer 2016.

80. Pritchard CC, Mateo J, Walsh MF, De Sarkar N, Abida W, Beltran H, et al. Inherited DNA-Repair Gene Mutations in Men with Metastatic Prostate Cancer. The New England journal of medicine 2016;375(5):443-53.
81. Kirkpatrick J. Radical prostatectomy versus watchful waiting in early prostate cancer. Journal of insurance medicine (New York, NY) 2002;34(2):131-2.
82. Widmark A, Klepp O, Solberg A, Damber JE, Angelsen A, Fransson P, et al. Endocrine treatment, with or without radiotherapy, in locally advanced prostate cancer (SPCG-7/SFUO-3): an open randomised phase III trial. Lancet (London, England) 2009;373(9660):301-8.
83. Warde P, Mason M, Ding K, Kirkbride P, Brundage M, Cowan R, et al. Combined androgen deprivation therapy and radiation therapy for locally advanced prostate cancer: a randomised, phase 3 trial. Lancet (London, England) 2011;378(9809):2104-11.
84. Tanderup K, Menard C, Polgar C, Lindegaard JC, Kirisits C, Potter R. Advancements in brachytherapy. Advanced drug delivery reviews 2016.
85. Jin C, Fan Y, Meng Y, Shen C, Wang Y, Hu S, et al. A meta-analysis of cardiovascular events in intermittent androgen-deprivation therapy versus continuous androgen-deprivation therapy for prostate cancer patients. Prostate cancer and prostatic diseases 2016.
86. Horwitz SB. Mechanism of action of taxol. Trends in pharmacological sciences 1992;13(4):134-6.
87. Schiff PB, Horwitz SB. Taxol stabilizes microtubules in mouse fibroblast cells. Proc Natl Acad Sci U S A 1980;77(3):1561-5.
88. Clarke SJ, Rivory LP. Clinical pharmacokinetics of docetaxel. Clinical pharmacokinetics 1999;36(2):99-114.
89. Royer I, Monsarrat B, Sonnier M, Wright M, Cresteil T. Metabolism of docetaxel by human cytochromes P450: interactions with paclitaxel and other antineoplastic drugs. Cancer research 1996;56(1):58-65.
90. Monegier B, Gaillard C, Sablé S, Vuilhorgne M. Structures of the major human metabolites of docetaxel (RP 56976 - Taxotere®). Tetrahedron Letters 1994;35(22):3715-18.
91. Verweij J, Clavel M, Chevalier B. Paclitaxel (Taxol) and docetaxel (Taxotere): not simply two of a kind. Annals of oncology : official journal of the European Society for Medical Oncology / ESMO 1994;5(6):495-505.
92. Kruijtzer CM, Beijnen JH, Schellens JH. Improvement of oral drug treatment by temporary inhibition of drug transporters and/or cytochrome P450 in the gastrointestinal tract and liver: an overview. The oncologist 2002;7(6):516-30.
93. Mellado B, Jimenez N, Marin-Aguilera M, Reig O. Diving Into Cabazitaxel's Mode of Action: More Than a Taxane for the Treatment of Castration-Resistant Prostate Cancer Patients. Clinical genitourinary cancer 2016;14(4):265-70.
94. Goldberg AA, Titorenko VI, Beach A, Sanderson JT. Bile acids induce apoptosis selectively in androgen-dependent and -independent prostate cancer cells. PeerJ 2013;1:e122.
95. Teixeira AL, Gomes M, Nogueira A, Azevedo AS, Assis J, Dias F, et al. Improvement of a Predictive Model of Castration-Resistant Prostate Cancer:

Functional Genetic Variants in TGFbeta1 Signaling Pathway Modulation. PloS one 2013;8(8):e72419.
96. Giannakakou P, Gussio R, Nogales E, Downing KH, Zaharevitz D, Bollbuck B, et al. A common pharmacophore for epothilone and taxanes: molecular basis for drug resistance conferred by tubulin mutations in human cancer cells. Proceedings of the National Academy of Sciences of the United States of America 2000;97(6):2904-9.
97. Nettles JH, Li H, Cornett B, Krahn JM, Snyder JP, Downing KH. The binding mode of epothilone A on alpha,beta-tubulin by electron crystallography. Science (New York, NY) 2004;305(5685):866-9.
98. Darshan MS, Loftus MS, Thadani-Mulero M, Levy BP, Escuin D, Zhou XK, et al. Taxane-induced blockade to nuclear accumulation of the androgen receptor predicts clinical responses in metastatic prostate cancer. Cancer research 2011;71(18):6019-29.
99. Ueda K, Cardarelli C, Gottesman MM, Pastan I. Expression of a full-length cDNA for the human "MDR1" gene confers resistance to colchicine, doxorubicin, and vinblastine. Proceedings of the National Academy of Sciences of the United States of America 1987;84(9):3004-8.
100. Gottesman MM, Fojo T, Bates SE. Multidrug resistance in cancer: role of ATP-dependent transporters. Nature reviews Cancer 2002;2(1):48-58.
101. O'Neill AJ, Prencipe M, Dowling C, Fan Y, Mulrane L, Gallagher WM, et al. Characterisation and manipulation of docetaxel resistant prostate cancer cell lines. Molecular cancer 2011;10:126.
102. Giannelli G, Koudelkova P, Dituri F, Mikulits W. Role of epithelial to mesenchymal transition in hepatocellular carcinoma. Journal of hepatology 2016;65(4):798-808.
103. van Roy F, Berx G. The cell-cell adhesion molecule E-cadherin. Cellular and molecular life sciences : CMLS 2008;65(23):3756-88.
104. Lee GA, Hwang KA, Choi KC. Roles of Dietary Phytoestrogens on the Regulation of Epithelial-Mesenchymal Transition in Diverse Cancer Metastasis. Toxins 2016;8(6).
105. Barriga EH, Mayor R. Embryonic cell-cell adhesion: a key player in collective neural crest migration. Current topics in developmental biology 2015;112:301-23.
106. Miyamoto Y, Sakane F, Hashimoto K. N-cadherin-based adherens junction regulates the maintenance, proliferation, and differentiation of neural progenitor cells during development. Cell adhesion & migration 2015;9(3):183-92.
107. Bryan RT. Cell adhesion and urothelial bladder cancer: the role of cadherin switching and related phenomena. Philos Trans R Soc Lond B Biol Sci 2015;370(1661):20140042.
108. Gonzalez DM, Medici D. Signaling mechanisms of the epithelial-mesenchymal transition. Science signaling 2014;7(344):re8.
109. Mak P, Jaggi M, Syed V, Chauhan SC, Hassan S, Biswas H, et al. Protein kinase D1 (PKD1) influences androgen receptor (AR) function in prostate cancer cells. Biochemical and biophysical research communications 2008;373(4):618-23.

110. Edwards J, Bartlett JM. The androgen receptor and signal-transduction pathways in hormone-refractory prostate cancer. Part 2: Androgen-receptor cofactors and bypass pathways. BJU Int 2005;95(9):1327-35.
111. Zhou J, Scholes J, Hsieh JT. Signal transduction targets in androgen-independent prostate cancer. Cancer metastasis reviews 2001;20(3-4):351-62.
112. Silvestris N, Leone B, Numico G, Lorusso V, De Lena M. Present status and perspectives in the treatment of hormone-refractory prostate cancer. Oncology 2005;69(4):273-82.
113. Chau CH, Figg WD. Molecular and phenotypic heterogeneity of metastatic prostate cancer. Cancer Biol Ther 2005;4(2):166-7.
114. Quinn DI, Henshall SM, Sutherland RL. Molecular markers of prostate cancer outcome. Eur J Cancer 2005;41(6):858-87.
115. Wang G, Wang J, Sadar MD. Crosstalk between the androgen receptor and beta-catenin in castrate-resistant prostate cancer. Cancer research 2008;68(23):9918-27.
116. Chesire DR, Isaacs WB. Ligand-dependent inhibition of beta-catenin/TCF signaling by androgen receptor. Oncogene 2002;21(55):8453-69.
117. Chesire DR, Ewing CM, Gage WR, Isaacs WB. In vitro evidence for complex modes of nuclear beta-catenin signaling during prostate growth and tumorigenesis. Oncogene 2002;21(17):2679-94.
118. Jaggi M, Johansson SL, Baker JJ, Smith LM, Galich A, Balaji KC. Aberrant expression of E-cadherin and beta-catenin in human prostate cancer. Urol Oncol 2005;23(6):402-6.
119. Kallakury BV, Sheehan CE, Ross JS. Co-downregulation of cell adhesion proteins alpha- and beta-catenins, p120CTN, E-cadherin, and CD44 in prostatic adenocarcinomas. Hum Pathol 2001;32(8):849-55.
120. Jaggi M, Chauhan SC, Du C, Balaji KC. Bryostatin 1 modulates beta-catenin subcellular localization and transcription activity through protein kinase D1 activation. Molecular cancer therapeutics 2008;7(9):2703-12.
121. Li DQ, Kumar R. Mi-2/NuRD complex making inroads into DNA-damage response pathway. Cell cycle (Georgetown, Tex) 2010;9(11):2071-9.
122. Pakala SB, Rayala SK, Wang RA, Ohshiro K, Mudvari P, Reddy SD, et al. MTA1 promotes STAT3 transcription and pulmonary metastasis in breast cancer. Cancer research 2013;73(12):3761-70.
123. Dias SJ, Zhou X, Ivanovic M, Gailey MP, Dhar S, Zhang L, et al. Nuclear MTA1 overexpression is associated with aggressive prostate cancer, recurrence and metastasis in African Americans. Scientific reports 2013;3:2331.
124. Tuncay Cagatay S, Cimen I, Savas B, Banerjee S. MTA-1 expression is associated with metastasis and epithelial to mesenchymal transition in colorectal cancer cells. Tumour biology : the journal of the International Society for Oncodevelopmental Biology and Medicine 2013;34(2):1189-204.
125. Manavathi B, Kumar R. Metastasis tumor antigens, an emerging family of multifaceted master coregulators. The Journal of biological chemistry 2007;282(3):1529-33.
126. Manavathi B, Singh K, Kumar R. MTA family of coregulators in nuclear receptor biology and pathology. Nuclear receptor signaling 2007;5:e010.

127. Kumar R, Wang RA, Bagheri-Yarmand R. Emerging roles of MTA family members in human cancers. Seminars in oncology 2003;30(5 Suppl 16):30-7.
128. Toh Y, Nicolson GL. The role of the MTA family and their encoded proteins in human cancers: molecular functions and clinical implications. Clinical & experimental metastasis 2009;26(3):215-27.
129. Kumar R, Wang RA, Mazumdar A, Talukder AH, Mandal M, Yang Z, et al. A naturally occurring MTA1 variant sequesters oestrogen receptor-alpha in the cytoplasm. Nature 2002;418(6898):654-7.
130. Carlin D, Sepich D, Grover VK, Cooper MK, Solnica-Krezel L, Inbal A. Six3 cooperates with Hedgehog signaling to specify ventral telencephalon by promoting early expression of Foxg1a and repressing Wnt signaling. Development (Cambridge, England) 2012;139(14):2614-24.
131. Rykx A, De Kimpe L, Mikhalap S, Vantus T, Seufferlein T, Vandenheede JR, et al. Protein kinase D: a family affair. FEBS Lett 2003;546(1):81-6.
132. Bowden ET, Barth M, Thomas D, Glazer RI, Mueller SC. An invasion-related complex of cortactin, paxillin and PKCmu associates with invadopodia at sites of extracellular matrix degradation. Oncogene 1999;18(31):4440-49.
133. Jaggi M, Du C, Zhang W, Balaji KC. Protein kinase D1: a protein of emerging translational interest. Front Biosci 2007;12:3757-67.
134. Jaggi M, Rao PS, Smith DJ, Wheelock MJ, Johnson KR, Hemstreet GP, et al. E-cadherin phosphorylation by protein kinase D1/protein kinase C{mu} is associated with altered cellular aggregation and motility in prostate cancer. Cancer Res 2005;65(2):483-92.
135. Tandon M, Salamoun JM, Carder EJ, Farber E, Xu S, Deng F, et al. SD-208, a novel protein kinase D inhibitor, blocks prostate cancer cell proliferation and tumor growth in vivo by inducing G2/M cell cycle arrest. PloS one 2015;10(3):e0119346.
136. Sundram V, Chauhan SC, Jaggi M. Emerging Roles of Protein Kinase D1 in Cancer. Molecular Cancer Research 2011.
137. Lei M, Zavodszky M, Kuhn L, Thorpe MF. Sampling Protein Conformations and Pathways. Journal of Computational Chemistry 2004.
138. Aggarwal M, Mondal A. Role of N-Terminal Hydrophobic Region in modulating the Subcellular Localization and Enzyme Activity of the Bisphosphate Nucelotidase from Debaryomyces hansenii. Eukaryotic Cell 2006.
139. Ubersax JA, Ferrell JE. Mechanisms of specificity in protein phosphorylation. Nature Reviews: Molecular Cell Biology 2007.
140. Fu Y, Rubin C. Protein kianse D: coupling extracellular stimuli to the regulation of cell physiology. EMBO Rep 2011.
141. Oancea E, Bezzerides V, Greka A, Clapham D. Mechanism of Persistent Protein Kinase D1 Translocation and Activation. Developmental Cell 2003.
142. Cowell C, Doppler H, Yan I, Hausser A, Umezawa Y, Storz P. Mitochondrial diacylglycerol intiates protein-kinase-D1-mediated ROS signaling. Journal of Cell Science 2009.
143. Rey O, Rozengurt E. Regulated nucleocytoplasmic transport of protein kinase D in response to G protein-coupled receptor activation. Journal of Biological Chemistry 2001.

144. Baron CL, Malhotra V. Role of diacylglycerol in PKD recruitment to the TGN and protein transport to the plasma membrae. Science 2002.
145. Campelo F, Malhotra V. Membrane Fission: The Biogenesis of Transport Carriers. Annual Review of Biochemistry 2012.
146. Bossard B, Polishchuk R, Malhotra V. Dimeric PKD regulates membrane fission to form transport carriers at the TGN. Journal of Cellular Biology 2007.
147. Gschwendt M, Johannes F, Kittstein W, Marks F. Regulation of protein kinase Cmu by basic peptides and heparin. Putative role of an acidic domain in the activation of the kinase. Journal of Biological Chemistry 1997.
148. Waldron R, Rozengurt E. Protein kinase C phosphorylates protein kinase D activation loop Ser744 and Ser748 and releases autoinhibition by the pleckstrin homology. Journal of Biological Chemistry 2003.
149. Iglesias T, Rozengurt E. Protein Kinase D Activation by Mutations within Its Pleckstrin Homology Domain. The Journal of Biological Chemistry 1998.
150. Steinberg S. Regulation of Protein Kinase D1 Activity. Molceular Pharmacology 2012.
151. Vertommen D, Rider M, Ni Y, Waelkens E, Merlevede W, Vandenheede J, et al. Regulation of Protein Kinase D by Multisite Phosphorylation: Identification of Phosphorylation Sites by Mass Spectrometry and Characterization by Site-Directed Mutagenesis. The Journal of Biological Chemistry 2000.
152. Rybin V, Guo J, Steinberg S. Protein Kinase D1 Autophosphorylation via Distinct Mechanisms at Ser 744/Ser 748 and Ser 916. The Journal of Biological Chemistry 2009.
153. Avkiran M, Rowland A, Cuello F, Haworth R. Protein Kinase D in the Cardiovascular System; Emerging Roles in Health and Disease. Circulation Research 2008.
154. Rozengurt E, Rey O, Waldron R. Protein kinase D signaling. Journal of Biological Chemistry 2005.
155. Waldron R, Iglesias T, Rozengurt E. Phosphorylation-dependent protein kinase D activation. Electrophoresis 1999.
156. Lau W, Chan A, Poon L, Zhu J, Wong Y. GBy-mediated activation of protein kinase D exhibits subunit specificity and requires GBy-responsive phospholipase CB isoforms. Cell Communication & Signaling 2013.
157. Vantus T, Vertommen D, Saelens X, Rykx A, De Kimpe L, Vancauwenbergh S, et al. Doxorubicin-induced activation of protein kinase D1 through caspase-mediated proteolytic cleavage: identification of two cleavage sites by microsequencing. Cell Signal.
158. Haussermann S, Kittstein W, Rincke G, Johannes F, Marks F, Gschwendt M. Proteolytic cleavage of protein kinase cmu upon induction of apoptosis is U937 cells. FEBS Lett 1999.
159. Doppler H, Bastea L, Eiseler T, Storz P. Neuregulin mediates F-actin-driven cell migration through inhibition of protein kinase D1 via Rac1 protein. The Journal of Biological Chemistry 2013.
160. Ziegler S, Eiseler T, Scholz R-P, Beck A, Link G, Hausser A. A novel protein kinase D phosphorylation site in the tumor suppressor Rab interactor 1 is critical for coordination of cell migration. Molecular Biology of the Cell 2011.

161. Du C, Zhang C, Hassan S, Biswas M, Balaji K. Protein kinase D1 suppresses epithelial-to-mesenchymal transition through phosphorylation of snail. Cancer Research 2010.
162. Watkins J, Lewandowski K, Meek S, Storz P, Toker A, Piwnica-Worms H. Phosphorylation of the Par-1 polarity kinase by protein kinase D regulates 14-3-3 binding and membrane association. PNAS 2008.
163. Mak P, Jaggi M, Syed V, Chauhan SC, Hassan S, Biswas H, et al. Protein kinase D1 (PKD1) influences androgen receptor (AR) function in prostate cancer cells. Biochem Biophys Res Commun 2008.
164. Eiseler T, Doppler H, Yan I, Goodison S, Storz P. Protein kinase D1 regulates matrix metalloproteinase expression and inhibits breast cancer cell invasion. Breast Cancer Research 2009.
165. Jaggi M, Rao P, Smith D, Wheelock M, Johnson K, Hemstreet G, et al. E-Cadherin Phosphorylation by Protein Kinase D1/Protein Kinase Cmu is Associated with Altered Cellular Aggregation and Motility in Prostate Cancer. Cancer Research 2005.
166. Du C, Zhang C, Li Z, Biswas MHU, Balaji KC. Beta-Catenin Phosphorylated at Threonine 120 Antagonizes Generation of Active Beta-Catenin by Spatial Localization in trans-Golgi Network. PLoS ONE 2012.
167. Du C, Jaggi M, Zhang C, Balaji KC. Protein Kinase D1-Mediated Phosphorylation and Subcellular Localization of β-catenin. Cancer Research 2009.
168. Storz P, Doppler H, Toker A. Protein Kinase Cdelta Selectively Regulates Protein Kinase D-Dependent Activation of NF-kappaB in Oxidative Stress Signaling. Molecular and Cellular Biology 2004.
169. Kisfalvi K, Hurd C, Guha S, Rozengurt E. Induced Overexpression of Protein Kinase D1 Stimulates Mitogenic Signaling in Human Pancreatic Carcinoma PANC-1 Cells. Journal of Cellular Physiology 2010.
170. Rozengurt E, Guha S, Sinnett-Smith J. Gastrointestinal peptide signalling in health and disease. The European journal of surgery Supplement : = Acta chirurgica Supplement 2002(587):23-38.
171. Fu Y, Rubin CS. Protein kinase D: coupling extracellular stimuli to the regulation of cell physiology. EMBO reports 2011;12(8):785-96.
172. Kedei N, Telek A, Czap A, Lubart ES, Czifra G, Yang D, et al. The synthetic bryostatin analog Merle 23 dissects distinct mechanisms of bryostatin activity in the LNCaP human prostate cancer cell line. Biochemical pharmacology 2011;81(11):1296-308.
173. Winegarden JD, Mauer AM, Gajewski TF, Hoffman PC, Krauss S, Rudin CM, et al. A phase II study of bryostatin-1 and paclitaxel in patients with advanced non-small cell lung cancer. Lung cancer (Amsterdam, Netherlands) 2003;39(2):191-6.
174. Ardekani AM, Fard SS, Jeddi-Tehrani M, Ghahremanzade R. Bryostatin-1, Fenretinide and 1alpha,25 (OH)(2)D(3) Induce Growth Inhibition, Apoptosis and Differentiation in T and B Cell-Derived Acute Lymphoblastic Leukemia Cell Lines (CCRF-CEM and Nalm-6). Avicenna journal of medical biotechnology 2011;3(4):177-93.

175. Clamp AR, Blackhall FH, Vasey P, Soukop M, Coleman R, Halbert G, et al. A phase II trial of bryostatin-1 administered by weekly 24-hour infusion in recurrent epithelial ovarian carcinoma. British journal of cancer 2003;89(7):1152-4.
176. Kamboj VP, Setty BS, Chandra H, Roy SK, Kar AB. Biological profile of Centchroman--a new post-coital contraceptive. Indian journal of experimental biology 1977;15(12):1144-50.
177. Misra NC, Nigam PK, Gupta R, Agarwal AK, Kamboj VP. Centchroman--a non-steroidal anti-cancer agent for advanced breast cancer: phase-II study. International journal of cancer Journal international du cancer 1989;43(5):781-3.
178. Nigam M, Ranjan V, Srivastava S, Sharma R, Balapure AK. Centchroman induces G0/G1 arrest and caspase-dependent apoptosis involving mitochondrial membrane depolarization in MCF-7 and MDA MB-231 human breast cancer cells. Life sciences 2008;82(11-12):577-90.
179. Srivastava VK, Gara RK, Bhatt ML, Sahu DP, Mishra DP. Centchroman inhibits proliferation of head and neck cancer cells through the modulation of PI3K/mTOR pathway. Biochemical and biophysical research communications 2011;404(1):40-5.
180. Khan S, Ebeling MC, Chauhan N, Thompson PA, Gara RK, Ganju A, et al. Ormeloxifene suppresses desmoplasia and enhances sensitivity of gemcitabine in pancreatic cancer. Cancer research 2015;75(11):2292-304.
181. Maher DM, Khan S, Nordquist JL, Ebeling MC, Bauer NA, Kopel L, et al. Ormeloxifene efficiently inhibits ovarian cancer growth. Cancer letters 2015;356(2 Pt B):606-12.
182. Khan S, Chauhan N, Yallapu MM, Ebeling MC, Balakrishna S, Ellis RT, et al. Nanoparticle formulation of ormeloxifene for pancreatic cancer. Biomaterials 2015;53:731-43.
183. Singh MM. Centchroman, a selective estrogen receptor modulator, as a contraceptive and for the management of hormone-related clinical disorders. Medicinal research reviews 2001;21(4):302-47.
184. Jemal A, Simard EP, Dorell C, Noone AM, Markowitz LE, Kohler B, et al. Annual Report to the Nation on the Status of Cancer, 1975-2009, featuring the burden and trends in human papillomavirus(HPV)-associated cancers and HPV vaccination coverage levels. J Natl Cancer Inst 2013;105(3):175-201.
185. Schneikert J, Behrens J. The canonical Wnt signalling pathway and its APC partner in colon cancer development. Gut 2007;56(3):417-25.
186. Korkaya H, Paulson A, Charafe-Jauffret E, Ginestier C, Brown M, Dutcher J, et al. Regulation of mammary stem/progenitor cells by PTEN/Akt/beta-catenin signaling. PLoS biology 2009;7(6):e1000121.
187. Greenspan EJ, Madigan JP, Boardman LA, Rosenberg DW. Ibuprofen inhibits activation of nuclear {beta}-catenin in human colon adenomas and induces the phosphorylation of GSK-3{beta}. Cancer Prev Res (Phila) 2011;4(1):161-71.
188. Moon RT, Kohn AD, Ferrari GVD, Kaykas A. WNT and [beta]-catenin signalling: diseases and therapies. Nat Rev Genet 2004;5(9):691-701.
189. MacDonald BT, Tamai K, He X. Wnt/beta-catenin signaling: components, mechanisms, and diseases. Dev Cell 2009;17(1):9-26.

190. Verheyen EM, Gottardi CJ. Regulation of Wnt/beta-catenin signaling by protein kinases. Developmental dynamics : an official publication of the American Association of Anatomists 2010;239(1):34-44.
191. Korinek V, Barker N, Morin PJ, van Wichen D, de Weger R, Kinzler KW, et al. Constitutive transcriptional activation by a beta-catenin-Tcf complex in APC-/- colon carcinoma. Science 1997;275(5307):1784-7.
192. van de Wetering M, Sancho E, Verweij C, de Lau W, Oving I, Hurlstone A, et al. The beta-catenin/TCF-4 complex imposes a crypt progenitor phenotype on colorectal cancer cells. Cell 2002;111(2):241-50.
193. Sundram V, Chauhan SC, Jaggi M. Emerging Roles of Protein Kinase D1 in Cancer. Mol Cancer Res 2011;9(8):985-96.
194. Rozengurt E, Rey O, Waldron RT. Protein kinase D signaling. The Journal of biological chemistry 2005;280(14):13205-8.
195. Eiseler T, Doppler H, Yan IK, Goodison S, Storz P. Protein kinase D1 regulates matrix metalloproteinase expression and inhibits breast cancer cell invasion. Breast Cancer Res 2009;11(1):R13.
196. Eiseler T, Doppler H, Yan IK, Kitatani K, Mizuno K, Storz P. Protein kinase D1 regulates cofilin-mediated F-actin reorganization and cell motility through slingshot. Nat Cell Biol 2009;11(5):545-56.
197. Hassan S, Biswas MH, Zhang C, Du C, Balaji KC. Heat shock protein 27 mediates repression of androgen receptor function by protein kinase D1 in prostate cancer cells. Oncogene 2009;28(49):4386-96.
198. Du C, Zhang C, Hassan S, Biswas MH, Balaji KC. Protein kinase D1 suppresses epithelial-to-mesenchymal transition through phosphorylation of snail. Cancer Res 2010;70(20):7810-9.
199. Biswas MH, Du C, Zhang C, Straubhaar J, Languino LR, Balaji KC. Protein kinase D1 inhibits cell proliferation through matrix metalloproteinase-2 and matrix metalloproteinase-9 secretion in prostate cancer. Cancer Res 2010;70(5):2095-104.
200. Peterburs P, Heering J, Link G, Pfizenmaier K, Olayioye MA, Hausser A. Protein kinase D regulates cell migration by direct phosphorylation of the cofilin phosphatase slingshot 1 like. Cancer Res 2009;69(14):5634-8.
201. Jaggi M, Rao PS, Smith DJ, Hemstreet GP, Balaji KC. Protein kinase C mu is down-regulated in androgen-independent prostate cancer. Biochem Biophys Res Commun 2003;307(2):254-60.
202. Borges S, Doppler H, Perez EA, Andorfer CA, Sun Z, Anastasiadis PZ, et al. Pharmacologic reversion of epigenetic silencing of the PRKD1 promoter blocks breast tumor cell invasion and metastasis. Breast cancer research : BCR 2013;15(2):R66.
203. Du C, Jaggi M, Zhang C, Balaji KC. Protein kinase D1-mediated phosphorylation and subcellular localization of beta-catenin. Cancer Res 2009;69(3):1117-24.
204. Kisfalvi K, Hurd C, Guha S, Rozengurt E. Induced overexpression of protein kinase D1 stimulates mitogenic signaling in human pancreatic carcinoma PANC-1 cells. J Cell Physiol 2010;223(2):309-16.
205. Syed V, Mak P, Du C, Balaji KC. Beta-catenin mediates alteration in cell proliferation, motility and invasion of prostate cancer cells by differential

expression of E-cadherin and protein kinase D1. J Cell Biochem 2008;104(1):82-95.
206. Johnson KR, Lewis JE, Li D, Wahl J, Soler AP, Knudsen KA, et al. P- and E-cadherin are in separate complexes in cells expressing both cadherins. Exp Cell Res 1993;207(2):252-60.
207. Sundram V, Chauhan SC, Ebeling M, Jaggi M. Curcumin attenuates beta-catenin signaling in prostate cancer cells through activation of protein kinase D1. PLoS One 2012;7(4):e35368.
208. Gupta BK, Maher DM, Ebeling MC, Sundram V, Koch MD, Lynch DW, et al. Increased expression and aberrant localization of mucin 13 in metastatic colon cancer. J Histochem Cytochem 2012;60(11):822-31.
209. Chauhan SC, Ebeling MC, Maher DM, Koch MD, Watanabe A, Aburatani H, et al. MUC13 mucin augments pancreatic tumorigenesis. Mol Cancer Ther 2012;11(1):24-33.
210. Yallapu MM, Maher DM, Sundram V, Bell MC, Jaggi M, Chauhan SC. Curcumin induces chemo/radio-sensitization in ovarian cancer cells and curcumin nanoparticles inhibit ovarian cancer cell growth. J Ovarian Res 2010;3:11.
211. Chauhan SC, Vannatta K, Ebeling MC, Vinayek N, Watanabe A, Pandey KK, et al. Expression and functions of transmembrane mucin MUC13 in ovarian cancer. Cancer research 2009;69(3):765-74.
212. Eiseler T, Hausser A, De Kimpe L, Van Lint J, Pfizenmaier K. Protein kinase D controls actin polymerization and cell motility through phosphorylation of cortactin. J Biol Chem 2010;285(24):18672-83.
213. Eiseler T, Schmid MA, Topbas F, Pfizenmaier K, Hausser A. PKD is recruited to sites of actin remodelling at the leading edge and negatively regulates cell migration. FEBS Lett 2007;581(22):4279-87.
214. Clevers H. Wnt/beta-catenin signaling in development and disease. Cell 2006;127(3):469-80.
215. Du C, Jaggi M, Zhang C, Balaji KC. Protein Kinase D1-Mediated Phosphorylation and Subcellular Localization of {beta}-Catenin. Cancer Res 2009;69(3):1117-24.
216. Bastea LI, Doppler H, Balogun B, Storz P. Protein kinase D1 maintains the epithelial phenotype by inducing a DNA-bound, inactive SNAI1 transcriptional repressor complex. PLoS One 2012;7(1):e30459.
217. Borges S, Doppler H, Perez EA, Andorfer CA, Sun Z, Anastasiadis PZ, et al. Pharmacologic reversion of epigenetic silencing of the PRKD1 promoter blocks breast tumor cell invasion and metastasis. Breast Cancer Res 2013;15(2):R66.
218. Doppler H, Bastea LI, Eiseler T, Storz P. Neuregulin mediates F-actin-driven cell migration through inhibition of protein kinase D1 via Rac1 protein. J Biol Chem 2013;288(1):455-65.
219. Storz P. Protein kinase D1: a novel regulator of actin-driven directed cell migration. Cell Cycle 2009;8(13):1975-6.
220. Eisenberg-Lerner A, Kimchi A. PKD is a kinase of Vps34 that mediates ROS-induced autophagy downstream of DAPk. Cell Death Differ 2012;19(5):788-97.

221. Eisenberg-Lerner A, Kimchi A. DAP kinase regulates JNK signaling by binding and activating protein kinase D under oxidative stress. Cell Death Differ 2007;14(11):1908-15.
222. Eisenberg-Lerner A, Kimchi A. PKD at the crossroads of necrosis and autophagy. Autophagy 2012;8:3:433-34.
223. Sullivan R, Graham C. Hypoxia-driven selection of the metastatic phenotype. Cancer Metastasis Rev 2007;26(2):319-31.
224. Semenza GL. Targeting HIF-1 for cancer therapy. Nat Rev Cancer 2003;3(10):721-32.
225. Qin L, Zeng H, Zhao D. Requirement of protein kinase D tyrosine phosphorylation for VEGF-A165-induced angiogenesis through its interaction and regulation of phospholipase Cgamma phosphorylation. J Biol Chem 2006;281(43):32550-8.
226. Ha CH, Jhun BS, Kao HY, Jin ZG. VEGF stimulates HDAC7 phosphorylation and cytoplasmic accumulation modulating matrix metalloproteinase expression and angiogenesis. Arterioscler Thromb Vasc Biol 2008;28(10):1782-8.
227. Ha CH, Wang W, Jhun BS, Wong C, Hausser A, Pfizenmaier K, et al. Protein kinase D-dependent phosphorylation and nuclear export of histone deacetylase 5 mediates vascular endothelial growth factor-induced gene expression and angiogenesis. J Biol Chem 2008;283(21):14590-9.
228. Wheelock MJ, Johnson KR. Cadherins as modulators of cellular phenotype. Annu Rev Cell Dev Biol 2003;19:207-35.
229. Semenas J, Allegrucci C, Boorjian SA, Mongan NP, Persson JL. Overcoming drug resistance and treating advanced prostate cancer. Current drug targets 2012;13(10):1308-23.
230. Prados J, Melguizo C, Ortiz R, Perazzoli G, Cabeza L, Alvarez PJ, et al. Colon cancer therapy: recent developments in nanomedicine to improve the efficacy of conventional chemotherapeutic drugs. Anti-cancer agents in medicinal chemistry 2013;13(8):1204-16.
231. Chen J, Ding Z, Peng Y, Pan F, Li J, Zou L, et al. HIF-1alpha inhibition reverses multidrug resistance in colon cancer cells via downregulation of MDR1/P-glycoprotein. PloS one 2014;9(6):e98882.
232. Ganju A, Yallapu MM, Khan S, Behrman SW, Chauhan SC, Jaggi M. Nanoways to overcome docetaxel resistance in prostate cancer. Drug resistance updates : reviews and commentaries in antimicrobial and anticancer chemotherapy 2014;17(1-2):13-23.
233. Liu J, Wang H, Ma F, Xu D, Chang Y, Zhang J, et al. MTA1 regulates higher-order chromatin structure and histone H1-chromatin interaction in-vivo. Molecular oncology 2014.
234. Kaur E, Gupta S, Dutt S. Clinical implications of MTA proteins in human cancer. Cancer metastasis reviews 2014;33(4):1017-24.
235. Liu J, Xu D, Wang H, Zhang Y, Chang Y, Zhang J, et al. The subcellular distribution and function of MTA1 in cancer differentiation. Oncotarget 2014;5(13):5153-64.

236. Levenson AS, Kumar A, Zhang X. MTA family of proteins in prostate cancer: biology, significance, and therapeutic opportunities. Cancer metastasis reviews 2014;33(4):929-42.
237. Gururaj AE, Singh RR, Rayala SK, Holm C, den Hollander P, Zhang H, et al. MTA1, a transcriptional activator of breast cancer amplified sequence 3. Proceedings of the National Academy of Sciences of the United States of America 2006;103(17):6670-5.
238. Yu L, Su YS, Zhao J, Wang H, Li W. Repression of NR4A1 by a chromatin modifier promotes docetaxel resistance in PC-3 human prostate cancer cells. FEBS letters 2013;587(16):2542-51.
239. Sundram V, Ganju A, Hughes JE, Khan S, Chauhan SC, Jaggi M. Protein kinase D1 attenuates tumorigenesis in colon cancer by modulating beta-catenin/T cell factor activity. Oncotarget 2014;5(16):6867-84.
240. Chong RA, Wu K, Spratt DE, Yang Y, Lee C, Nayak J, et al. Pivotal role for the ubiquitin Y59-E51 loop in lysine 48 polyubiquitination. Proc Natl Acad Sci U S A 2014;111(23):8434-9.
241. Simpson MA, Weigel JA, Weigel PH. Systemic blockade of the hyaluronan receptor for endocytosis prevents lymph node metastasis of prostate cancer. International journal of cancer Journal international du cancer 2012;131(5):E836-40.
242. Li J, Ye L, Sun PH, Satherley L, Hargest R, Zhang Z, et al. MTA1 Is Up-regulated in Colorectal Cancer and Is Inversely Correlated with Lymphatic Metastasis. Cancer genomics & proteomics 2015;12(6):339-45.
243. Fuhrmann J, Rurainski A, Lenhof HP, Neumann D. A new Lamarckian genetic algorithm for flexible ligand-receptor docking. Journal of computational chemistry 2010;31(9):1911-18.
244. Ansari MF, Siddiqui SM, Ahmad K, Avecilla F, Dharavath S, Gourinath S, et al. Synthesis, antiamoebic and molecular docking studies of furan-thiazolidinone hybrids. European Journal of Medicinal Chemistry 2016;124:393-406.
245. Abassi YA, Xi B, Zhang W, Ye P, Kirstein SL, Gaylord MR, et al. Kinetic cell-based morphological screening: prediction of mechanism of compound action and off-target effects. Chemistry & biology 2009;16(7):712-23.
246. Nakazawa M, Kyprianou N. Epithelial-mesenchymal-transition regulators in prostate cancer: Androgens and beyond. The Journal of steroid biochemistry and molecular biology 2016.
247. Trudel D, Fradet Y, Meyer F, Harel F, Tetu B. Significance of MMP-2 expression in prostate cancer: an immunohistochemical study. Cancer research 2003;63(23):8511-5.
248. Itoh T, Tanioka M, Matsuda H, Nishimoto H, Yoshioka T, Suzuki R, et al. Experimental metastasis is suppressed in MMP-9-deficient mice. Clinical & experimental metastasis 1999;17(2):177-81.
249. Stearns M, Stearns ME. Evidence for increased activated metalloproteinase 2 (MMP-2a) expression associated with human prostate cancer progression. Oncology research 1996;8(2):69-75.
250. Ross JS, Kaur P, Sheehan CE, Fisher HA, Kaufman RA, Jr., Kallakury BV. Prognostic significance of matrix metalloproteinase 2 and tissue inhibitor of

metalloproteinase 2 expression in prostate cancer. Modern pathology : an official journal of the United States and Canadian Academy of Pathology, Inc 2003;16(3):198-205.
251. Sack JS, Kish KF, Wang C, Attar RM, Kiefer SE, An Y, et al. Crystallographic structures of the ligand-binding domains of the androgen receptor and its T877A mutant complexed with the natural agonist dihydrotestosterone. Proceedings of the National Academy of Sciences 2001;98(9):4904-09.
252. Kim S, Wu JY, Birzin ET, Frisch K, Chan W, Pai L-Y, et al. Estrogen receptor ligands. II. Discovery of benzoxathiins as potent, selective estrogen receptor α modulators. Journal of medicinal chemistry 2004;47(9):2171-75.
253. Mewshaw RE, Bowen SM, Harris HA, Xu ZB, Manas ES, Cohn ST. ERβ ligands. Part 5: Synthesis and structure–activity relationships of a series of 4′-hydroxyphenyl-aryl-carbaldehyde oxime derivatives. Bioorganic & medicinal chemistry letters 2007;17(4):902-06.
254. Grossmann TN, Yeh JT-H, Bowman BR, Chu Q, Moellering RE, Verdine GL. Inhibition of oncogenic Wnt signaling through direct targeting of β-catenin. Proceedings of the National Academy of Sciences 2012;109(44):17942-47.
255. Berg S, Bergh M, Hellberg S, Högdin K, Lo-Alfredsson Y, Söderman P, et al. Discovery of novel potent and highly selective glycogen synthase kinase-3β (GSK3β) inhibitors for Alzheimer's disease: design, synthesis, and characterization of pyrazines. Journal of medicinal chemistry 2012;55(21):9107-19.

VITA

Aditya Ganju was born in New Delhi, India in the year 1988. He obtained Bachelor of Technology degree (Biotechnology) in May 2010 from Jaypee Institute of Information Technology, Noida, U.P., India and Masters of Science (Biotechnology) in May 2011 from department of biotechnology, Georgetown University, Washington DC, USA. From May 2011 to December 2011, he has worked in Protein Information Resource (PIR), Georgetown University, Washington DC. From January 2011 to August 2011, he worked as a Research Associate (RA) in Dr. Meena Jaggi's Lab. He was matriculated in the PhD program in Basic Biomedical Sciences with major in Cancer Biology at University of South Dakota, Vermillion, SD, USA in August 2012. In June 2013, he transferred to the University of Tennessee Health Science Center, Memphis, TN, USA. In 2015, he received first prize for best poster presentation at Graduate Research Day (GRD) at UTHSC. He has presented his research works in regional and national level conferences. He has authored and co-authored in eight peer reviewed scientific articles. He is the member of AACR since 2013 and AAPS since 2016. He received his doctorate degree with major in Bioanalysis in December 2016.

LIST OF RELATED PUBLICATIONS

1. Ganju A, Khan S, Hafeez BB, Behrman SW, Yallapu MM, Chauhan SC, et al. miRNA nanotherapeutics for cancer. Drug discovery today 2016. [Epub ahead of print]

2. Ganju A, Yallapu MM, Khan S, Behrman SW, Chauhan SC, Jaggi M. Nanoways to overcome docetaxel resistance in prostate cancer. Drug resistance updates : reviews and commentaries in antimicrobial and anticancer chemotherapy 2014;17(1-2):13-23.